

# Controlling entanglement via parity measurements and semi-classical approach to ultrafast thermalization dynamics



Im Fachbereich Physik der Freien Universität Berlin eingereichte Dissertation zur  
Erlangung des Grades eines Doktors der Naturwissenschaften (Dr. rer. nat.)

Berlin, Juli 2017

vorgelegt von

Clemens Meyer zu Rheda



Erste Gutachterin: Dr. Tamara Nunner

Zweiter Gutachter: Prof. Felix von Oppen, PhD

Termin der Disputation: 30. Oktober 2017

## **Selbstständigkeitserklärung**

Ich versichere hiermit, dass ich alle Hilfsmittel und Hilfen, auf deren Grundlage ich diese Arbeit selbstständig verfasst haben, angegeben habe. Ferner versichere ich, dass diese Arbeit nicht schon einmal in einem früheren Promotionsverfahren angenommen oder als ungenügend beurteilt worden ist.

Clemens Meyer zu Rheda

# Contents

Deutsche Zusammenfassung	7
English summary	9
Preface	11
<b>I Controlling entanglement via parity measurements</b>	<b>13</b>
<b>1 Introduction</b>	<b>15</b>
<b>2 Entanglement</b>	<b>19</b>
2.1 Introduction to entanglement . . . . .	19
2.2 Entanglement measures . . . . .	20
2.2.1 Schmidt decomposition . . . . .	21
2.2.2 von Neumann entropy . . . . .	24
2.2.3 Entanglement of formation . . . . .	27
2.2.4 Entanglement concurrence . . . . .	29
<b>3 Quantum measurements</b>	<b>31</b>
3.1 General measurements . . . . .	31
3.1.1 Projective measurements . . . . .	32
3.1.2 General measurements as projections . . . . .	34
3.2 Von Neumann measurements . . . . .	36
3.2.1 Measurement strength . . . . .	40
3.3 Continuous measurements . . . . .	41
3.4 Measurement control . . . . .	46
3.4.1 Markovian Feedback . . . . .	47
3.4.2 Bayesian Feedback . . . . .	47
<b>4 Measurement and entanglement</b>	<b>51</b>
4.1 Parity measurements . . . . .	51
4.1.1 Bell states . . . . .	52

4.1.2	Conditional concurrence . . . . .	53
4.2	Electronic Mach-Zender interferometer . . . . .	54
4.2.1	Physical model . . . . .	55
4.3	Microscopic model . . . . .	57
4.3.1	Single electron passing . . . . .	58
4.3.2	Parity meter conditions . . . . .	59
4.3.3	Continuous electron detection . . . . .	61
4.3.4	Dephasing mechanisms . . . . .	62
4.4	Markovian feedback . . . . .	63
4.5	Bayesian feedback . . . . .	67
4.6	Numerical simulations . . . . .	69
4.6.1	Markovian feedback . . . . .	70
4.6.2	Bayesian feedback . . . . .	70
5	Summary and conclusions	77
II	Ultrafast thermalization and equilibration dynamics	79
6	Introduction	81
7	Boltzmann equation	85
7.1	Classical part . . . . .	85
7.2	Two term approximation . . . . .	87
7.3	Collision part . . . . .	87
7.3.1	Single particle collisions . . . . .	88
7.3.1.1	Impurity scattering . . . . .	89
7.3.1.2	Phonon scattering . . . . .	91
7.3.2	Two particle collisions . . . . .	98
7.3.2.1	Electron-electron scattering . . . . .	99
8	Ballistic-diffusive crossover	103
8.1	Introduction . . . . .	103
8.2	Ballistic-diffusive equation . . . . .	104
8.3	Diffusion and wave equations . . . . .	105
8.4	Mean square displacement . . . . .	106
8.5	Solution to the ballistic-diffusive equation . . . . .	107
9	Thermalization	111
9.1	Introduction . . . . .	111
9.2	Thermalization of the electron system . . . . .	112
9.3	Approaching the equilibrium . . . . .	113

<i>CONTENTS</i>	5
<b>10 Two temperature model</b>	<b>119</b>
<b>10.1 Extension of the two temperature model . . . . .</b>	<b>122</b>
<b>11 Summary and conclusions</b>	<b>125</b>
<b>List of publications</b>	<b>137</b>
<b>Curriculum vitae</b>	<b>139</b>
<b>Acknowledgements</b>	<b>141</b>





# Deutsche Zusammenfassung

Diese Arbeit besteht aus zwei Teilen. Im ersten Teil analysieren wir das Messen, Kontrollieren und Stabilisieren von Quantenverschränkung. Wir nehmen ein einfaches System, bestehend aus zwei gekoppelten Qubits, als Grundlage, um die Quantenverschränkung als die fundamentale Einheit der Quanteninformationstheorie einzuführen. Diese Einführung dient zugleich der Entwicklung des mathematischen Formalismus.

Auf ähnliche Weise führen wir dann Quantenmessungen als eine weitere fundamentale Säule der Quantentheorie ein. Ausgehend von einer axiomatischen Definition entwickeln wir eine physikalische Theorie für Messungen in der Quantenwelt, die auf dem von-Neumann-Formalismus beruht.

Mit beiden Werkzeugen ausgerüstet präsentieren wir eine Modellarchitektur, um den beeinflussenden Charakter von Quantenmessungen zur Generation und Kontrolle von Quantenverschränkung auszunutzen. Wir zeigen wie ein elektronisches Mach-Zehnder Interferometer einzustellen ist um die Parität zweier an die jeweiligen Arme gekoppelten Qubits zu messen. Es zeigt sich, dass die Messung der Parität dabei zur Verschränkung beider Qubits führt. Die mikroskopische Einstellung des Mach-Zehnder Interferometers führt allerdings zu einem internen Dephasing im geraden Partitätsunterraum. Um dieses Dephasing, das der Verschränkung entgegenwirkt, zu kontrollieren, führen wir eine Rückkopplungsschleife ein, die das am Ende des Mach-Zehnder Interferometer aufgenommene Signal ausnutzt, um die Fluktuationen im geraden Unterraum auszugleichen.

Um die Quantenverschränkung beider Qubits auch gegen externe Einflüsse zu schützen, zeigen wir wie eine zweite Rückkopplungsschleife in das System integriert werden kann. Diese zweite Schleife beruht auf einer zweiten Messung und erlaubt durch ihren Bayesischen Charakter die Quantenverschränkung zwischen beiden Qubits auch gegen externe Einflüsse zu stabilisieren.

Im zweiten Teil dieser Arbeit nutzen wir den Boltzmann Formalismus um die Annäherung eines angeregten Elektronensystems an ein neues Gleichgewicht zu untersuchen. Wir führen die Boltzmann Gleichung mit den relevanten Kollisionsintegralen ein, um sowohl das Streuen von Elektronen an Störstellen im Gitter, als auch die Effekte von Interaktionen zwischen Elektronen, sowie die Kollisionen von Elektronen mit Phononen zu beschreiben.

Aus der Boltzmann Gleichung, mit dem Kollisionsintegral für das Stoßen an Störstellen, leiten wir eine Differenzialgleichung her, die die Entwicklung von ballistischem zu diffusivem Transport beschreibt. Diese Gleichung lässt sich analytisch lösen.

Weiterhin untersuchen wir die Thermalisierung der Elektronen im Energieraum unter Hinzunahme des Elektron-Elektron Kollisionsintegrals. Die resultierende Gleichung lösen wir semi-analytisch, sodass die zeitliche Entwicklung über viele Größenordnungen verfolgt wird und somit die Annäherung an ein neues Quasi-Gleichgewicht gezeigt werden kann.

Diese Entwicklung nutzen wir dann, um das Zwei-Temperatur-Model, das die Interaktion zwischen Elektron- und Phonontemperatur beschreibt, weiterzuentwickeln. Wir zeigen dabei, dass die Thermalisierung des Elektronensystems zu einem verzögerten Energieaustausch mit dem Gitter führt.



# English summary

The content of this thesis involves two main topics. In the first part we analyze the measurement, control and stabilization of entanglement. We introduce the concepts of entanglement as the fundamental unit of quantum information theory with a focus on a coupled two qubit system. Using this system we present a mathematical formalism of entanglement.

In a similar manner we introduce quantum measurements as another fundamental building block of quantum theory. From an axiomatic definition we derive a physically accessible theory of quantum measurements based on von Neumann measurements.

With both formalisms developed, we present a model architecture to use the interfering nature of quantum measurements to create and control quantum entanglement. We show how to tune an electronic Mach-Zehnder interferometer that is coupled to two qubits so that it acts as a parity meter. The measurement of parity is shown to be able to create entanglement between both qubits. As the use of a Mach-Zehnder interferometer as a parity meter introduces intrinsic dephasing within the even subspace, we create a feedback loop based on the outcome of the parity measurement that counters this dephasing.

To also stabilize the created entanglement against external influences, we proceed to introduce a second feedback loop based on a second joint measurement. The Bayesian nature of this feedback is shown to allow for the stabilization against external noise sources.

In the second part of this thesis, we employ the semi-classical Boltzmann formalism to analyze the approach of equilibrium by an excited electron system. We introduce the Boltzmann equation and the relevant collision integrals to account for impurity scattering, collisions between electrons and interactions between the electron bath and the surrounding phonon bath.

From the Boltzmann equation, enhanced with impurity scattering, we derive a differential equation that describes the transition from ballistic to diffusive transport. We show the analytical solution to this equation.

Including electron-electron interactions into the Boltzmann equation the thermalization of electron bath in energy space is analyzed. We solve the resulting equation semi-analytically so that the time evolution for many orders of magnitude can be derived and the approach to a new quasi-equilibrium is shown.

With the dynamics of this approach at hand, we extend the two temperature model that describes the interaction between electrons and lattice temperatures. Including the thermalization of electrons in the derivation leads to a delayed interaction between electron bath and phonon bath.



# Preface

This work consists of two parts. In the first we present the creation and control of entanglement between two qubits. We introduce the electronic Mach-Zehnder interferometer as a parity meter to create entanglement and show how the addition of feedback loops can be used to stabilize the created entanglement against dephasing.

In the second part we present a semi-classical approach to equilibration based on the Boltzmann equation. We show that with the inclusion of impurity scattering the transition from ballistic to diffusive transport can be described while the electron-electron interactions lead to the thermalization of the electron system. The obtained dynamics are then used to derive an model for the exchange of energy between electron and phonon systems.



## Part I

# Controlling entanglement via parity measurements





# Chapter 1

## Introduction

While the advocates of any new technology tend to foretell the dawn of a technological revolution, the advent of quantum computational devices is associated with a particular abundance of superlative prophecies. Providing *quantum supremacy* over classical computers the prospect of exploiting quantum phenomena excites scientists and laymen alike, letting the *economist* rejoice: "The era of quantum technology is almost here." [1]

What is to be understood by the word *almost*, however, is up for debate and leaders of the field tend to be reluctant to make predictions [2, 3]. This hesitation is by no means due to a lack of enthusiasm, but rather gives credit to the elusiveness of quantum technologies' fundamental currency: entanglement.

Challenging fights have to be fought at multiple fronts: the creation, control and manipulation, and finally the readout of entanglement all present open fields of research. It turns out that the peculiarities of quantum physics on the one hand provide the prospect of novel application, but complicate the development on the other hand. In particular it is impossible to measure a quantum system without distorting it. In the extreme case the measurement leads to a total collapse of the system's wave function and the loss of all phase coherence.

In the present text we, however, present a setup that uses the collapsing mechanism of a quantum measurement to create entanglement. The locality of the measurement has to be abandoned and a joint measurement of two systems is put in place instead [4, 5, 6, 7, 8, 9, 10, 11]. In the present context the parity of a two qubit system is measured and it is well known that with a properly initialized two qubit state the resulting parity eigenstates are fully entangled Bell states [12].

The implementation of a parity measurement has been proposed and realized in different experimental architectures, most notably in the realm of circuit quantum electron dynamics [13, 14], using superconducting qubits [15, 16], in three and two-dimensional architectures [17]. On the other hand the

creation of an electronic Mach-Zehnder interferometer [18, 19, 20] coupled to two double dot qubits has been proposed to realize a parity meter in the domain of quantum transport [21].

To use a Mach-Zehnder interferometer as a parity meter it has to be tuned in a way that it only distinguishes two resulting sub-spaces, spanned by the even and odd parity states. However, it has been predicted theoretically and confirmed in experiments that a Mach-Zehnder interferometer that is fine tuned to match the parity conditions necessarily brings about an intrinsic dephasing within the even subspace that prevents the creation of entangled states. While such a parity meter does create fully entangled odd Bell states and the creation is traceable due to the parity meter outcome, this outcome is stochastic and on average half the cases have to be discarded.

In the present work we analyze the microscopic transport problem of individual electrons traveling through the Mach-Zehnder interferometer [22] to understand the origin of the mentioned dephasing. Its source is traced back to a continuous measurement-outcome-dependent back action in the form of a fluctuating phase induced by the passing electrons. The details of these fluctuations are lost in a macroscopic account of the measurement process leading to an averaged dephasing.

Having singled out the nature of the unwanted dephasing process we propose a feedback mechanism that employs the microscopic relation between measurement outcome and fluctuating phase so that said stochasticity is cancelled in real time and the corresponding dephasing is avoided. We name this feedback *Markovian* to emphasize its dependency only on the momentary stochastic measurement outcome [23, 24, 25].

However, the employed continuous weak measurement does not acquire information about any external sources of dephasing such as noise from a coupling to the environment or the initialization of the qubits. To stabilize the double qubit system and thus the created entanglement against such external influences we analyze the implementation of a second feedback loop based on a second measurement. As this feedback is based on probabilistic information acquired by the weak measurement it is named *Bayesian feedback* [26, 27].

We show that with the combination of both feedback loops a deterministic creation and the subsequent stabilization of entanglement against external influences is achieved even for environmental dephasing of the order of the measurement rate. The stabilized partial entanglement can in principle be used to distill fully entangled qubits in more elaborate architectures based on future developments [28, 29, 30].

In the following we start by introducing the concept of quantum entanglement to the unfamiliar reader in chapter 2. The concept is explained first heuristically and then by the development of several ideas on how to quantify entanglement, the entanglement measures. In chapter 3 we turn then

to the second main ingredient of the present text, quantum measurements. Here we take the opposite approach and start from an axiomatic definition of a quantum measurement only to introduce more physical aspects later. With the necessary tools at hand we then combine both entanglement and measurement by introducing a way of creating entanglement with quantum measurements in chapter 4. We introduce the architecture of an electronic Mach-Zehnder interferometer to act as a parity meter between two qubits systems and propose and simulate the inclusion of two feedback loops to stabilize the created entanglement.



## Chapter 2

# Entanglement

### 2.1 Introduction to entanglement

When the new theory of quantum mechanics emerged in the beginning of the 20th century it was able to solve many of the open questions in fundamental physics that were baffling physicists at the time. The new phenomena and their implications, however, interfered with the physical intuition that scientists developed over the course of the history of the field, so that the theory was confronted with an seemingly unfair distrust. The most striking of these new phenomena, that have no direct classical counterpart and have kept puzzling the physics community ever since, certainly is the notion of entanglement. For this reason Schrödinger not only listed it as *one* but as *the* most fundamental concept of quantum mechanics.

“When two systems, of which we know the states by their respective representatives, enter into temporary physical interaction due to known forces between them, and when after a time of mutual influence the systems separate again, then they can no longer be described in the same way as before, viz. by endowing each of them with a representative of its own. I would not call that one but rather the characteristic trait of quantum mechanics, the one that enforces its entire departure from classical lines of thought. By the interaction the two representatives [...] have become entangled.”

Now we would like to interpret entanglement as a subjective characteristic of a system. However, we are better off by thinking of it as a state of the system. To use the words of Schrödinger, of a system being entangled.

Nonetheless a certain notion of quantification of entanglement is necessary to make it not only a source of bafflement but a physical characteristic or quantity of a system. Here quantification shall be taken to have the classical meaning of “attaching a number to it”.

In the following we start to introduce the simplest entangled system, the connection of two two-level systems. This is not just a very easily accessible model system but has direct application in quantum information analysis where a two level system is called a qubit, the quantum mechanical equivalent of the classical fundamental unit of signal processing, the bit.

Incidentally two entangled qubits also play a prominent role in the following analysis when we present a way to physically create and stabilize such a system with the help of another fundamental ingredient to the theory of quantum physics, quantum measurement.

## 2.2 Entanglement measures

Having introduced the notion of entanglement, or rather the possibility of quantum systems to be entangled, the direct follow up question comes naturally: Is entanglement quantifiable or is it a dichotomous characteristic of a quantum state. Can it be compared in mathematical treatment to the potential energy of a classical system, that can take any value on a continuous spectrum (that might be bounded). Or is its nature of a more fundamental kind, like charge, in the sense that a particle either is charged or it is not (notwithstanding that a collection of charges can then again be counted).

With this in mind it is necessary first to notice that not all quantum systems are entangled. And in fact it is quite straightforward to come up with unentangled ones. Take for example a system comprised of two subsystems (system one  $|\phi_1\rangle$  and system two  $|\phi_2\rangle$ ) that do not have to have any further characteristics. In the literature, systems of this nature are often referred to as bipartite and we make due use of this term.

The state of the complete system is then the tensor product of both states  $|\psi\rangle = |\phi_1\rangle |\phi_2\rangle$ . Imagine now a measurement of an observable  $A$  of system one. We turn to a more complete theory of quantum measurements in chapter 3 so for now the standard notion of a measurement being connected to an observable and the outcome of a measurement being connected to the corresponding eigenvalue, leaving the system in the eigenstate, does suffice. An operation that measures an observable on system one<sup>1</sup> and does nothing on system two thus casts the complete system into the state  $|\psi'\rangle = |a\rangle |\phi_2\rangle$ .

Now although a measurement was performed and the state of the first system changed (maybe quite dramatically), the second system is untouched and remains in the same state as before the measurement. We may therefore separate both systems and continue to treat them as independent. Any system that has this features is called *separable*. The notation we used ( $|\psi\rangle = |\phi_1\rangle |\phi_2\rangle$ ), that implicitly assumes the (tensor)-product between both states gives rise to another name for the same thing, a *product state*.

---

<sup>1</sup>The measurement operator in this case takes the form  $\sum_a a |a\rangle \langle a|$  leaving the system in an eigenstate  $|a\rangle$  corresponding to the measurement outcome and eigenvalue  $a$ .

As this measurement here takes the role of the forces that Schrödinger imagined to act between the combined system, and we can still separate the systems after the measurement, the total system can not be entangled by the understanding of entanglement we have given so far. This allows for a first definition of entanglement:

**Definition:** A bipartite state  $|\psi\rangle$  is *unentangled* if and only if it is separable.

By this definition we have a means to transfer the somewhat weary description of two systems influencing each other and no longer being able to be called independent to the common mathematical description of a system's state as a state in a Hilbert space. Unentangled states (and for that matter entangled states) are therefore a certain subclass of states in Hilbert space. The definition above is rather unsatisfactory, however, as it allows us to identify some states as being unentangled but does not provide any means for testing a general state as to its entanglement. In particular, just because a separation of a bipartite state *seems* not to be possible, we can not know for sure. We therefore need to dig further to obtain a meaningful definition of entanglement of bipartite systems.

### 2.2.1 Schmidt decomposition

We have introduced the first connection between the loosely defined term “entangled” and the language that is used in quantum mechanics, namely states and Hilbert spaces. To progress further along these lines we need to introduce some formal tools that help dealing with the bipartite systems at hand. Let us introduce here then the *Schmidt decomposition*, a decomposition that will turn out to be of substantial help when dealing with composite systems. Here we loosely follow Ekert et al. [31].

As already introduced we start with two systems  $A$  and  $B$  that are described or associated with the two Hilbert spaces  $H_A$  and  $H_B$ . Without limiting the applicability we limit the treatment to Hilbert spaces of the same dimension  $\dim H_A = \dim H_B = n$ . The composite or total system encompassing both  $A$  and  $B$  is then connected to a Hilbert space formed by the tensor product  $H_A \otimes H_B$ . As both separate Hilbert spaces have their own bases choosing two orthonormal ones  $\{|i\rangle\}$  and  $\{|j\rangle\}$  we can write any state of the composite system as

$$|\psi\rangle = \sum_{i,j} a_{i,j} |i\rangle |j\rangle. \quad (2.2.1)$$

Again the tensor product sign between the two ket vectors is implied. The number of terms in this sum can obviously be up to  $n^2 = \dim^2 H_A$ , the square of the dimension of either part. The aim of the Schmidt decomposition is

now to show that for a suitably chosen basis  $|i'\rangle$  of the second space we can reduce the terms in the expansion to a maximum of  $n$  as

$$|\psi\rangle = \sum_i p_i |i\rangle |i'\rangle. \quad (2.2.2)$$

To prove this we expand the matrix  $(a_{i,j})$  via singular value decomposition  $(a_{i,j}) = UPV^*$ . The properties of the singular value decomposition state that here  $U$  and  $V^*$  are unitary matrices while  $P$  is a diagonal matrix with elements that are non-negative. The state (2.2.1) can therefore be rewritten as

$$\begin{aligned} |\psi\rangle &= \sum_{i,j,k} U_{ik} P_{kk} V_{kj}^* |i\rangle |j\rangle = \sum_k P_{kk} \left( \sum_i U_{ik} |i\rangle \right) \left( \sum_j V_{kj}^* |j\rangle \right) \\ &= \sum_k P_{kk} |k\rangle |k'\rangle. \end{aligned} \quad (2.2.3)$$

As the unitarity of  $U$  and  $V^*$  preserves the nature of the bases  $\{|i\rangle\}$  and  $\{|j\rangle\}$  we recovered the decomposition (2.2.2) where the expansion coefficients  $p_i$  turn out to be the singular values.

The first observation that reveals the use of the Schmidt decomposition in the treatment of entangled bipartite systems springs readily in sight. When there is *only one* singular value (zero valued entries on the diagonal of  $P$  do not constitute singular values) the system clearly is a product state and separable and thus unentangled. The number of non-zero singular values can therefore be a (admittedly rather crude) measure of entanglement in a bipartite system. To give this notion more gravitas the number is also coined the *Schmidt number*. We make note: A bipartite system is entangled if it has a Schmidt number larger than one.

The singular value decomposition therefore constitutes an operational procedure to determine if a bipartite system is entangled or not. We write the state in the Schmidt decomposition and count the number of terms. Any more than one and the state is entangled in some sense of the word.

As the Schmidt decomposition makes use of bases of the two sub-Hilbert spaces  $H_A$  and  $H_B$  it is also of quite some use in the density matrix formalism. The density matrix of our bipartite state (2.2.2) in the basis  $\{|i\rangle |i'\rangle\}$  takes the form

$$\rho = |\psi\rangle \langle\psi| = \sum_{i,j} p_i p_j |i\rangle |i'\rangle \langle j| \langle j'|, \quad (2.2.4)$$

where we remember that the coefficients  $p_j$  are real and non-negative. This density matrix represents the full system. While in the state vector formalism there is no direct way to separate a sub-system from the other, in the case of a density matrix we may trace out any one of the sub-systems and are



then left with a so-called reduced density matrix pertaining to the remaining system. Tracing over the degrees of freedoms of the second we thus arrive at

$$\rho_1 = \text{tr}_2 \rho = \sum_i p_i^2 |i\rangle \langle i|, \quad (2.2.5)$$

as the basis  $\{|i'\rangle\}$  is orthonormal. Again the expansion coefficients of the Schmidt decomposition appear, albeit here as squares. In the present case they constitute the eigenvalue of the reduced density matrix pertaining to the sub-system at hands. As they are non-negative and real the reduced density matrix also uniquely determines these coefficients and we may equally well define the *Schmidt number* as the number of non-zero eigenvalues of the reduced density matrix after tracing out any one sub-system. This method therefore constitutes another operational way of obtaining the Schmidt number of a bipartite system.

To shed a little practical light on the rather theoretical introduction let us take an example bipartite system that is made up of two spin-1/2 particles. In the most general case such a system consists of a linear combination of all spin-up and spin-down combinations

$$|\psi\rangle = \alpha |00\rangle + \beta |01\rangle + \gamma |10\rangle + \delta |11\rangle \quad (2.2.6)$$

where we used the common notation of ones and zeros for spin-up and spin-down particles. The coefficients  $\alpha$  to  $\delta$  are complex so with the restriction of normalization there are seven variables to fill. So let us restrict the current analysis to a simpler set of states, namely

$$|\psi(s)\rangle = \cos(s) |01\rangle - \sin(s) |10\rangle, \quad s \in [0, 2\pi]. \quad (2.2.7)$$

Now for values of  $s$  that are a multiple of  $\pi/2$  the state  $|\psi\rangle$  clearly is a product state where one of the particles is in state spin-up and the other in spin-down. A measurement along the spin axis of any single particle always returns the same outcome in this case. A value of  $s = \pi/4$  constitutes the familiar spin singlet state  $|\text{singlet}\rangle = 1/\sqrt{2}(|01\rangle - |10\rangle)$ , that is obviously not separable. A continuous change of the parameter  $s$  therefore changes the state  $|\psi(s)\rangle$  from an unentangled product state to an entangled singlet. It is remarkable here that *only* the exact multiples of  $\pi/2$  are unentangled states while all other values of  $s$  result in some sort of entangled state. For any (small)  $\varepsilon > 0$  an entangled state  $|\psi(\varepsilon)\rangle$  can be turned into a product state by changing the variable by  $-\varepsilon$ . On the other hand no state around  $s = \pi/4$  can be unentangled by a change of  $-\varepsilon$ .

While the notion of entanglement has until now been treated in a rather dichotomous fashion a notion of distance of an entangled state from the product state emerges readily. The remainder of the section is devoted to finding a formal definition of this heuristic notion of the “amount” of entanglement.

First, however, we calculate the reduced state of the first spin system that is obtained by tracing out the second's degrees of freedom. The full density matrix of state (2.2.7) reads

$$\rho = \begin{pmatrix} 0 & 0 & 0 & 0 \\ 0 & \cos^2(s) & -\sin(s)\cos(s) & 0 \\ 0 & -\sin(s)\cos(s) & \sin^2(s) & 0 \\ 0 & 0 & 0 & 0 \end{pmatrix} \quad (2.2.8)$$

so that the reduced state of the first is given by

$$\rho_1 = \begin{pmatrix} \cos^2(s) & 0 \\ 0 & \sin^2(s) \end{pmatrix} \quad (2.2.9)$$

and as expected we have two non-zero eigenvalues for any entangled state. Here we may notice that a single non-zero eigenvalue, or a Schmidt number of one, corresponds to a pure state of the sub-system while an entangled state corresponds to a mixed state of the subsystem. In particular the singlet state with  $s = \pi/4$ , that we earlier identified heuristically as the farthest away from the unentangled state, here corresponds to the fully mixed state

$$\rho_1(\text{singlet}) = \begin{pmatrix} \frac{1}{2} & 0 \\ 0 & \frac{1}{2} \end{pmatrix}. \quad (2.2.10)$$

In this sense the degree that the density matrix of the subsystems is mixed can be regarded as a measure of the degree of entanglement between the two subsystems. As the mixedness of a density matrix can be quantified by the quantum entropy it is only natural to proceed along these lines to also find a measure of entanglement.

### 2.2.2 von Neumann entropy

We established the connection between an entangled bipartite state and the *mixedness* of the reduced density matrix of the sub-systems. To quantify the degree to which a density matrix can be called mixed we now introduce the notion of quantum entropy in the form of the *von Neumann entropy*  $S$  that is defined via the density matrix  $\rho$  of a state

$$S(\rho) = -\text{tr}(\rho \log_2 \rho). \quad (2.2.11)$$

For normalization purposes we take the logarithm to be of base two here. In the case of a singlet we have calculated the reduced density matrix of a sub-system (2.2.10) so that the entropy reads

$$S(\rho_1) = -\text{tr}(\rho_1 \log_2 \rho_1) = -\sum_i p_i^2 \log_2 p_i^2 = 1. \quad (2.2.12)$$

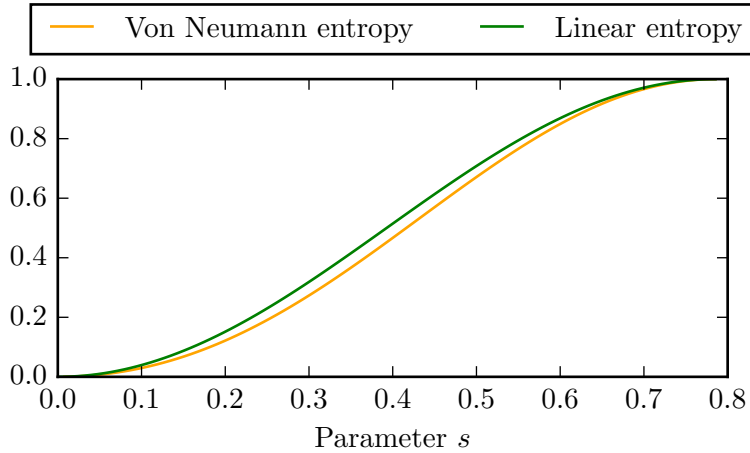


Figure 2.2.1: The entropy of the reduced density matrix that is obtained by tracing over one of the sub-systems of state (2.2.7). It ranges from zero corresponding to a product state to one for a maximally entangled singlet state. Both the von Neumann entropy and its approximation, the linear entropy, are shown.

The last equation also points out that the entropy of any pure density matrix is zero, as it has only one entry on the diagonal, that is unity. The corresponding unentangled state of the bipartite system therefore leads to a vanishing entropy. To visualize this correspondence between entanglement and entropy of the sub-system, the entropy of state (2.2.9) is plotted in figure 2.2.1 with respect to the variable  $s$ . It shows a smooth function that monotonically increases from zero for the product state to one for the singlet. As the von Neumann entropy is bound between zero and one we therefore conclude that indeed the singlet constitutes a maximally entangled state. In the sub-set spanned by the two vectors  $|01\rangle$  and  $|10\rangle$  the von Neumann entropy therefore serves as a measure for the entanglement between the two sub-systems. As it turns out it is indeed a useful measure of entanglement for all bipartite composite systems.

The von Neumann entropy therefore gives an operational measure of entanglement of a bipartite system. However, it does not reveal any insights to the physical nature of entanglement itself. Before we introduce a measure of entanglement that is rooted in such a physical interpretation we draw attention to yet another connection between the von Neumann entropy and the mixedness of the reduced state. Expanding the logarithm in equation (2.2.11) we have

$$S(\rho) \approx \underbrace{1 - \text{tr}\rho^2}_{\text{linear entropy}} + \frac{1}{2} \text{tr}(\rho(\rho - 1)^2). \quad (2.2.13)$$

The first order in this expansion, constituting the first two terms, is called *linear entropy* and we will denote it by  $S_L(\rho)$ . Demanding that the maximally mixed state gives an entropy of one, with the proper normalization we may take this as a measure of entanglement as well. Given this direct correspondence between entanglement and entropy it is easy to mistake both as being the same. If one speaks of the entropy of a system in this context one always means, however, the entropy of the reduced density matrix. Keeping this distinction in mind we may use both terms interchangeably. The linear entropy of our sample state (2.2.7) then gives the corresponding linear entanglement

$$E_L = 2(1 - \text{tr}_A \rho_A^2) = 2(1 - \cos^4(s) - \sin^4(s)) \quad (2.2.14)$$

where  $\rho_A$  denotes the reduced density matrix after tracing out system  $B$ . Both linear and full entropy may therefore serve as a measure of entanglement. As shown in figure 2.2.1 both measures do not fully coincide. This ambiguity is somewhat irritating when thinking of entanglement as a physical property of the system but is rooted in the technical approach to the matter. It turns out, however, that the von Neumann entropy is naturally connected to a more physical interpretation of entanglement, that is connected with the distillation of entanglement.

Coining the term distillation, Bennet et al. [28] devised a method to concentrate entanglement. Concentration here is to be understood in the following way. Imagine a set of  $n$  bipartite states; for simplicity they shall consist of two two-level systems as above. These  $n$  copies of the bipartite states  $|\psi\rangle$  are taken to be partially entangled, meaning that their entanglement entropy is somewhere between one and zero. Each of these states is physically separated in the same way where the first part is taken care of by an agent called Alice and the second by an agent called Bob. As described above, the entanglement of each system is given by the von Neumann entropy  $S$  of its parts.

Bennet et al. now devised a procedure by which from these  $n$  partially entangled bipartite states  $m$  fully entangled singlets can be *distilled* by operations that are done locally by Alice and Bob. Both participants may further communicate classically. Such operations are therefore labeled LOCC, for *local operations and classical communication*.

For a large number of shared states  $n$  the fraction of fully entangled singlets that can be distilled by this procedure approaches the von Neumann entropy  $S$

$$\frac{m}{n} \rightarrow S(|\psi\rangle). \quad (2.2.15)$$

Therefore the entropy of the sub-systems is not only a convenient measure that is operationally accessible. It is also a very natural way to quantify entanglement. In this way the singlet is a basic unit for the quantification of entanglement.

With these ideas we now have a fully applicable system to quantify the entanglement of a bipartite quantum state. This is applicable if the knowledge about the state is complete, in the sense that the state is a *pure* state. If information about the state is incomplete we speak of the system as being in a mixed state. Another way of thinking about mixed states is as an *ensemble* of states; however, it should be always kept in mind that also a single state of a system can be mixed.

We already encountered mixed states arising as the left-over part of a composite state when the other part is traced out. The entanglement between the two parts turns into mixedness of the single system as we have seen. This is yet another way to think of mixed states, where here the missing knowledge is due to the locally invisible connection to a different system, the entanglement.

To complete this introduction to entanglement we now turn to the problem of defining entanglement for a mixed state, so that we are able to treat all possible configurations of bipartite states in the following.

### 2.2.3 Entanglement of formation

The entanglement of pure states of a bipartite system can be naturally described by the von Neumann entropy of its parts. The applicability of this procedure is limited in two ways. Firstly a bipartite state may not be in a pure state but in a mixed state. Secondly a system may have more than two parts, sometimes being described as being multipartite.

The quantification and even the interpretation of entanglement in a composite system consisting of more than two parts is an open field of discussion and research [32, 33].

Here we limit the presentation to mixed bipartite states. The entanglement of low-dimensional bipartite systems, such as a two qubit system, has been well understood and documented [34]. As the present work is concerned with exactly such a system, composed of two qubits, we limit the presentation to such systems. While several approaches exist, we here present one that is connected to the physical interpretation of entanglement given above, the connection between the von Neumann entropy and the distillation of entanglement.

As mentioned in the previous section a set of partially entangled states can be used to create a subset of fully entangled singlets by a procedure called entanglement distillation. As this process is reversible, with the given number of singlets an ensemble of partially entangled states can be created as well, again by only using local operations and classical communication. The final state here is a pure state. With the singlet as the basic unit of entanglement the number of singlets needed to form the desired ensemble can therefore be thought of as the amount of entanglement that is needed to form such an ensemble. This notion of entanglement -as a quantity that's

inserted into an ensemble to create it- gives rise to the name *entanglement of formation* [35]. This concept can be used to quantify the entanglement of mixed states.

To understand the usefulness and need of these concepts let us see how the entanglement of a mixed state may be calculated. A mixed state  $\rho$  can be thought of as an ensemble of pure states, each pure state composing a certain fraction of the ensemble

$$\rho = \sum_i p_i |\psi_i\rangle \langle \psi_i|. \quad (2.2.16)$$

Knowing the procedure for quantification of entanglement of a pure state we may calculate the entropy for every term in the sum  $E(|\psi_i\rangle)$ . Now this entanglement equals to the fraction  $n/m$  of  $n$  singlets that are needed to create  $m$  copies of the state  $|\psi_i\rangle$

$$n_i = m_i E(|\psi_i\rangle). \quad (2.2.17)$$

Equivalently we need

$$\frac{n_i p_i}{m_i} = p_i E(|\psi_i\rangle) \quad (2.2.18)$$

singlets to create the fraction  $p_i$  of states  $|\psi_i\rangle$ . The total number of singlets to create an ensemble of pure states, each represented by a fraction  $p_i$ , is therefore

$$\text{total \# singlet} = \sum_i p_i E(|\psi_i\rangle). \quad (2.2.19)$$

As in this ensemble each state  $|\psi_i\rangle$  is represented by a fraction  $p_i$ , this also gives the probability to end up with the state  $|\psi_i\rangle$  when drawing a random state from the ensemble. In other words we have thus created an ensemble that exactly corresponds to the mixed state  $\rho$  of equation (2.2.16).

Dividing the total number of singlets necessary for this creation (2.2.19) by the total number of created states

$$\text{total \# states} = \sum_i m_i \quad (2.2.20)$$

gives a measure for the entanglement that was needed in the formation. The keen eye immediately spots a problem with this approach, however. The expansion (2.2.16) is not uniquely defined. For example, the state

$$\rho = \frac{1}{2} (|00\rangle \langle 00| + |11\rangle \langle 11|) \quad (2.2.21)$$

is clearly a mixture of separable pure states and should therefore not be considered entangled. No singlet therefore is needed in the creation of such a state. But the ambiguity of expansion allows for a different form to express this state:

$$\rho = \frac{1}{2} [(|00\rangle + |11\rangle)(\langle 00| + \langle 11|) + (|00\rangle - |11\rangle)(\langle 00| - \langle 11|)] \quad (2.2.22)$$

using two states that are fully entangled (the states used are part of the three triplet states). As every pure state in this expansion is entangled we have to conclude that also their weighted sum is entangled. In this case it seems that we have to spend singlets to create such a state. As the final state is the same, however, and nature should not be bothered by the specific notation, we conclude that we *could* spend singlets in the formation of such state but we *don't have to*. Including these thoughts in the analysis amounts to defining

$$E(\rho) = \min \sum_i p_i E(|\psi_i\rangle). \quad (2.2.23)$$

The entanglement of a mixed state shall be the minimum of all possible expansions (2.2.16).

While physically this is satisfactory, as it again defines entanglement as the amount of singlets needed to create the entangled state, we can not rejoice unrestrictedly as again we are left with a definition that does not permit easy calculation. Calculating the entanglement of *all* possible expansions is hardly a convenient method.

If we give up the physicality of entropy as a measure of entanglement we may, however, turn to the *entanglement concurrence* as a way to quantify entanglement of mixed states via an operational procedure.

#### 2.2.4 Entanglement concurrence

The introduction of entanglement of formation as a measure of entanglement of mixed states came naturally through the interpretation of entanglement already used for pure states. However, it lacked an operationally feasible procedure. Hill and Wothers [36, 37] devised a method to calculate the entanglement of formation of a two qubit system using a quantity that has little physical interpretation but is closely connected to the entanglement of formation. They coined the term *concurrence*. The entanglement concurrence can be calculated by standard operations on the composite state. We present here the method for a general two qubit system  $\rho$ .

1. Given the state  $\rho$  calculate the so called spin-flipped state.

$$\tilde{\rho} = (\sigma_y \otimes \sigma_y) \rho^* (\sigma_y \otimes \sigma_y),$$

where  $\rho^*$  is the complex conjugate of  $\rho$  in the standard basis and  $\sigma_y$  is the second Pauli matrix.

2. Calculate the eigenvalues  $\mu_i$  of the product  $\rho\tilde{\rho}$ .

3. Calculate the square-roots of these eigenvalues,  $\lambda_i = \sqrt{\mu_i}$ .
4. The concurrence  $C$  is then defined as

$$C(\rho) = \max\left(0, \lambda_1 - \sum_{i=2}^4 \lambda_i\right), \quad (2.2.24)$$

where  $\lambda_1$  is the maximum of  $\{\lambda_i\}$ .

The concurrence is a monotonically increasing function between zero and one, zero denoting a separable state and no entanglement and one for a fully entangled state that incidentally has to be pure. As such it is suited to serve as a measure for entanglement in its own right.

However, as mentioned above, the concurrence is also connected to the entanglement of formation  $E(\rho)$ , the formula being

$$E(\rho) = H\left(\frac{1 + \sqrt{1 - C^2}}{2}\right), \quad (2.2.25)$$

with the function  $H(x) = -x \log_2 x - (1 - x) \log_2 (1 - x)$ .

In this short introduction to quantum entanglement we have now presented physical interpretations of entanglement and operational methods for its quantification for both pure and mixed two qubit systems. Next we turn to another fundamental topic of quantum theory, the measurement.



## Chapter 3

# Quantum measurements

In the previous chapter quantum entanglement was introduced as probably *the essence* of quantum theory. A close runner up in this category are quantum measurements. In the present chapter we therefore introduce the mathematical background of the measurement process in quantum theory. While in this case there is of course an analogous classical concept of a measurement, the nuances introduced by quantum theory are at the same time subtle and fundamental. To emphasize this novelty we introduce quantum measurement on a similarly formal basis as quantum entanglement.

### 3.1 General measurements

Fundamentally, a measurement in quantum theory is a change of state that results in a certain gain of information. The particularity of this change of state is so fundamental to quantum theory that in an axiomatic formulation of quantum mechanics the measurement process is introduced as a postulate. We quote the measurement postulate here from Nielsen and Chuang [38]

#### Measurement postulate

“Quantum measurements are described by a collection  $\{M_m\}$  of *measurement operators*. These are operators acting on the state space of the system being measured. The index  $m$  refers to the measurement outcomes that may occur in the experiment. If the state of the quantum system is  $|\psi\rangle$  immediately before the measurement then the probability that result  $m$  occurs is given by

$$p(m) = \langle \psi | M_m^\dagger M_m | \psi \rangle, \quad (3.1.1)$$

and the state after the measurement is

$$\frac{M_m |\psi\rangle}{\sqrt{\langle \psi | M_m^\dagger M_m | \psi \rangle}}. \quad (3.1.2)$$

The measurement operators satisfy the *completeness relation*,

$$\sum_m M_m^\dagger M_m = \mathbb{1}. \quad (3.1.3)$$

The measurement postulate provides us with a formalism that can be applied to any measurement. We therefore use the term *general measurement* to refer to such a collection  $\{M_m\}$  of measurement operators.

### 3.1.1 Projective measurements

While an axiomatic basis is welcome to bolster the theoretical construct quantum theory is build on, it is somewhat hard to relate to. Even a formal introduction to quantum theory tends to skip the formalism of general measurements and introduces a related concept instead, the *projective measurement*. Here we introduce projective measurements as a subset of general measurements.

In the previous section we introduced general measurement as a set of operators  $\{M_m\}$  acting on a state  $|\psi\rangle$  with properties (3.1.2) and (3.1.3). Imagine now two subsequent measurements of the same kind. The first  $M_m$  with outcome  $m$  leaves the system in the state  $|\psi'\rangle = M_m |\psi\rangle / p(m)$ . Measuring this resulting state again, this time with the outcome  $m'$ , yields

$$|\psi''\rangle = \frac{M_{m'}}{\sqrt{p'(m')}} |\psi'\rangle = \frac{M_{m'}}{\sqrt{p'(m')}} \frac{M_m}{\sqrt{p(m)}} |\psi\rangle \quad (3.1.4)$$

where the probability for the second measurement outcome  $m'$  has to be updated to take the form

$$p'(m') = \langle \psi' | M_{m'}^\dagger M_{m'} | \psi' \rangle. \quad (3.1.5)$$

Up to now these are just two general measurements performed one after the other. We now make an important assumption about the set of measurement operators  $\{M_m\}$ . On the one hand we take them to be hermitian, so  $M_m^\dagger = M_m$ . And on the other hand we take them to form an orthogonal set

$$M_{m'} M_m = \delta_{mm'} M_m. \quad (3.1.6)$$

This immediately results in a drastic simplification of the second measurement. The outcome probability now reduces to

$$p'(m') = \begin{cases} 1 & m = m' \\ 0 & \text{else} \end{cases} \quad (3.1.7)$$

so that the result of the second measurement is already determined by the outcome of the first. From a classical viewpoint this seems rather unpectacular. Performing a measurement on the same system twice should better

return the same outcome twice. And once the system is determined by the first measurement the second has no choice but to concur.

The quantum world, however, generally leaves open a door for ambiguity even in such a seemingly clear cut case. The simplest case is measuring the spin of a particle. Let the first measurement, say along the  $\hat{z}$ -axis, determine the spin to be pointing upwards along that axis. A second measurement along another axis, for instance pointing along  $\hat{x}$ -axis is again completely undetermined.

In the present case not only is the result of the second measurement determined by the first, but also the state is not affected by the second measurement,  $|\psi''\rangle = |\psi'\rangle$ . We may therefore think of the initial state *collapsing* into a state  $|\psi_m\rangle$  with the outcome  $m$  and refusing to change afterwards. This final state also only depends on the measurement outcome and not on the initial state. Mathematically the system's state is *projected* onto a final state, so that we speak of *projective measurements* and introduce the corresponding *projection operators*  $\Pi$ .

The projection onto a state  $|\psi_m\rangle$  is given by  $\Pi_m = |\psi_m\rangle\langle\psi_m|$ . This already hints to a close relation between projections and observables. Remembering that observables of a system are represented by hermitian operators  $\hat{O}$ . We use the spectral decomposition to write

$$\hat{O} = \sum_m m |m\rangle\langle m| = \sum_m m \Pi_m, \quad (3.1.8)$$

where the projection operators involve the eigenstates of the observable. Notice also that the set of projection operators  $\{\Pi_m\}$  satisfies the restrictive assumptions we made about measuring operators in this section. As they are related to the eigenstates of an observable they are automatically mutually orthogonal. And as the observable is hermitian also the projection operators are.

We have therefore found that projective measurements in the usual formulation known from introductory quantum mechanics classes are a subset of general measurements. Their intimate relation to observables of the system makes them natural to use. Also, projective measurements can be applied to a vast variety of physical measuring processes. However, there are a number of important experimental setups where projective measurements fail to provide the necessary formalism. For instance a projection is always connected to the same Hilbert space and cannot be used in contexts where particles are created or destroyed.

Consider for example the measurement of a photon. Measuring the photon itself necessarily leads to its destruction, the resulting state is the vacuum. It is hardly of any sense to try to measure the vanished photon again and of even less sense to expect the same result as before. A projective measurement may be thought of as collapsing the state to the vacuum in

this case. But the repeatability of projective measurements that was a key ingredient to the formulation is lost in this interpretation.

We conclude therefore that projective measurements are, due to their straightforward mathematical applicability, convenient where they can be used. But they have to be supplemented by the formalism of general measurements to be able to treat all physical measurement processes.

### 3.1.2 General measurements as projections

In the previous section projective measurements were introduced. As always in mathematical formulations, the orthogonality of these projective measurements provides a considerably easier treatment of the measurement process. On the other hand the connection to a measurement result, as just the eigenvalue of an observable in the final eigenstate the system collapses upon, admitted the most painless approach to this unintuitive matter.

However, it was pointed out that projective measurements cannot be applied to all experimental setups and general measurements have to be kept around. This statement can be softened somewhat [38]. Projective measurements are a sub-set of general measurements in the same Hilbert space, so that an expansion of the set of measurement operators generalizes from projective to general measurements. We now proceed in the different direction and show that every general measurement can be performed with projective measurements, albeit now on an enlarged Hilbert space. So from projective to general measurements we therefore extended the set of measurement operators and from general to projective measurements we extend the dimension of Hilbert space.

A general measurement was defined as a set of operators acting on a state in some Hilbert space. Let this state be labeled by  $|\psi\rangle$  and the encompassing Hilbert space by  $H$ . The measurement operators shall again be called  $\{M_m\}$ . We have seen that this set of measurement operators can not be represented by projective operators in the same Hilbert space  $H$ , so the idea is to enlarge the space the projections operate on. Take therefore a separate Hilbert space of dimension  $n$  that we call  $V$ . This Hilbert space is spanned by a basis and as there are as many basis vectors as dimensions each basis vector can be labeled in correspondence with a measurement operator so that we denote this basis of  $V$  as  $\{|m\rangle\}$ . Up to now this extra space has only auxiliary status so that it is often called *ancilla*. In the proceedings we will discover, however, that a physical interpretation can be attached to this ancilla. In the same way as the system is in an initial state  $|\psi\rangle$  we assume the ancilla to be in some specific state  $|\phi\rangle$ . With these prerequisites we define an operator  $U$  that acts on a state of Hilbert space  $H$  only

$$U |\psi\rangle = \sum_m M_m \otimes \mathbb{1}_V |\psi\rangle |\phi\rangle. \quad (3.1.9)$$

Here the tensor product between both states is implicitly assumed. This operator defines a map  $U : H \rightarrow H \otimes V$  that preserves the inner product

$$\begin{aligned} \langle \psi' | U^\dagger U | \psi \rangle &= \sum_{mm'} \langle \psi' | \langle m' | \left( M_{m'}^\dagger \otimes \mathbb{1}_V \right) (M_m \otimes \mathbb{1}_V) | \psi \rangle | m \rangle \\ &= \sum_{mm'} \langle \psi' | M_{m'}^\dagger M_m | \psi \rangle \langle m' | m \rangle \\ &= \sum_m \langle \psi' | M_m^\dagger M_m | \psi \rangle = \langle \psi' | \psi \rangle \end{aligned} \quad (3.1.10)$$

of the space  $H$ , where we have used the completeness of the set of measurement operators in the last equality. While  $U$  in this definition is taking a state from space  $H$  to the enlarged space  $H \otimes V$  we can extend the operation to be a unitary endomorphism on the space  $H \otimes V$ . We continue to denote this operation as  $U$  because the actions on  $H$  coincide and therefore both can not be distinguished.

Consider now an action that is complementary to the previously defined, acting only on the ancilla and leaving the space  $H$  untouched. In particular the action on the ancilla shall be a projection, as anticipated. A thus enhanced projection operator takes the form

$$\Pi_m = \mathbb{1}_H \otimes |m\rangle \langle m|. \quad (3.1.11)$$

This projection can be applied<sup>1</sup> to the evolved composite state  $U |\psi\rangle |\phi\rangle$  so that we have

$$|\Psi\rangle = U |\psi\rangle |\phi\rangle \rightarrow |\Psi'\rangle = \frac{\Pi_m}{p(m)} U |\psi\rangle |\phi\rangle, \quad (3.1.12)$$

where we introduced

$$\begin{aligned} p(m) &= \langle \psi | \langle \phi | U^\dagger \Pi_m U | \psi \rangle | \phi \rangle \\ &= \sum_{m'm''} \langle \psi | U_{m''}^\dagger U_{m'} | \psi \rangle \langle m'' | m \rangle \langle m | m' \rangle \\ &= \langle \psi | U_m^\dagger U_m | \psi \rangle \end{aligned} \quad (3.1.13)$$

which turns out to be exactly the probability (3.1.1) connected to the measurement outcome  $m$  of the general measurement  $\{M_m\}$ . The resulting state after the projection (3.1.12) then takes the form

$$|\Psi'\rangle = \frac{\Pi_m}{\langle \psi | U_m^\dagger U_m | \psi \rangle} U |\psi\rangle |\phi\rangle = \frac{M_m |\psi\rangle}{\underbrace{\langle \psi | U_m^\dagger U_m | \psi \rangle}_{\text{system}}} |m\rangle. \quad (3.1.14)$$

<sup>1</sup>When applying a projection it is common to emphasize the non unitary nature of the operation by connecting initial and final state by an arrow.

As suggested in the last equality the resulting state is a product state. The part of the system is in a state that coincides with the resulting state of a general measurement in the original Hilbert space  $H$  as defined in (3.1.2). And the probability of the resulting state is connected to the measurement operator  $M_m$  and thus to the measurement outcome  $m$ . It is again exactly the postulated probability (3.1.1). Both operations  $U$  and  $\Pi_m$  were defined only by the general measurement operators  $\{M_m\}$ . We have therefore presented how projectively measuring an auxiliary system that is artificially introduced can mimic general measurement on the original system. This may seem to be of rather academic use but notice the resulting state of the ancilla. It is exactly in the basis state that corresponds to the measurement outcome  $|m\rangle$  so that by observing the ancilla and determining its state all necessary information about the original system can be obtained.

This notion of using an auxiliary system to gain information about an otherwise inaccessible system is at the core of every scientific process. Usually the ancilla is then called a detector or measurement device. In the next section we expand this interpretation to give a physical description of the measurement process with the help of an auxiliary system.

## 3.2 Von Neumann measurements

In the previous introduction to quantum measurements we focussed on a rather mathematical formulation of the matter. This technical approach is indeed quite useful to begin with, as one is less tempted to mix mathematical postulates of quantum theory and a mental picture of physical processes. Without being restricted by descriptive thinking one can make use of the powerful machinery of the mathematical formulation to create a solid foundation of quantum theory.

Once this objective is achieved, however, the need to bridge the mathematical and the physical world becomes more urgent. Peres succinctly phrased it as

“Quantum phenomena do not occur in a Hilbert space. They occur in a laboratory.”

A. Peres

The first mathematical description of the newly developed quantum theory was given by von Neumann in his groundbreaking treatise “*Mathematische Grundlagen der Quantenmechanik*.” [39]. Even at this early stage von Neumann tried to give not just a physical interpretation of the measurement process but also developed a formulation according to such a physical interpretation. He introduced a second system that served as a detector. This detector should be thought of as an intermediary between the quantum world

of a Hilbert space and the every-day world of a laboratory, with all the devices that physicists use. In this sense the detector should be describable by a Hamiltonian on the one hand and have a (quasi)-classical state on the other.

Take an isolated system with Hamiltonian  $H_0$  that is in a known state  $|\psi\rangle$ . The measurement is connected to an observable with the hermitian operator  $\hat{A}$  that acts on the system state. We may thus write the system state in the eigenbasis of the measurement observable

$$|\psi\rangle = \sum_a \alpha_a |a\rangle, \quad (3.2.1)$$

where  $\hat{A}|a\rangle = a|a\rangle$  and  $\alpha_a = \langle a|\psi\rangle$ , or in other words  $a$  is the eigenvalue pertaining to the eigenstate  $|a\rangle$  and  $\alpha_a$  the overlap of the system state and the eigenstate  $|a\rangle$ . The measuring device on the other hand was said to be of such fashion that it could be “read out” by the physicist operating the laboratory. To this end it is modeled as a many-body system with a single degree of freedom, in this case taken to be position in space.

When both systems, the state to be measured and the measuring device, are brought into close vicinity they interact and evolve together. For a Hamiltonian that is continuous in time the evolution of the composite system is unitary and the common Hamiltonian is taken to be

$$\begin{aligned} H(t) &= H_0 + H_{\text{detector}} + H_{\text{int}} \\ &= H_0 + \frac{\hat{p}^2}{2m} + \lambda g(t) \hat{A} \otimes \hat{p}. \end{aligned} \quad (3.2.2)$$

To first order the Hamiltonian is therefore split into a system Hamiltonian  $H_0$  that can be time-dependent in principle, a detector Hamiltonian  $H_{\text{detector}}$  and the interaction Hamiltonian  $H_{\text{int}}$ . Notice that in this formulation all Hamiltonians act on the composite Hilbert space of system and detector but  $H_0$  and  $H_{\text{detector}}$  only concern the degrees of freedom of system and detector, respectively. Whenever the dimensionality of an operator seems to be amiss we shall read it amended with the fitting tensor product. So in equation (3.2.2) the first term in fact reads  $H_0 \otimes \mathbb{1}_{\text{detector}}$ . For the sake of clarity the above notation of equation (3.2.2) is used when no ambiguity demands otherwise. As we are only interested in a physical description of the measurement process, we ignore the inherent evolution of the measurement device and take  $H_{\text{detector}} = 0$ , having a comparatively heavy device in mind.

The whole measurement process is governed by the interaction Hamiltonian  $H_{\text{int}}$  that couples the two Hilbert spaces. Its particular effect is to connect the observable  $\hat{A}$  with the degree of freedom of the detector. The Hamiltonian is supplemented with a parameter  $\lambda$  to denote the interaction strength and a time dependence  $g(t)$  with compact support that starts at  $t = 0$  and ends at the measurement time  $\tau_m$ .

In general, an observable may have an intrinsic time-dependence and could thus evolve during the measurement process. Here we assume that the time-scales of observable and measurement process can be separated so that we have  $[H_0, \hat{A}] = 0$  while the measurements lasts. In the interaction picture [40] the evolution of the composite state of system and detector under the measurement is due to the evolution operator

$$\begin{aligned} U(t) &= \exp \left[ -\frac{i}{\hbar} \int_0^t dt' H_{\text{int}} \right] = \exp \left[ -\frac{i\lambda}{\hbar} \int_0^t dt' g(t') \hat{A} \otimes \hat{p} \right] \\ &= \exp \left[ -\frac{i\lambda}{\hbar} \hat{A} \otimes \hat{p} \right], \end{aligned} \quad (3.2.3)$$

if the time  $t$  is to be taken after the measurement time  $\tau_m$ . With the spectral decomposition of the observable

$$\hat{A} = \sum_a |a\rangle a \langle a| \quad (3.2.4)$$

the evolution operator then takes the form

$$U(t) = \sum_a |a\rangle \exp \left[ -\frac{i\lambda a}{\hbar} \hat{p} \right] \langle a|. \quad (3.2.5)$$

Having understood how the composite system evolves under the measurement process we need a quantum mechanical description of the measurement device. As the detector is modeled as a single degree of freedom, the quantum mechanical uncertainty suggests to view it as a (gaussian) wave packet in position space. Taken its expectation value to be  $x_0$  initially, the whole composite system takes the form  $|\Psi\rangle = |\psi\rangle \otimes |\phi(x_0)\rangle$  and evolves under the evolution operator (3.2.5)

$$\begin{aligned} |\Psi(t)\rangle &= U(t) |\psi\rangle \otimes |\phi(x_0)\rangle \\ &= \sum_a |a\rangle \exp \left[ -\frac{i\lambda a}{\hbar} \hat{p} \right] \langle a| \left( \sum_{a'} \alpha_{a'} |a'\rangle \otimes |\phi(x_0)\rangle \right) \\ &= \sum_a \exp \left[ -\frac{i\lambda a}{\hbar} \hat{p} \right] \alpha_a |a\rangle \otimes |\phi(x_0)\rangle. \end{aligned} \quad (3.2.6)$$

As  $\hat{p}$  acts on the detector space and serves as a generator of translation it shifts every wave packet in the sum by  $\lambda a$

$$|\Psi(t)\rangle = \sum_a \alpha_a |a\rangle \otimes |\phi(x_0 - \lambda a)\rangle. \quad (3.2.7)$$

Due to the common evolution the system and the detector have therefore become entangled. The end of the measurement process amounts to removing



the detector from the vicinity of the measured system so that any further interaction between system and measurement device is due to the entangled nature of the composite state.

Once the device is separated from the system the next step can be taken, that is the “reading out” of the detector. If the system is traced out, the detector is in a mixed state while unobserved. When we now imagine the laboratory assistant taking a look at the detector to determine its precise location the result is a collapse of its wave function to the eigenstate corresponding to the observed location. Here the attentive reader might feel cheated as we began the section with the promise of a mathematical description of the physical process. Only to now somehow have shifted the magical measurement from the measured system to a different system called “measuring device”. And the final step from quantum state to classical measurement result, the crux of the whole formalism, is muffled into the coy words “reading out”. Fundamentally this objection is correct and the reason why the measurement postulate is indeed a postulate of quantum theory. It can not be circumvented.

However, all is not lost. We might not have at hand a formalism that sheds light on the measurement postulate itself, but the above description did separate the measured system from the measurement process. We are now free to make some assumptions about the measurement device to help the interpretation. For example we take it to be quasi-classical and therefore possessing quantum and classical features. All these assumptions do not concern the measured system and are therefore in a certain sense universal.

To proceed with the formalism we therefore have to put “reading out” of the measurement device into quantum language. This brings us back to the projection of a state onto an eigenstate with the corresponding eigenvalue as measurement result. Observing the device at position  $\bar{q}$  therefore projects the state (collapses the wave function) onto state  $|\bar{q}\rangle$ . The corresponding projection operator that only operates on the detector space is

$$\Pi_{\bar{q}} = \mathbb{1}_{\psi} \otimes \frac{|\bar{q}\rangle \langle \bar{q}|}{\sqrt{p(\bar{q})}}, \quad (3.2.8)$$

with the probability  $p(\bar{q})$  of a certain detector outcome  $\bar{q}$ . To apply the projection onto the detector state we write  $|\phi(x_0 - \lambda a)\rangle$  as a Gaussian wave packet as discussed above. To ease notation we assume the detector to be initially centered at  $x_0 = 0$ :

$$\begin{aligned} \Pi_{\bar{q}} |\Psi\rangle &= \sum_a \alpha_a |a\rangle \otimes \frac{1}{(\pi\Delta^2)^{\frac{1}{4}}} \int dq \exp\left[-\frac{(q - \lambda a)^2}{2\Delta^2}\right] |q\rangle \\ &= \frac{1}{(\pi\Delta^2)^{\frac{1}{4}} \sqrt{p(\bar{q})}} \sum_a \alpha_a \exp\left[-\frac{(\bar{q} - \lambda a)^2}{2\Delta^2}\right] |a\rangle \otimes |\bar{q}\rangle \\ &= |\Psi'(\bar{q})\rangle \otimes |\bar{q}\rangle, \end{aligned} \quad (3.2.9)$$

where the width of the Gaussian wave packet is given by its standard deviation  $\Delta$ . The final state of system and detector (3.2.9) is obviously a product state so that system and measurement device can henceforth be regarded as separate. The system is now in a superposition similar to the initial state (3.2.1) only that now the eigenstates are additionally weighted by an exponential factor depending on the measurement outcome  $\bar{q}$ . Furthermore, the probability distribution of the measurement outcome is linked to the initial state via the spectral decomposition

$$p(\bar{q}) = \text{tr}(\Pi_{\bar{q}}|\Psi\rangle\langle\Psi|) = \frac{1}{\sqrt{\pi\Delta^2}} \sum_a |\alpha_a|^2 \exp\left[-\frac{(q-\lambda a)^2}{\Delta^2}\right]. \quad (3.2.10)$$

Using the probability distribution of  $\bar{q}$  to calculate the expectation value of the measurement device's position after the measurement we notice that it is connected to the expectation value of the observable  $\hat{A}$  via

$$\langle\bar{q}\rangle = \int d\bar{q} \bar{q} p(\bar{q}) = \lambda \langle\hat{A}\rangle. \quad (3.2.11)$$

It is only through this relation that the information we obtain from reading out the detector reveals information about the initial state of the system. A single measurement is bound to give no information about the measured system due to the stochastic nature of quantum measurement processes. Repeating the above procedure on many copies of a system in the initial state  $|\psi\rangle$  the resulting detector outcomes  $\bar{q}$  spread according to the probability distribution (3.2.10) and we may determine the average, that coincides with the expectation value, with increasing precision.

### 3.2.1 Measurement strength

There are two parameters left undefined in the above formalism. On the one hand we introduced an interaction strength  $\lambda$  that was already named measurement strength and on the other hand the Gaussian wave packet that is used to describe the quantum state of the measurement device prior to the measurement has a width  $\Delta$ . Indeed both parameters are related to the strength of the measurement. Here the measurement strength should be understood as the impact the measurement has on the measured system, in other words, the strength of the back-action. After the detector is removed we have seen the system to be in the final state

$$|\psi'(\bar{q})\rangle \propto \sum_a \alpha_a \exp\left[-\frac{(\bar{q}-\lambda a)^2}{2\Delta^2}\right] |a\rangle. \quad (3.2.12)$$

In the strong measurement limit  $\lambda\Delta a \gg \Delta^2$  for any measurement result  $\bar{q}$  only one exponential factor is non-zero. The resulting state therefore is the corresponding eigenstate  $|a\rangle$ . The measurement of the observable  $\hat{A}$  leads to a collapse of the systems state onto one of the eigenstates of  $\hat{A}$ : We have described a projective measurement.

In the opposite case of a weak measurement, characterized by the width of the Gaussian peaks in (3.2.10) greatly exceeding their separation  $\Delta \gg \lambda\Delta a$ , the exponentials in the final state (3.2.12) have approximately the same value so that the change to the state is negligible. The measurement therefore has no (or a very small) effect on the system.

Another useful way to think about the relation between  $\lambda$  and  $\Delta$  is from the point of view of the measurement device. The measurement strength  $\lambda$  relates the expectation value of the measured observable with the shift of the position of the detector (3.2.11). All things equal the measurement of two states with a different expectation value for  $\hat{A}$  cause a different average shift of the detector. The measurement strength  $\lambda$  is therefore amplifying the difference of both states by translating it into a large shift of detector expectation value. This larger shift, however, has to be put in relation to the general uncertainty of the detector position, here given by the width of its wave packet  $\Delta$ . If the measurement of two states with different expectation values for an observable results in a detector shift clearly discernible despite the positional uncertainty we speak of a strong measurement. Or in this context of a measurement strong enough to distinguish both states.

### 3.3 Continuous measurements

In the previously presented formalism the duration of the measurement was not taken into account. We assumed that the measurement device was brought into contact with the system, the composite system evolved, and the measurement device was read out, all within a timeframe that was taken to be short compared to any dynamic of the system. The result of the measurement was a single point in space, the position of the detector after the measurement. In practice, however, most measuring devices return constant information about the measured system, think of an Ampere-meter for instance.

Therefore we present here a treatment of a continuous measurement of a two level system [41, 42]. We model this two level system as a double quantum dot that is occupied by an electron.<sup>3</sup> The electron occupying each of the dots represents the basis states  $|0\rangle$  and  $|1\rangle$ . The system is placed

---

<sup>2</sup>Here  $\Delta a$  is the maximum distance between two consecutive eigenvalues. This distance has to be small compared to the width of the gaussian distributions, so that the distributions are overlapping strongly.

<sup>3</sup>Incidentally this system is of academic interest, but is also used in the application of the following chapter.

in the vicinity of a low transmission quantum point contact (QPC) with a current  $I(t)$  flowing through. The potential of the tunnel junction is modulated by the occupational state of the quantum double dot, so that the resulting current carries information about the two level system. In this sense the tunnel junction is a detector with the continuous measurement result  $I(t)$ .

The composite system is governed by the second-quantized Hamiltonian,

$$H = H_{\text{DD}} + H_{\text{QPC}} + H_{\text{int}} \quad (3.3.1)$$

with the double dot Hamiltonian  $H_{\text{DD}} = \frac{\varepsilon}{2} (c_1^\dagger c_1 - c_0^\dagger c_0) + \Delta (c_1^\dagger c_0 + c_0^\dagger c_1)$ , where  $c_i$  ( $c_i^\dagger$ ) is the annihilation (creation) operator for the qubit state  $|i\rangle$ . Both states are therefore separated by an energy splitting  $\varepsilon$  while the second part allows for tunneling between both operational states. In the following we first ignore this tunneling to later include it in the formalism. The quantum point contact is modeled by two reservoirs with tunneling between them,  $H_{\text{QPC}} = \sum_r E_r a_r^\dagger a_r + \sum_l E_l a_l^\dagger a_l + \sum_{r,l} T (a_r^\dagger a_l + a_l^\dagger a_r)$ . The interaction between double dot and quantum point contact then is the modulated tunneling based on the occupational state of the double dot  $H_{\text{int}} = \sum_{r,l} \Delta T c_1^\dagger c_1 (a_r^\dagger a_l + a_l^\dagger a_r)$ . The tunneling between the leads has an amplitude of  $T$ , if the electron occupies state  $|0\rangle$ , and an amplitude  $T + \Delta T$  when occupying state  $|1\rangle$ . This difference in tunneling amplitude translates into different average currents

$$I_0 = 2\pi T^2 \rho_r \rho_l \frac{e^2 V}{\hbar} \quad (3.3.2)$$

$$I_1 = 2\pi (T + \Delta T)^2 \rho_r \rho_l \frac{e^2 V}{\hbar} = I_0 + \Delta I \quad (3.3.3)$$

where  $\rho_i$  is the density of states in the  $i$ -lead and  $V$  the bias voltage across the junction.

To describe the continuous nature of the measurement we assume that information gain is low and therefore the back-action on the double dot system due to the measurement is also low. In other words it takes a long time until the measurement result is conclusive and the double dot state collapses to one of the operational states. Many electrons should therefore pass through the tunneling junction so that we can average over timespans that allow for interpretation of a passing current.

For the resulting current this assumption amounts to a current difference between the two states that is small compared to the average current

$$\Delta I = I_1 - I_0 \ll \bar{I} \equiv \frac{I_0 + I_1}{2}. \quad (3.3.4)$$

If the information of the detector current is discarded the tunneling junction is nothing more than an environment of the double dot system that leads to

decoherence of the double dot state. A pure state therefore loses coherence at the rate[42]

$$\Gamma_d = \frac{(\sqrt{I_0} - \sqrt{I_1})^2}{2e} \approx \frac{(\Delta I)^2}{8e\bar{I}} = \frac{(\Delta I)^2}{4S_I} \quad (3.3.5)$$

where  $S_I = 2eI$  is the Schottky shot noise of the tunneling junction. If the intrinsic evolution of the double dot is set aside, the density matrix of the measured system therefore only loses its coherence and thus

$$\rho(t) = \begin{pmatrix} \rho_{00} & \rho_{01}e^{-\Gamma_d t} \\ \rho_{10}e^{-\Gamma_d t} & \rho_{11} \end{pmatrix}. \quad (3.3.6)$$

When the measurement result is, however, not discarded but recorded we must use the gained information to infer the evolution of the measured system. In the classical case where there is no tunneling between the two states ( $\Delta = 0$ ) the occupation has a purely probabilistic nature. The diagonal entries of the density matrix reflect the probabilistic knowledge about the system while the off-diagonal terms are zero. This situation amounts to the electron decisively occupying one of the states, although, we do *not know* which state it is. The situation is classical in the sense that while the state of the system is unknown to the observer, it is not in principle unknowable.

Now the current  $I(t)$  is a highly fluctuating quantity and as a measurement result we therefore use the time averaged current over the measurement time  $\tau$ . Assuming this time is long enough to encompass many electrons passing the tunneling junction we have

$$\langle I \rangle = \frac{1}{\tau} \int_0^\tau dt I(t). \quad (3.3.7)$$

This averaged current serves as the measurement output at any given time. Assume now the electron is occupying the lower dot. The probability distribution for an outcome  $\langle I \rangle$  thus is

$$P_0(\langle I \rangle, \tau) = \frac{1}{\sqrt{2\pi D}} \exp \left[ -\frac{(\langle I \rangle - I_0)^2}{2D} \right] \quad (3.3.8)$$

where the width of the distribution is related to the shot noise and the measurement duration  $\tau$  via

$$D = \frac{S_I}{\tau}. \quad (3.3.9)$$

The longer the measurement the narrower the distribution becomes, as expected. For an electron occupying the higher dot the distribution is analogous, but centered around  $I_1$ .

The aggregate probability distribution for the current when only probabilistic information about the occupational state of the electron is available then reads

$$P(\langle I \rangle, \tau) = \frac{\rho_{00}}{\sqrt{2\pi D}} \exp\left[-\frac{(\langle I \rangle - I_0)^2}{2D}\right] + \frac{\rho_{11}}{\sqrt{2\pi D}} \exp\left[-\frac{(\langle I \rangle - I_1)^2}{2D}\right]. \quad (3.3.10)$$

As the probability distribution of the measurement result  $\langle I \rangle$  therefore depends on the state of the electron, the result reveals information about the system that has to be used to update the probabilities via the standard Bayes formalism of posterior probabilities [43].

The posterior probability that an event  $A$  occurs provided the evidence  $X$  is a conditional probability that is defined as

$$P(A|X) \equiv P(A) \frac{P(X|A)}{P(X)} \quad (3.3.11)$$

where  $P(A)$  is the probability of the event  $A$  and  $P(X)$  analogously for  $X$ .

In the present case this translates to the occupational probabilities

$$\begin{aligned} \rho_{00}(\tau) &= \rho_{00}(0) \frac{P_0(\langle I \rangle, \tau)}{P(\langle I \rangle, \tau)} \\ \rho_{11}(\tau) &= 1 - \rho_{00}(\tau). \end{aligned} \quad (3.3.12)$$

So far we have only analyzed the system when treated classically. When the system is in a quantum state the off-diagonal terms of the density matrix are non-zero. If the state, however, is fully coherent and thus a pure state the off-diagonal terms relate to the diagonal ones via

$$|\rho_{01}(0)| = \sqrt{\rho_{00}(0) \rho_{11}(0)}. \quad (3.3.13)$$

While the diagonal term still represent the occupational probabilities the off-diagonal term are not directly accessible. We have, however, the upper limit

$$|\rho_{01}(\tau)| \leq \sqrt{\rho_{00}(\tau) \rho_{11}(\tau)}. \quad (3.3.14)$$

Let us compare this with the decoherence of a double dot due to an external noise source or environment (3.3.6). For this let us calculate the effect of the measurement averaged over many realizations of the system. Averaging over many realizations here amounts to averaging over the measurement output so that the upper bound for the off-diagonal terms becomes

$$\int d\langle I \rangle P(\langle I \rangle, \tau) \sqrt{\rho_{00}(\tau) \rho_{11}(\tau)} = \sqrt{\rho_{00}(0) \rho_{11}(0)} \exp\left[-\frac{(\Delta I)^2}{4S_I} \tau\right]. \quad (3.3.15)$$

Comparison with (3.3.6) shows that this gives the same decoherence rate as an external noise source so that we conclude that the *only* source of decoherence is due to the loss of measurement information. Keeping track of the current  $\langle I \rangle$  and updating the state via equations (3.3.12) therefore does not affect the purity of the state so that it remains pure during the measurement.

Above we have presented the evolution of a qubit under measurement (given a measurement outcome  $\langle I \rangle$ ) over a time period of  $\tau$ . We took this measurement time to be long enough so that in the given example of a tunneling junction enough electrons would pass through to be able to treat the flow as a current. In other words we implement a low pass filter that averages the effect of individual electrons passing through

$$\tau \gg \frac{e^2}{S_I}. \quad (3.3.16)$$

This ensures suppression of the quantum noise in the treatment of the current by treating the detector as an ampere meter and thus measuring current. The time interval can be taken to be arbitrarily small.

In a weak coupling regime the information gained within this timeframe is small and therefore the back action on the measured system is small as well. We may linearize the evolution to deduce a dynamic equation. In practice this amounts to the iteration of

1. Start with a system  $\rho(0)$ .
2. Draw a random instantaneous current  $\langle I \rangle$  from the distribution (3.3.10).
3. Calculate the evolved system  $\rho(\tau)$  from the current via (3.3.12).
4. Repeat from 1. with updated system  $\rho(\tau)$ .

On the other hand we have[41]

$$\begin{aligned} \rho_{00}(\tau) &= \frac{\rho_{00}(0) \exp\left[-\frac{(\langle I \rangle - I_0)^2}{D}\right]}{\rho_{00}(0) \exp\left[-\frac{(\langle I \rangle - I_0)^2}{D}\right] + (1 - \rho_{00}(0)) \exp\left[-\frac{(\langle I \rangle - I_1)^2}{D}\right]} \\ &\approx \rho_{00}(0) - \rho_{00}(0)(1 - \rho_{00}(0)) \frac{2\Delta I}{S_I} (\langle I \rangle - \bar{I}) \tau. \end{aligned} \quad (3.3.17)$$

The continuous limit with the instantaneous current  $I(t)$  is then

$$\dot{\rho}_{00} = -\rho_{00}(0)(1 - \rho_{00}(0)) \frac{2\Delta I}{S_I} (I(t) - \bar{I}). \quad (3.3.18)$$

This equation now serves as the evolution equation of a qubit under measurement.

In the derivation above we disregarded the internal evolution of the qubit due to its Hamiltonian  $H_{\text{DD}} = \frac{\varepsilon}{2} (c_1^\dagger c_1 - c_0^\dagger c_0) + \Delta (c_1^\dagger c_0 + c_0^\dagger c_1)$ . This is applicable when the dynamics that governs this evolution is slow compared to the tunneling of electrons through the barrier. In practice we can assume the qubit to be frozen for every instantaneous current  $\langle I \rangle$ , or in other words

$$\frac{\sqrt{\varepsilon^2 + 4\Delta^2}}{\hbar} \ll \frac{S_I}{e^2}, \quad (3.3.19)$$

and [44, 41] the resulting stochastic differential equations become

$$\dot{\rho}_{00} = -\dot{\rho}_{11} = -\frac{2\Delta}{\hbar} \text{Im}(\rho_{01}) - \rho_{00}(0) (1 - \rho_{00}(0)) \frac{2\Delta I}{S_I} (I(t) - \bar{I}) \quad (3.3.20)$$

$$\begin{aligned} \dot{\rho}_{01} = & \frac{i\varepsilon}{\hbar} \rho_{01} + \frac{i\Delta}{\hbar} (\rho_{00} - \rho_{11}) \\ & - (\rho_{00} - \rho_{11}) \frac{\Delta I}{S_I} (I(t) - \bar{I}) \rho_{01}. \end{aligned} \quad (3.3.21)$$

These describe the evolution of the qubit for any continuously measured detector outcome  $I(t)$ . Notice here that for proper determination of the qubit state the whole history of  $I(t)$  has to be known and taken into account.

Having now introduced the various mathematical descriptions of the measurement process we next turn to make the information gained during the measurement process useful. In particular we present two approaches on how the continuously acquired knowledge about a system can be used to control and stabilize its dynamical evolution.

### 3.4 Measurement control

In the preceding section of the chapter we have been concerned with finding information about a certain system. This acquiring of information is formally done in a measurement process and we have presented several descriptions of the details of measurement procedures. While obtaining the desired information can be reward enough in itself, it can also be used to control the measured system by changing its parameters depending on the measurement outcome.

The loop of measurement and parameter control is so natural that we hardly notice applying it every day for instance in measuring the temperature of a room (by feeling cold or warm) and adjusting its parameters (by tuning up the heating or opening a window). As control of a system constitutes the core of any engineering problem a depth of formalism has been developed. In the following we therefore just briefly introduce two approaches, the well known classical feedback and its maybe not so well know analog for quantum systems.



### 3.4.1 Markovian Feedback

To introduce the simplest feedback loop it is appropriate to use the most basic system. Take a temperature bath that is connected to a heat sink and a heat source. A thermometer measures the bath's temperature  $T(t)$  and we assume control over the heat source, i.e., we may control the amount of heat  $\delta Q_{\text{in}}(t)$  that is transferred into the system at any given moment.

To keep the bath at a desired fixed temperature  $T_0$  the amount of heat lost in the sink has to be countered by an equal amount of heat inserted from the source. Having no knowledge about the sink's dynamics but only of the current measured temperature  $T(t)$  we quickly find a linear relation between measurement outcome and required heat

$$\delta Q_{\text{in}}(t) = C(T_0 - T(t)), \quad (3.4.1)$$

where the proportionality factor is the heat capacity of the system. With this relation we may connect the heat source with the measurement device and the system stays at constant temperature without further ado.

In the present context we coin the name *Markovian feedback* for the above situation. This is to emphasize the classical nature of the system that can be applied to quantum systems as well [23, 24, 25]. The only uncertainty is the random change of heat dissipation through the sink. But as the measurement device precisely follows this dissipation the control loop can pick up any movements. At any given point the system therefore is in a well known state. This neat feature of classical systems only carries over to the quantum realm in the case of quantum non demolition measurements [26] so that in the general case we have to be more creative.

### 3.4.2 Bayesian Feedback

In the previous section we focussed on stabilizing a system under external influences via feedback control. The general idea was to adjust the driving parameters based on a continuously updated knowledge about the state of the system.

The basic prerequisites for this approach are on the one hand that we are able to monitor the system precisely, so that in any instance we have a complete knowledge about its state. Or at the very least a complete knowledge about the part of the system that is subject to the feedback stabilization. On the other hand we assumed that the effect of changing the system's external parameters, the process we call feedback, has a one to one correspondence with the reaction of the system. While some relation is of cause necessary to speak of control of the system we particularly assumed a linear relation between the discrepancy of actual and desired state of the system vs. the action taken in feedback control.

These two assumptions are valid for a vast number of systems that are subject to feedback control. The linear relation between discrepancy and action in particular allows for an electronic implementation of stabilizing loops so that these controls can be incorporated into the devices themselves. As the origin of the theory of feedback control [45] lies in the realm of engineering it is of no surprise that its tools are tailored to be applied to classical systems.

For quantum systems we have a stochastic uncertainty build in the foundations of the theory so that we are compelled to reexamine the above assumptions. As it has been established well enough, not least in this chapter, in the process of a quantum measurement the gathering of information about the system is necessarily associated with back-action on the measured system. The strength of this back-action is correlated with the decisiveness of the gathered information, peaking in the extreme case of complete knowledge with a total collapse of the wave function. The projective nature of this back-action contradicts the idea of continuous measurement and simultaneous feedback control. Being therefore limited to continuous weak measurements, as for instance introduced in section 3.3, the theory has to be expanded to cover these new type of cases where the measurement is the driving force of the evolution of system. This starkly contrasts the classical case where the measurement *follows* the evolution of the system.

To introduce these new concepts we follow Ruskov et al. [46] in presenting the continuous measurement of a qubit. This feedback has been studied and implemented in solid state qubits [47, 27] as well as in a circuit QED environment [48]. Above we have coined the update of the density matrix by information gathered through a continuous measurement as “Bayesian”. To emphasize the use of these techniques we continue to use this term to refer to the feedback control mechanisms that are incorporated into the coming analysis.

To reduce the problem to the fundamental concepts at hand we assume a qubit Hamiltonian  $H = \Delta (c_1^\dagger c_0 + c_0^\dagger c_1)$  corresponding to  $H = \Delta \sigma_x$  in qubit space. The evolution of the unmeasured qubit therefore is a rotation around the  $x$ -axis, while the weak measurement in  $z$ -direction returns information about the qubit’s “position” along that axis. As mentioned, the measurement process is inherently invasive so that at the same time as it returns information about the state it also serves as another driver of rotation. The important difference is evident already in this simple setup. While the rotation per time interval  $\tau$  due to the Hamiltonian is determined strictly by  $\Delta$ , the back-action due to the measurement depends not only on the measurement result  $I(t)$  but also on the qubit state  $\rho(t)$ . This extra dependency prohibits any kind of direct feedback control as introduced in the preceding section so that a more elaborate scheme has to be implemented.

We have seen that a given density matrix of a qubit that is measured

by a nearby QPC has to be updated via the equations (3.3.20, 3.3.21) for any measured current  $I(t)$ . While a direct feedback mechanism fails to incorporate the dependency on the current qubit state  $\rho(t)$  we thus use these equations to calculate the system state at any given time. Without measurement the unperturbed qubit follows a rotation governed by

$$\dot{\rho}_{00} = -\dot{\rho}_{11} = -\frac{2\Delta}{\hbar} \text{Im}\rho_{12} \quad (3.4.2)$$

$$\dot{\rho}_{12} = \frac{\Delta}{\hbar} (\rho_{00} - \rho_{11}), \quad (3.4.3)$$

so that, with the condition of positive diagonal entries of the density matrix, we have

$$\rho_{00}(t) = \frac{1}{2} \left( 1 + \cos \left( \frac{2\Delta}{\hbar} t \right) \right) \quad (3.4.4)$$

$$\rho_{12}(t) = \frac{\dot{\rho}_{12}}{2} \sin \left( \frac{2\Delta}{\hbar} t \right). \quad (3.4.5)$$

The phase  $\phi_0(t) = 2\Delta t/\hbar \pmod{2\pi}$  of the unperturbed motion has to be compared to the actual phase

$$\phi(t) = \arctan \left( 2 \frac{\text{Im}\rho_{12}}{\rho_{00} - \rho_{11}} \right) \quad (3.4.6)$$

of the measured system. On the momentary phase difference  $\delta\phi(t)$  now a direct feedback can be applied by changing the rotation frequency  $\Delta$  proportionally

$$\frac{\Delta'}{\Delta} = 1 + F\delta\phi(t), \quad (3.4.7)$$

with the dimensionless proportionality factor  $F$  to control the feedback strength. Ruskov et al. show via numerical simulations that for a feedback factor approaching unity the asymptotic amplitude of oscillations also saturates essentially at one.

This short introduction to the control of a continuously measured system concludes the present chapter of quantum measurements. In the following we apply the previously presented ideas by combining the concepts of quantum entanglement and quantum measurement in a physical setup to create and stabilize entanglement via a quantum measurement.



## Chapter 4

# Measurement and entanglement

As announced we now present the creation and stabilization of fully entangled two qubit states. In the preceding chapters we introduced the general formalism of quantum entanglement and quantum measurements including feedback loops, so that we are now in a position to apply these concepts to a given system. As a proof on concept we focus on the entanglement of two qubits. The means of creating entanglement here is a parity measurement on both. The necessary concepts are presented in the following sections first briefly theoretically (4.1) and then within an experimentally feasible context of a Mach-Zehnder interferometer (4.2).

We continue to analyze the dephasing that is present intrinsically due to the special architecture of the Mach-Zehnder interferometer and the additional dephasing mechanisms present in any experimental context. The study of these dephasing mechanism readily admits the inclusion of a feedback loop to stabilize the intrinsic dephasing (4.4) as well as the external one (4.5).

Including both feedback loops in the measurement process then leads to stable maximally entangled Bell-states that are the fundamental building blocks of any quantum computational setup.

### 4.1 Parity measurements

The expression *parity* has a wide range of meanings in physics so that we are bound to give a proper definition for the system at hand. As mentioned in the introduction the present chapter is concerned with the creation of entanglement between two qubits so that the given Hilbert space it spanned by the states

$$H = \text{span} \{ |\uparrow\uparrow\rangle, |\uparrow\downarrow\rangle, |\downarrow\uparrow\rangle, |\downarrow\downarrow\rangle \}. \quad (4.1.1)$$

Here  $\uparrow$  and  $\downarrow$  denote the spin polarization along the  $z$ -axis. We define those states that are a linear combination of the basis states with both spins pointing in the same direction as even. Thus the even subspace of  $H$  is spanned by  $\{|\uparrow\uparrow\rangle, |\downarrow\downarrow\rangle\}$  leaving the odd subspace to be spanned by  $\{|\downarrow\uparrow\rangle, |\uparrow\downarrow\rangle\}$ . The corresponding observable shall be denoted by  $\hat{P}$  and as both subspaces are two dimensional the eigenvalues pertaining to the even and odd parity are degenerate. With the given definition of even and odd subspaces it is readily verified that the operator  $\hat{P} = \sigma_z \otimes \sigma_z$ , where  $\sigma_z$  denotes the Pauli matrix, incorporates the given subspaces as eigenspaces to its eigenvalues one and minus one.

### 4.1.1 Bell states

Until now we have described the two qubit system with the computational basis. This is straightforward and intuitive as each computational basis state can be created by local operations on each qubit. In the following we, however, deal with the two qubit system in the context of entangled states. One immediate consequence is that the states involved are no longer locally producible so the computational basis tends to loose its favorability. Instead we now introduce four different basis states, the Bell states

$$|\Psi_e^\pm\rangle = \frac{1}{\sqrt{2}} (|\uparrow\uparrow\rangle \pm |\downarrow\downarrow\rangle) \quad (4.1.2)$$

$$|\Psi_o^\pm\rangle = \frac{1}{\sqrt{2}} (|\uparrow\downarrow\rangle \pm |\downarrow\uparrow\rangle). \quad (4.1.3)$$

Notice first that all of the Bell states are fully entangled. This is verified by calculating, for instance, the von Neumann entropy (cf. chapter 2.2.2) of their reduced states. Incidentally, the state  $|\Psi_o^+\rangle$  is exactly the singlet state already introduced. As these Bell states are fully entangled they serve as the ideal results of any apparatus that claims to create entanglement between two qubits.

Another thing to notice is that the Bell states are again eigenstates of the parity operator. Indeed we have

$$\hat{P} |\Psi_e^\pm\rangle = |\Psi_e^\pm\rangle \quad (4.1.4)$$

$$\hat{P} |\Psi_o^\pm\rangle = -|\Psi_o^\pm\rangle, \quad (4.1.5)$$

so that the subscript e/o is duly justified. As eigenstates of the parity operator the Bell states remain intact under parity measurements. Conversely, a parity measurement can thus also be used to create such a Bell state. Now the parity operator has degenerate eigenvalues so the parity measurement of an arbitrary state does not necessary result in a Bell state but just in a superposition of either even or odd Bell states.

Take, however, the initial state

$$\begin{aligned} |\psi\rangle &= \frac{1}{\sqrt{2}} (|\uparrow\rangle + |\downarrow\rangle) \otimes \frac{1}{\sqrt{2}} (|\uparrow\rangle + |\downarrow\rangle) \\ &= \frac{1}{2} (|\uparrow\uparrow\rangle + |\uparrow\downarrow\rangle + |\downarrow\uparrow\rangle + |\downarrow\downarrow\rangle) \end{aligned} \quad (4.1.6)$$

that obviously is a product state and thus can be prepared locally. Applying the parity operator to  $|\psi\rangle$  projects the state to

$$|\psi'\rangle = \hat{P} |\psi\rangle = \frac{1}{\sqrt{2}} (|\Psi_e^+\rangle - |\Psi_o^+\rangle) \quad (4.1.7)$$

so that each parity eigenvalue corresponds to a unique eigenstate. The parity measurement thus creates a determined fully entangled Bell state for both measurement outcomes.

A simple Hamiltonian for the qubits of the form  $H = \sum_{i=1,2} \frac{\varepsilon}{2} \sigma_z^i$ , where  $\sigma_z^i$  mark the Pauli matrices for the respective qubits, leads to a free evolution of the projected state

$$|\psi'(t)\rangle = \frac{1}{2} \left( e^{-\frac{\varepsilon t}{\hbar}} |\uparrow\uparrow\rangle + |\uparrow\downarrow\rangle + |\downarrow\uparrow\rangle + e^{\frac{\varepsilon t}{\hbar}} |\downarrow\downarrow\rangle \right) \quad (4.1.8)$$

$$= \frac{1}{\sqrt{2}} \left( \cos \frac{\varepsilon t}{\hbar} |\Psi_e^+\rangle + \sin \frac{\varepsilon t}{\hbar} |\Psi_e^-\rangle + |\Psi_o^+\rangle \right). \quad (4.1.9)$$

A measurement resulting in an even outcome thus projects the initial state  $|\psi\rangle$  onto the even Bell state  $|\Psi_e^+\rangle$  and the evolution of the system results in a subsequent oscillation between both even Bell states. If the measurements give back an odd result the state is frozen, however, in the odd Bell state  $|\Psi_o^+\rangle$  and no oscillation occurs. While the Bell states are fully entangled, the knowledge of the measurement outcome is crucial to determine the state of the system. In the next section we therefore define a new type of entanglement measure to incorporate this necessary knowledge into the entanglement measure.

### 4.1.2 Conditional concurrence

In the previous section we introduced the parity measurement as a means to create a maximally entangled Bell state. With the right initial state any given outcome of the parity measurement resulted in a uniquely determined Bell state. For any single measurement the entanglement is therefore maximal. In an experiment or simulation, however, this single measurement procedure is repeated many times to form an ensemble, any analysis has so be done regarding this statistical ensemble of states, hence its density matrix. Here, however, we run into a problem with the parity measurement given above. For the initial state (4.1.6) the outcome of each measurement result is of equal probability, the statistical ensemble after the measurement therefore

consists of even Bell states  $|\Psi_e^+\rangle$  and odd Bell states  $|\Psi_o^+\rangle$  of equal proportion. It is easy to verify that this amounts to a fully mixed final ensemble. With the definition of entanglement of mixed states, the entanglement concurrence, given in the previous chapter 2 this results in zero entanglement in the ensemble.

The problem here is that the knowledge of the single measurement results was discarded in the averaging process. To include this knowledge in the analysis we define the *conditional concurrence* as the concurrence of the statistical ensemble postselected on the measurement result. In practice this means that for every repetition of the measurement the result is collected into one of two bundles depending on the measurement outcome. All states with a measurement outcome of even parity are then averaged together to form the statistical ensemble  $\rho_e$  and all state with an odd measurement outcome form the statistical ensemble  $\rho_o$ . Averaging over both ensembles again gives the original full ensemble. In the postselected density matrices the knowledge of the measurement result is now included, however, and the entanglement of both is nonzero.

For the present case of projective measurements this method seems to be somewhat artificial but once the measurement procedure is simulated in detail via a weak von Neumann measurement the conditional concurrence serves as a valuable tool to describe the entanglement created with the measurement outcome included in the analysis.

Having now introduced the parity measurement as a means to create fully entangled Bell states and having further expanded the definition of entanglement to incorporate the measurement results we now turn to an experimental setup to actually perform a parity measurement on two qubits.

## 4.2 Electronic Mach-Zender interferometer

The physical implementation of a parity measurement has been achieved in various architectures. In the framework of three-dimensional circuit quantum electrodynamics a continuous parity measurement of two superconducting qubits has been accomplished by Riste et al. employing phase-sensitive parametric amplification [14, 49, 50]. The advantage of this approach is the relatively easy extension of the protocol to architectures involving macroscopic separation of the qubits [51]. On the other hand the possibility of surface coding can be employed in the realization of parity measurements in two dimensional planar circuit quantum electrodynamics [17].

But transport-based setups can also act as a parity meter. Already the simultaneous measurement of two adjacent double quantum dot qubits by a quantum point contact can distinguish Bell states of different parity and thus serves as a proto-parity meter [12]. Operating, however, two quantum point contacts to form a Mach-Zehnder interferometer [52, 53] allows for the



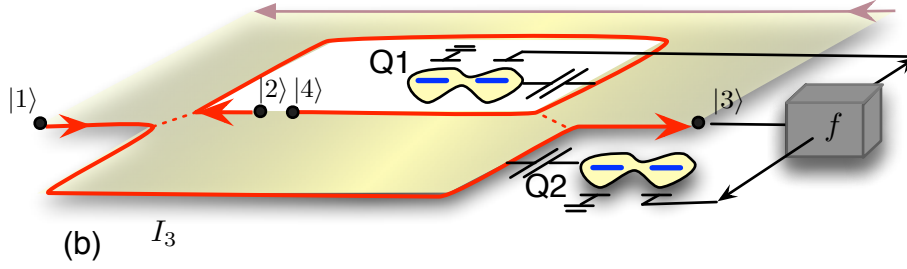


Figure 4.2.1: The Mach-Zehnder interferometer is established with two quantum point contacts acting as beam splitters. The electrons are injected in lead  $|1\rangle$  and read out in lead  $|3\rangle$ . The two charge qubits  $Q1$  and  $Q2$  are controlled by a feedback loop that continuously adjusts their bias energies. Figure from [22].

creation of a true parity meter [21, 54]. The excellent coherence properties [19, 55, 56, 57, 58] make the electronic Mach-Zehnder interferometer an ideal candidate for a quantum detector [54, 59]. In the following we briefly review this architecture qualitatively as it forms the basis of our further analysis.

#### 4.2.1 Physical model

This electronic equivalent of the well known optical Mach-Zehnder interferometer is formed by a two dimensional electron gas operated in the quantum Hall regime. The quantized motion is effectively limited to one-dimensional chiral edge states corresponding to the arms of the traditional interferometer. Quantum point contacts are used to split the incoming particle beam and recombine both paths on the other side.

The electrons traveling through the arm  $i = 1, 2$  gain a phase  $\chi_i$  due to the different effects of the interferometer [21]

$$\begin{aligned}\chi_1 &= k(d - L) + \theta_{\text{up}} + \Delta\chi_1 \frac{1 - \hat{\sigma}_z^1}{2} \\ \chi_2 &= k(d - L) + \theta_{\text{down}} + \Delta\chi_2 \frac{1 + \hat{\sigma}_z^2}{2}.\end{aligned}\quad (4.2.1)$$

Firstly the length of the arms  $d$ , assumed to be equal for both arms, leads to a phase of  $kd$  and we subtract the part of the arm  $L$  where the electron is in range of the interaction potential of the double dots as the phase acquired in this section depends on the occupation of the double dots. These occupation-dependent phases hence lead to the last terms in (4.2.1) where  $\hat{\sigma}_z^i$  is the Pauli matrix of the double dot connected to arm  $i$ . The strength of the coupling between arms and double dots is incorporated into the parameters  $\Delta\chi_i$ . Note therefore that these can be readily tuned by adjusting the individual coupling

strengths. Finally the magnetic flux threading the sample induces another phase difference  $\theta_{\text{up}} - \theta_{\text{down}} = 2\pi\Phi/\Phi_0$  with  $\Phi_0 = e/h$  the flux quantum.

Depending on the occupation of the double dots the phase difference  $\Delta\Phi$  acquired between the two arms takes four different values corresponding to the four computational states (4.1.1) of

$$\begin{aligned}\Delta\Phi_{\uparrow\uparrow} &= 2\pi\Phi/\Phi_0 - \Delta\chi_2 \\ \Delta\Phi_{\downarrow\uparrow} &= 2\pi\Phi/\Phi_0 + \Delta\chi_1 - \Delta\chi_2 \\ \Delta\Phi_{\uparrow\downarrow} &= 2\pi\Phi/\Phi_0 \\ \Delta\Phi_{\downarrow\downarrow} &= 2\pi\Phi/\Phi_0 + \Delta\chi_1.\end{aligned}\tag{4.2.2}$$

As the current  $I$  measured in output lead 3, as depicted in figure 4.2.1, of the second quantum point contact is proportional to the transmission probability [21] from lead 1 to lead 3

$$T_{31} = T_L R_R + T_R R_L + 2\sqrt{T_L R_R T_R R_L} \cos \Delta\Phi\tag{4.2.3}$$

the four different phase differences (4.2.2) lead to four different average currents as detector output. Remembering that a parity meter shall only distinguish between the parity subspaces and yield the same output for any linear combination of states within one subspace we mark the first parity condition

$$\Delta\chi_1 = \Delta\chi_2 = \Delta\chi.\tag{4.2.4}$$

As mentioned above this can be achieved by tuning the coupling strength between interferometer arms and double dots. With this condition met the current reduces to three possible values as depicted in the first panel of figure 4.2.1.

While the odd subspace indeed is represented by only one detector outcome the measurement result still distinguishes between different states in the even subspace. Tuning the magnetic flux threading the sample, however, so that the odd detector outcome coincides with the maximum (or minimum) possible outcome

$$2\pi\Phi/\Phi_0 = 0 \bmod 2\pi,\tag{4.2.5}$$

as shown in the second panel of figure 4.2.1, the resulting current for both even states now coincide. Thus a true parity meter with only the two possible detector outcomes  $I_o$  and  $I_e$ , corresponding to the odd and even parity space, emerges.

It is worth noting already at this stage that with this realization of a parity meter there is an intrinsic difference between the measurement of both parity subspaces. The first parity condition ensures that all electrons acquired the same phase information in both arms for any state of the odd subspace. As they carry no such information difference there is no principle way of using them to distinguish between states of the odd subspace.

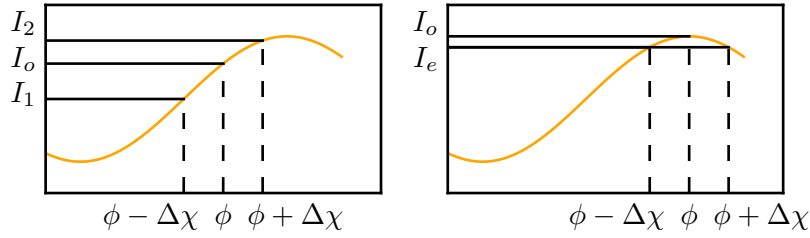


Figure 4.2.2: Fulfilling the two parity conditions (4.2.4) and (4.2.5) leads to only two values for the average current  $I(t)$  corresponding to the parity subspaces even and odd. The first parity condition leads to three remaining currents as shown in the left panel. Only if the flux  $\phi = 2\pi\Phi/\Phi_0$  is tuned so that it coincides with an extremum, as demanded by the second parity condition, two resulting possibilities for the current emerge and a parity meter is established.

The measurement for the even states, however, is achieved slightly differently. Here we make use of the cyclic nature of the transmission probability on the phase difference between both arms. Indeed for the two different even states a different *phase* is acquired by electrons traveling along both arms. Due to the fine-tuning of the interferometer's parameters these phase differences, however, do not correspond to different detector currents. In simple terms this means that the phase information is discarded.

To discard information that is in principle available leads to a decoherence, as was presented in chapter 2, and we therefore expect a dephasing of states within the even subspace. This dephasing was indeed confirmed experimentally [14] and the following analysis is based mainly on the hope to use a feedback mechanism to counter this dephasing. The mechanism to do so is to use the knowledge of acquired phase difference within the even subspace by explicit calculation.

We therefore proceed to develop a microscopic model to describe the passing of individual electrons through the Mach-Zehnder interferometer.

### 4.3 Microscopic model

*Part of the material presented in the following was already published by the author under the title "On-demand maximally entangled states with a parity meter and continuous feedback" [22].*

In the previous section we introduced the Mach-Zehnder interferometer as an implementation of a parity measurement of a two qubit system. In this section we now combine the formalism of quantum measurement theory presented in chapter 3 with the current physical setup. In particular we

devise a microscopical model of single electrons passing through the arms of the Mach-Zehnder interferometer and interacting with the double dot qubits on the way. The collection of single electrons passing allows for a description as a current so that we make the transition from a von Neumann type of measurement protocol to the formalism of continuous measurements.

As presented above the electrons moving through the arms of the Mach-Zehnder interferometer acquire a phase depending on the flux through the interferometer. While this phase is static in the sense that it applies to every electron regardless of the state of the qubits, there is another phase contribution due to the capacitive coupling of the double dots to the Mach-Zehnder interferometer arms. Each injected electron therefore acquires an additional phase that depends on the charge configuration of the double dot qubits  $|ss'\rangle$  and the path the electron travels. We write

$$\delta\varphi_u^{(ss')}, \delta\varphi_d^{(ss')} \quad (4.3.1)$$

for the phase acquired by an electron traveling through the upper (u) or lower (d) arm, that we leave undefined for the moment. The precise expressions are calculated via the Hamiltonian that describes the interaction between the charge of the double dot qubits (or the electron occupying the double dot) and the charge of the Mach-Zehnder interferometer arm as presented in the previous section 4.2.1. The double qubit system  $|ss'\rangle$  is spanned by the single qubit computational basis states via  $s, s' \in \{\uparrow, \downarrow\}$ . While the state of the passing electron is described by the exit node where it is detected. In practice the detection is executed only at one output port as particle conservation gives the corresponding number for the other.

### 4.3.1 Single electron passing

As mentioned, the passing electron acquires a phase depending on the state of the double qubit so that it serves as a detection mechanism (or rather serves as one component of the measurement process). The state of the detector is, however, only characterized by the number of electrons detected. We now proceed to show that this number of detected electrons indeed depends on the additional phase acquired by the passing of electrons and thus indirectly depends on the double qubit state. Before the measurement process the detector  $|\Phi_{\text{det}}\rangle$  and the double qubit system are just in a product state as no interaction has been taken place:

$$|\Psi\rangle = \left( \alpha^{(\uparrow\uparrow)} |\uparrow\uparrow\rangle + \alpha^{(\uparrow\downarrow)} |\uparrow\downarrow\rangle + \alpha^{(\downarrow\uparrow)} |\downarrow\uparrow\rangle + \alpha^{(\downarrow\downarrow)} |\downarrow\downarrow\rangle \right) \otimes |\Psi_{\text{det}}\rangle. \quad (4.3.2)$$

Each state being normalized we have

$$\left| \alpha^{(\uparrow\uparrow)} \right|^2 + \left| \alpha^{(\uparrow\downarrow)} \right|^2 + \left| \alpha^{(\downarrow\uparrow)} \right|^2 + \left| \alpha^{(\downarrow\downarrow)} \right|^2 = 1. \quad (4.3.3)$$

With the first electron that passes through the Mach-Zehnder interferometer and acquiring a state dependent phase the double qubit system and the detector become entangled (alas only weakly) [4, 8, 21]. As presented above, the detector has the physical form of an electron counter situated at the output leads of the Mach-Zehnder interferometer. The state of an electron passing through the interferometer and arriving at the detector is therefore spanned by the two possible output states  $\{|3\rangle, |4\rangle\}$ . The entangled state of electron at the output nodes and double qubit system then reads

$$|\Psi_1\rangle = \sum_{ss'} \alpha^{(ss')} |ss'\rangle \left( C_3^{(ss')} |3\rangle + C_4^{(ss')} |4\rangle \right) \quad (4.3.4)$$

where the coefficients  $C_i$  are given by the system parameters and incorporate the phases acquired by the electron [22]

$$C_3^{(ss')} = \sqrt{R_L R_R} e^{i2\pi\Phi/\Phi_0} e^{i\delta\varphi_u^{(ss')}} + \sqrt{T_L T_R} e^{i\delta\varphi_d^{(ss')}} \quad (4.3.5)$$

$$C_4^{(ss')} = i \left( \sqrt{R_L T_R} e^{i2\pi\Phi/\Phi_0} e^{i\delta\varphi_u^{(ss')}} - \sqrt{T_L R_R} e^{i\delta\varphi_d^{(ss')}} \right). \quad (4.3.6)$$

Here first we notice the term that is due to the well known Aharonov-Bohm flux  $2\pi\Phi/\Phi_0$ . This is induced by the vector potential that threads the sample. The second terms are the above mentioned extra phases that depend on the individual configuration of the double dot qubits. For ease of calculation we assume symmetric qubits that on the one hand result in  $R_R = R_L = \frac{1}{2}$  and on the other hand lead to a maximization of output signal strength as found experimentally [19, 52, 55]. The coefficients therefore take the form

$$C_3^{(ss')} = \frac{1}{2} \left( e^{i2\pi\Phi/\Phi_0} e^{i\delta\varphi_u^{(ss')}} + e^{i\delta\varphi_d^{(ss')}} \right) \quad (4.3.7)$$

$$C_4^{(ss')} = \frac{i}{2} \left( e^{i2\pi\Phi/\Phi_0} e^{i\delta\varphi_u^{(ss')}} - e^{i\delta\varphi_d^{(ss')}} \right). \quad (4.3.8)$$

Before generalizing to the passing of  $n$  electrons and treating them as a current we briefly discuss the parameter settings needed for the Mach-Zehnder interferometer to serve as a true parity detector.

### 4.3.2 Parity meter conditions

As presented above, the Mach-Zehnder interferometer is set up to serve as a parity detector. To this end the output has to have a distinct value for the even and odd subspaces, while no distinction can be made within each subspace. This is to demand that the probability to find the double qubits in an even state  $P_e$  or the odd state  $P_o$  is the same for both even and odd states

$$|\langle \uparrow\downarrow | \Psi_1 \rangle|^2 = |\langle \downarrow\uparrow | \Psi_1 \rangle|^2 = P_o \quad (4.3.9)$$

$$|\langle \downarrow\downarrow | \Psi_1 \rangle|^2 = |\langle \uparrow\uparrow | \Psi_1 \rangle|^2 = P_e, \quad (4.3.10)$$

where  $V$  is the bias voltage applied across the interferometer. These two probabilities translate into different mean currents in the output

$$I_o = \frac{2e^2V}{h}P_o, \quad I_e = \frac{2e^2V}{h}P_e. \quad (4.3.11)$$

To satisfy these parity conditions (4.2.4) and (4.2.5) in the present setting we have to tune the capacitive coupling between the interferometer arms and the double dots to obtain

$$\delta\varphi_u = \delta\varphi_d \equiv \delta\varphi, \quad (4.3.12)$$

on the one hand, and to adjust the Aharonov-Bohm flux to yield [21]

$$2\pi\frac{\Phi}{\Phi_0} = 0 \text{ mod } \pi, \quad (4.3.13)$$

on the other hand. While these two conditions allow for the interferometer to act as a parity meter we need to make further assumptions or rather demands as to the strength of the measurement. In particular the implementation of a continuous feedback loop can only be achieved if the detector is run in the weak measurement regime. The weak measurement strength ensures a weak measurement back-action so that the information gathered in the meantime can be used to adjust the feedback parameters without the system collapsing too much.

As in the previously introduced weak continuous measurement we operate the detector such that

$$\Delta I = I_o - I_e \ll I_o, I_e. \quad (4.3.14)$$

In the same manner we assume weak coupling between qubits and interferometer, and therefore the detector, to assume a detector output noise that is independent of the qubit states

$$S_{\text{II}} = \frac{S_{\text{II}}^o + S_{\text{II}}^e}{2}, \quad (4.3.15)$$

with the detector shot noise  $S_{\text{II}}^{o/e} = 2e^3V/hT_{31}^{o/e}(1 - T_{31}^{o/e})$  that is associated with the transmission probability of an electron that injected into lead one and detected in lead three, when the double qubits are in an even or odd state. Remember here again that the probabilities within one parity subspace are equal as the parity condition demands. The detector shot noise directly relates to the measurement rate [41] of the device

$$\Gamma_m = \frac{(\Delta I)^2}{4S_{\text{II}}}. \quad (4.3.16)$$

Notice also that a quantum limited parity meter, i.e., an ideal detector, acquires measurement information at the same rate as the system collapses. In

the present case this amounts to a measurement rate equal to the dephasing rate between both parity subspaces  $\Gamma_{\text{eo}} = \Gamma_{\text{m}}$ . To obtain an analytical expression for the dephasing rate between the parity subspaces we now extend the passing of a single electron to the flux and detection of a large number.

### 4.3.3 Continuous electron detection

Previously we have deduced an expression for the entangled state of the double qubit system and an electron that passed through the interferometer. When a bias voltage  $V$  is applied across the interferometer a flux of electrons is prompted through the interferometer. Monitoring this flux for a time  $\tau$  that is large compared to the passing time of a single electron

$$\tau \gg \frac{h}{eV} \quad (4.3.17)$$

ensures that a large number  $N \gg 1$  of independent electrons pass through and are detected on the output where the detector is situated. As the electrons are independent their order does not matter and only the total count of detecting  $n$  of the injected  $N$  electrons define the final state  $|\Psi_N\rangle$  via

$$|\Psi_N\rangle = \sum_n \sum_{(ss')} \binom{N}{n} \alpha^{(ss')} C_3^{(ss')n} C_4^{(ss')(N-n)} |n; N-n\rangle |ss'\rangle, \quad (4.3.18)$$

where we introduced the notation  $|n; N-n\rangle$  for the detection of  $n$  electrons in lead  $|3\rangle$  and conversely  $N-n$  in output lead  $|4\rangle$ . Notice here that the chirality of the edge states ensures that indeed every electron that is injected into lead  $|1\rangle$  exits through either  $|3\rangle$  or  $|4\rangle$ . Applying the central limit theorem onto (4.3.18) for a large number  $N \gg 1$  converts the binomial distribution to a normal one so that for the detection of a current

$$I_3 = \frac{ne}{\tau}$$

in lead  $|3\rangle$  we have to project the state (4.3.18) onto the state  $|n; N-n\rangle$  and obtain a final state

$$\begin{aligned} |\Psi_{\text{out}}\rangle &\propto \alpha^{(\uparrow\uparrow)} \frac{e^{-(I_3-I_e)^2/4D}}{\sqrt{4\pi D}} e^{iI_1\tau\delta\varphi/e} e^{i\pi(I_3-I_1)\tau/e} |\uparrow\uparrow\rangle \\ &+ \alpha^{(\downarrow\downarrow)} \frac{e^{-(I_3-I_e)^2/4D}}{\sqrt{4\pi D}} e^{iI_1\tau\delta\varphi/e} e^{-i\pi(I_3-I_1)\tau/e} |\downarrow\downarrow\rangle \\ &+ \frac{e^{-(I_3-I_o)^2/4D}}{\sqrt{4\pi D}} \left( \alpha^{(\uparrow\downarrow)} |\uparrow\downarrow\rangle + \alpha^{(\downarrow\uparrow)} e^{i2I_1\tau\delta\varphi/e} |\downarrow\uparrow\rangle \right) \end{aligned} \quad (4.3.19)$$

where the width of the normal distribution  $D$  that is centered around the average values for the even and odd currents is given by

$$D = \frac{S_{\text{II}}}{\tau} \quad (4.3.20)$$

and therefore connected to the detector shot noise. As expected the width of the distributions shrinks with time as more information is gathered about the systems state. When this width is small compared to the difference  $\Delta I = I_o - I_e$ , the measurement outcome can be attributed to one of the two parity subspaces so that indeed the measurement works as a parity meter.

#### 4.3.4 Dephasing mechanisms

Having derived the state of the double qubit based on a measured current at lead |3> in equation (4.3.19) one feature of the result immediately raises further need of investigation. The resulting state  $|\Psi_{\text{out}}\rangle$  does depend on the measured current in two ways. On the one hand the exponential factor shifts the weight between even and odd states as is expected as the natural back-action of a parity measurement. On the other hand there is a measurement dependent phase difference build up in the even subspace. No equivalent phase is present in the odd subspace, however. It becomes evident here that the two parity subspaces have a fundamental difference that arises due to the specific experimental realization of the Mach-Zehnder interferometer.

The measurement dependent phase difference within the even subspace coincidentally is proportional to part of the Hamiltonian. Before we exploit this fact via the introduction of a feedback mechanism we quickly derive the dephasing rates. While a four dimensional system is naturally connected with six dephasing rates in the present case of a parity meter these reduce to three. These are the dephasing within each subspace and the dephasing between the two subspaces.

The individual dephasing rates are readily obtained via the magnitude of the corresponding density matrix elements after averaging over many realizations.

$$\Gamma_{oo} = -\frac{1}{\tau} \log \left| \left\langle e^{i2I_1\tau\delta\varphi/e} \right\rangle \right| = 0 \quad (4.3.21)$$

$$\Gamma_{ee} = -\frac{1}{\tau} \log \left| \left\langle e^{i2\pi(I_3-I_1)\tau/e} \right\rangle \right| = \frac{4\pi^2}{e^2} S_{II} = \frac{4\pi^2}{e^2} \tau D \quad (4.3.22)$$

$$\Gamma_{eo} = -\frac{1}{\tau} \log \left| \left\langle e^{i\pi(I_3-I_1)\tau/e} \right\rangle \right| = \frac{\Gamma_{ee}}{4}. \quad (4.3.23)$$

As expected there is no extra dephasing in the odd subspace. As the parity meter is operated in such a way that a passing electron acquires the same phase for both odd states  $|\uparrow\downarrow\rangle$  and  $|\downarrow\uparrow\rangle$  there are no fluctuating (measurement dependent) contributions to the phase within that subspace. For a mathematical parity meter the same argument could be applied to the even subspace. As the measurement only distinguishes between the subspaces no extra back-action should be present within any subspace. However, the particular architecture of the present problem does distinguish



between the two even states  $|\uparrow\uparrow\rangle$  and  $|\downarrow\downarrow\rangle$  by introducing the extra phase difference  $2\pi(I_3 - I_1)\tau/e$ . An electron traveling through the interferometer therefore gains information about the even subspace so that the flip side is an additional dephasing.

Finally, we note that the dephasing rate between the two parity subspaces is the rate by which a superposition of even and odd states is pushed into an even or odd final state. In other words, this dephasing rate is the rate at which coherence between both measurement outcomes is destroyed. For an ideal detector this rate coincides with the rate of information gain, the measurement rate. Here the intrinsic dephasing rate within the even subspace is four times the decoherence rate. Any build-up of entanglement through the parity measurement is circumvented in the even subspace. In the following we therefore make use of the previously mentioned fact that the intrinsic phase difference in the even subspace is proportional to part of the double qubit Hamiltonian to devise an improved protocol, allowing creation of entanglement also in the even subspace.

## 4.4 Markovian feedback

Having introduced the formalism of a parity meter realized by a fine tuned Mach-Zehnder interferometer we noticed that extra dephasing is present in the even subspace. This dephasing is due to a measurement dependent, and therefore fluctuating, phase difference between the two even states. We now show that these phases can be dealt with by continuously fine tuning the Hamiltonian.

As both qubits are independent the Hamiltonian generating their free evolution is just the sum of each individual Hamiltonian

$$H_{\text{qb}} = \sum_{i=1,2} \frac{\varepsilon_i}{2} \sigma_z^i + \Delta_i \sigma_x^i \quad (4.4.1)$$

with the bias energies  $\varepsilon_i$  and the tunneling energies  $\Delta_i$  of the qubits  $i = 1, 2$  and their Pauli matrices  $\sigma_x$  and  $\sigma_z$ . For simplicity we again assume symmetric bias energies  $\varepsilon_i = \varepsilon$  and no tunneling  $\Delta_i = 0$  so that the parity is conserved  $[H_{\text{qb}}, \hat{P}] = 0$  and indeed the measurement of parity marks a quantum-non-demolition measurement.<sup>1</sup>

Comparing equation (4.3.19) and equation (4.1.8) we notice that the measurement dependent back-action on the double qubit state is proportional to the effect of a tunneling-free Hamiltonian. By adjusting the Hamiltonian's energy bias  $\varepsilon$  we can therefore implement a direct feedback that counters the

---

<sup>1</sup>Notice that a small tunneling rate is worked against by the separating effect of the parity measurement. The collapse due to the measurement leads to a freezing of the state in a quantum Zeno type of effect. [41, 60]

fluctuating part via

$$\varepsilon(t + \tau) = \varepsilon(t) + f\pi(I_3(t) - I_1)\frac{\hbar}{e}, \quad (4.4.2)$$

with the feedback parameter  $f$ . At any time therefore the adjustment works against the previously induced fluctuating part so that it is (partly) cancelled. As this feedback procedure does not require knowledge about the state itself but can be applied just based on the continuously measured detector outcome it is a direct feedback. To emphasize the absence of any memory effect and to contrast this type of feedback with the Bayesian feedback introduced in chapter 3.4.2 we coin the name Markovian feedback.

The feedback strength can be adjusted via the feedback parameter  $f$  that indeed represents the only free parameter of the feedback loop. This assumes the simultaneous change of bias energy in both qubits. Although in principle an individual feedback for each qubit could be implemented a different bias energy  $\varepsilon_i$  in both qubits leads to an additional fluctuating part in the odd subspace and thus to dephasing that would not be present without the feedback loop.

As suggested by the adjustment equation (4.4.2) the optimal value for the feedback parameter is  $f = 1$  that leads to an exact cancellation of the measurement induced fluctuations. Figure 4.4.1 shows the oscillating even and stable odd Bell states without feedback and with optimal feedback strength. Without feedback the even states decay quickly, as expected.

While the optimal feedback parameter strength is suggested by equation (4.4.2) and confirmed in the simulation in chapter 4.6 it can also be calculated via an analytical model based on the Langevin type of dynamics that the fluctuating phase exhibits. The phase difference that the double qubit system acquires during the time  $\tau$  in the even subspace is given by

$$\begin{aligned} \phi(t + \tau) - \phi(t) &= -\frac{\varepsilon\tau}{\hbar} + (1 - f)\frac{\tau 2\pi}{e}(I_3 - I_1) \\ &= -\frac{\varepsilon\tau}{\hbar} + (1 - f)\frac{\tau 2\pi}{e}\sqrt{D}\xi(t), \end{aligned} \quad (4.4.3)$$

where in the last equation we introduced the fluctuating variable  $\xi(t) = (I_3 - I_1)/\sqrt{D}$  that is governed by a white noise spectrum  $\langle \xi(t)\xi(t') \rangle = 2\delta(t - t')$ . The phase difference is thus brought into a Langevin type form with a random variable  $\xi$  so that after taking the limit of  $\tau \rightarrow 0$  we have

$$\dot{\phi}(t) = -\frac{\varepsilon}{\hbar} + (1 - f)\frac{2\pi}{e}\sqrt{D}\xi(t). \quad (4.4.4)$$

Starting from the Langevin form a Fokker-Planck equation for the underlying probability distribution  $P(\phi, t)$  of the phase  $\phi$  can be readily de-

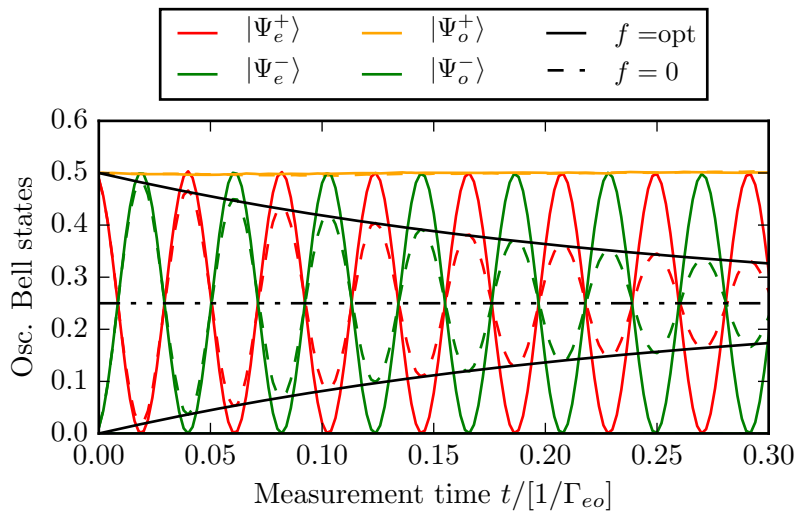


Figure 4.4.1: The amplitudes of the four Bell states as defined in section 4.1.1. For symmetric bias energies the even Bell states oscillate while the odd ones stay stable. Enveloping the oscillations the intrinsic dephasing within the even subspace leads to a decay of coherence if no feedback ( $f = 0$ , dashed lines) is present. Including the Markovian feedback at optimal strength ( $f = 1$ , solid lines) cancels the intrinsic dephasing so that stable oscillations are achieved. Cf. [22]

rived [61],

$$\begin{aligned}
\frac{d}{dt}P(\phi, t) &= (1-f)^2 \left(\frac{2\pi}{e}\right)^2 D \frac{d^2}{d\phi^2} P(\phi, t) \\
&= \frac{(1-f)^2 4\Gamma_{\text{eo}}}{\tau} \frac{d^2}{d\phi^2} P(\phi, t) \\
&= \frac{\Gamma_{\text{ee}}(f)}{\tau} \frac{d^2}{d\phi^2} P(\phi, t).
\end{aligned} \tag{4.4.5}$$

Here we have used the previously derived dephasing rate (4.3.22) and derived the diffusion coefficient  $\Gamma_{\text{ee}}(f)/\tau$  for the phase difference within the even subspace given a fluctuating detector outcome  $I_3$  that induces the Langevin dynamics. As mentioned above the dephasing rate between even and odd subspace is the same as the rate in which entanglement is created. We therefore make the rate  $\Gamma_{\text{eo}}$  the unit to measure  $\Gamma_{\text{ee}}$  against so that for optimal feedback we have to require that

$$\frac{\Gamma_{\text{ee}}(f)}{\Gamma_{\text{eo}}} = 4(1-f)^2 \rightarrow 0. \tag{4.4.6}$$

As expected from the preceding analysis a feedback parameter of  $f = 1$  leads to a vanishing dephasing rate in the even subspace while switching off the feedback mechanism via  $f = 0$  recovers the original dephasing rate (4.3.22). With the optimal feedback parameter identified a Markovian feedback loop can be introduced in the Mach-Zehnder interferometer measurement based on these calculations alone. In experimental situations it seems, however, more practical to exploit the proportional feature of this direct feedback to tune the feedback strength to give optimal results. This is particularly useful as the dephasing rate approaches zero quadratically with  $f$  approaching one so that an arbitrarily long coherence time can be reached for close to optimal feedback parameter  $f$ .

With the introduction of the Markovian feedback loop we have now presented a scheme to implement a true parity meter with a Mach-Zehnder interferometer where the mathematically induced additional measurement back-action is taken care of. However, there are plenty of other sources of dephasing mechanisms such as the initialization of the qubits, external influences and the fluctuations induced by constantly changing the bias energies of the qubit in the feedback loop. In the following we therefore address these additional sources of dephasing that may lead to a mixing of both parity subspaces by the means of employing a second measurement that drives a second feedback loop. As the dephasing is now not necessarily directly related to the measurement outcome but there is a more complicated relationship we turn to use Bayesian feedback as introduced in chapter 3.4.2 and expand this notion to the measurement of parity.

## 4.5 Bayesian feedback

In the previous analysis we have turned the Mach-Zehnder interferometer into a true parity meter without architecture-dependent extra dephasing in the even subspace. But there is an abundance of other sources of noise that do not directly link to the specific nature of a Mach-Zehnder interferometer. To stabilize a maximally entangled Bell state, or to at least stabilize a state with a decent amount of entanglement, we have to find a way of dealing with these sources of noise or the desired state will not exist for long.

As explained above the tunneling components of the Hamiltonian can be ignored as a sufficiently strong parity measurement suppresses the mixing of parity states due to the Hamiltonian in a quantum Zeno effect type of way. The same can be said about noise in the parameter  $\Delta$ . The effect of this noise can be split into a fluctuating mixing of parity spaces, that again is dealt with by a suitable measurement strength  $\Gamma_{e_0} \gg \Delta/\hbar$ , and fluctuations within each parity subspace.

On the other hand the Markovian feedback introduced in the previous section amounts to continuously changing the bias energies of the qubits so that necessarily some noise is induced here as well. The noise due to this initialization can be lumped together with the tunneling noise within the parity subspaces to effectively give one noise source per qubit

$$H_{\text{qb}} = \sum_{i=1,2} \left( \frac{\varepsilon_i}{2} + \xi_i(t) \right) \sigma_z^i, \quad (4.5.1)$$

where we assume non-symmetric bias energies as also the noise of each qubit in this case is independent. Notice that the back-action we dealt with in the previous section affected both qubits symmetrically due to the specific tuning of the Mach-Zehnder interferometer as a parity meter.

We introduced the noise of the system in the form of a fluctuating parameter  $\xi_i(t)$  with  $i = 1, 2$  that is drawn from a white noise distribution of width  $D_\xi$  assumed to be equal for both qubits. Consequently the additional noise sources lead to an additional dephasing within each subspace that is characterized by the dephasing rate  $\Gamma_\xi$ .

Now this dephasing obviously destroys any entanglement that is present in the system and therefore counteracts the creation of Bell states under the parity measurement. It is important to notice that this dephasing mechanism does not just cancel the entangling effect of the parity measurement but rather destroys the phase coherence of the qubits themselves so that Bell states can no longer be created via parity measurement.

The fact that the noise indeed does not affect the parity as we still have  $[H_{\text{qb}}, P] = 0$  is already a hint that the parity measurement result is not enough to create a feedback loop that cancels this type of dephasing. We therefore have to turn away from the Markovian feedback used up to

now and employ the technically more challenging but at the same time more powerful Bayesian feedback as introduced in chapter 3.4.2.

As mentioned, the parity measurement does not infer any information about the decoherence within each qubit. To employ a Bayesian feedback loop we therefore introduce another measurement of the form

$$P_x = \sigma_x \otimes \sigma_x \quad (4.5.2)$$

that gathers information about the fluctuating motion of each qubit. Indeed this operator can be used to distinguish between the states within each parity subspace while having the useful property of commuting with the parity itself  $[P, P_x] = 0$  so that the newly introduced measurement does not interfere with the parity measurement and the creation of entanglement.

This commutativity also makes possible an implementation of the second measurement without the addition of another detector in the Mach-Zehnder interferometer. One can pulse the parity measurement and rotate the qubits about  $\pi/2$  between all pulses so that the parity current alternates between measuring  $P$  and  $P_x$ .

As the additional measurement does not mix the parity subspaces the density matrix elements of the double qubit system connecting different parity states decay on the scale of the measurement time  $1/\Gamma_{e0}$  so that the state of the system is characterized by the two phases

$$\phi_e = \arctan \frac{\text{Re}\rho_{\uparrow\uparrow,\downarrow\downarrow}}{\text{Im}\rho_{\uparrow\uparrow,\downarrow\downarrow}} \quad (4.5.3)$$

$$\phi_o = \arctan \frac{\text{Re}\rho_{\uparrow\downarrow,\downarrow\uparrow}}{\text{Im}\rho_{\uparrow\downarrow,\downarrow\uparrow}}, \quad (4.5.4)$$

where  $\rho_{ss',s's'}$  is the double qubit density matrix spanned by the computational basis of the two qubits  $s, s' = \uparrow, \downarrow$ . This phase is the equivalent of the feedback phase (3.4.6) derived in the above introduction to Bayesian feedback 3.4.2. While in the formalism of chapter 3.4.2 one phase described the state of the qubit here we have two phases describing the state of the system. We proceed to show, however, that a joint feedback mechanism can be devised that incorporates both these phases and therefore cancels the dephasing in both subspaces simultaneously. One might object that for any single measurement the parity detection leads to a decay of the density matrix elements pertaining to the even or odd parity subspaces, depending on the measurement outcome. Any single measurement is therefore characterized by only one of these phases. Notice, however, that the dephasing introduced by the additional noise of (4.5.1) leads to a decoherence of the qubits even *before* the parity states are clearly separated. Any meaningful feedback mechanism therefore has to be employed from the beginning of the measurement and therefore need to include both phases.

As presented above we continue to compare the phases (4.5.3, 4.5.4) with the optimal values of a free evolution

$$\begin{aligned}\Delta\phi_e(t) &= (\varepsilon_1(t) + \varepsilon_2(t))\tau - \phi_e(t) \\ \Delta\phi_o(t) &= (\varepsilon_1(t) - \varepsilon_2(t))\tau - \phi_o(t).\end{aligned}\tag{4.5.5}$$

Here we have to understand the bias energies  $\varepsilon_1(t)$  and  $\varepsilon_2(t)$  as having the Markovian feedback (4.4.2) already included. Additionally to this Markovian adjustment the bias energies then have to be tuned in the Bayesian fashion to counter the discrepancy (4.5.5) via

$$\varepsilon_1(t) \rightarrow \varepsilon_1(t) + f_x \frac{\phi_e(t) + \phi_o(t)}{2}\tag{4.5.6}$$

$$\varepsilon_2(t) \rightarrow \varepsilon_2(t) + f_x \frac{\phi_e(t) - \phi_o(t)}{2}.\tag{4.5.7}$$

The Bayesian feedback mechanism can therefore be included with only one feedback parameter  $f_x$ . This greatly simplifies the implementation while it still remains experimentally challenging.

With the inclusion of Bayesian feedback into the measurement any desired maximally Bell state can be synthesized and stabilized. In the following we simulate these procedures with the help of numerical implementation of a von Neumann measurements.

## 4.6 Numerical simulations

In the previous section we introduced the Mach-Zehnder interferometer tuned as a parity meter to produce maximally entangled Bell states from two previously unentangled qubits. The specifics of the measurement architecture and the naturally occurring noise sources were shown to lead to a break down of these functionalities and were countered by the inclusion of a direct feedback (section 4.4) to address the architecture specific intrinsic dephasing and a Bayesian type of feedback (section 4.5) to address the general experimental noise sources.

In the present section we now simulate the measurement and the presented feedback loops numerically. To implement these simulations we start by incorporating the parity measurements. The inclusion of the feedback mechanisms then is straightforward. We start by considering two consecutive points in time (labeled  $i-1$  and  $i$ ) separated by the time  $\tau$  that fulfills the condition (4.3.17), so that in particular the measurement back-action onto the state is described by equation (4.3.19), while still small compared to the measurement time  $1/\Gamma_{eo}$ , so that quasi continuous feedback is possible. After the time  $\tau$  the system changes due to the free evolution of its Hamiltonian and a measurement result  $I_3^i$  is read out from the detector. This read-out of the detector is simulated by drawing a random value for  $I_3^i$  from

the probability distribution of  $I_3$ . The drawing of this value amounts to a projection of the detector state so that the resulting state of the double qubit system is now described by equation (4.3.19). Depending on the choice of Hamiltonian, i.e., the choice of which noise source to include, at this point the feedback loops can be included.

#### 4.6.1 Markovian feedback

We begin by dealing with the unavoidable intrinsic dephasing. As after drawing a random measurement outcome  $I_3^i$  the new system state is determined the bias energies are now adjusted via the Markovian feedback so that

$$\varepsilon_{i+1} = \varepsilon_i + f\pi (I_3^i - I_1) \frac{\hbar}{e}, \quad (4.6.1)$$

the discretized version of equation (4.4.2), becomes the bias energy for the next circle. As in the present case the measurement operator  $\hat{P}$  commutes with the Hamiltonian, the evolution and the measurement can be treated consecutively. Notice, however, that in the case of a general Hamiltonian (with tunneling within the qubits for instance) this assumption still holds for  $\tau \rightarrow 0$ .

Figure 4.4.1 shows the amplitudes of all Bell states without feedback and with optimal feedback strength. The odd states are stable as expected while the even states decay over time if the dephasing is not prevented by the Markovian feedback loop. While an optimal feedback strength cancels the intrinsic dephasing exactly any inclusion of feedback delays the dephasing as shown in figure 4.6.1. Operating the feedback loop close to the optimum therefore guarantees arbitrarily long coherence. Figure 4.6.2 then shows that for any finite dephasing

$$\frac{\Gamma_{ee}(f)}{\Gamma_{eo}} = 4(1-f)^2 \quad (4.6.2)$$

the creation of entanglement peaks at a finite time and subsequently the loss of coherence within the qubits prohibits any further entanglement. Assuming now optimal feedback to cancel the intrinsic dephasing we next turn to the additional dephasing mechanisms presented in section 4.5 and the implementation of a corresponding feedback loop.

#### 4.6.2 Bayesian feedback

As introduced in section 4.5 to work against the dephasing within each subspace due to fluctuating parts in the Hamiltonian we implement a Bayesian feedback loop based on an additional measurement of the operator  $P_x = \sigma_x \otimes \sigma_x$ . As this operator commutes with the parity operator we simulate this measurement directly after the parity measurement. The measurement



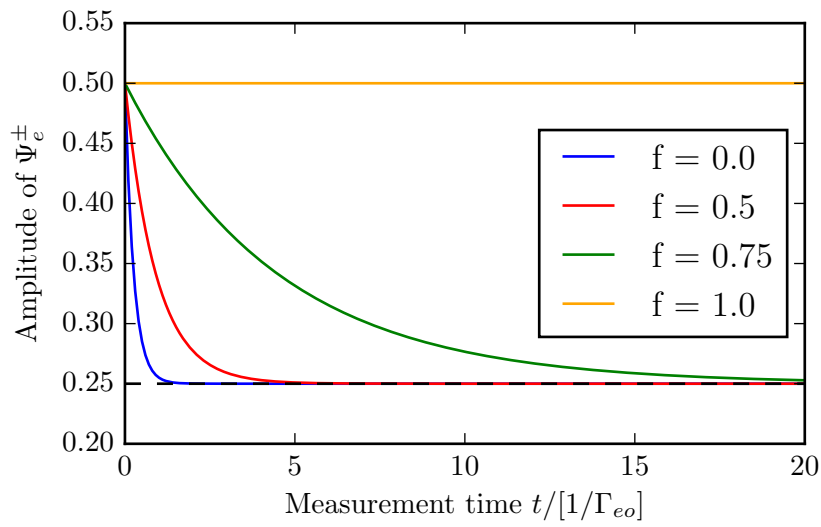


Figure 4.6.1: The decaying amplitudes of the oscillating Bell states within the even subspace (cf. section 4.1.1) are shown for different values of the feedback parameter  $f$ . No feedback leads to a quick loss of coherence while the optimal feedback of  $f = 1$  stabilizes the oscillation given that no other source of noise or decoherence is present. The different dephasing times translate into different amounts of entanglement created as presented in figure 4.6.2. The time is measured in units of the measurement time  $1/\Gamma_{eo}$ . Cf. [22]

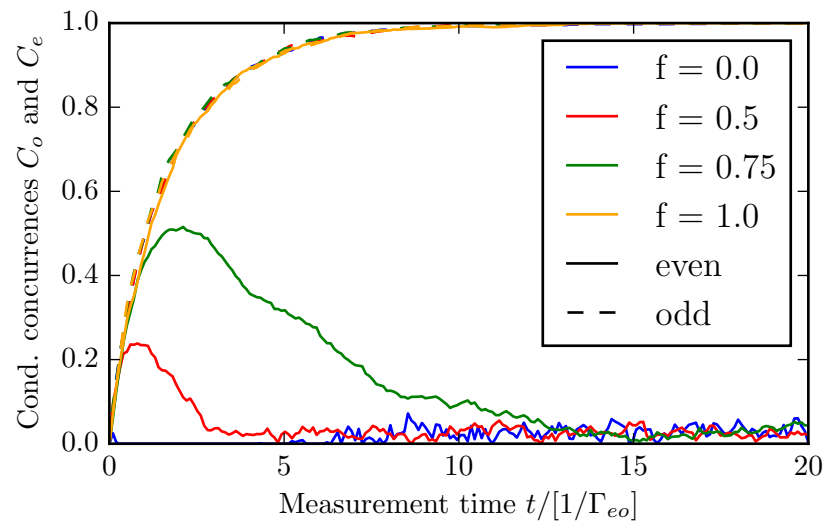


Figure 4.6.2: The amount of entanglement measured as the conditional concurrence is plotted for the even (solid lines) and odd (dashed lines) subspace. While creation of entanglement in the odd subspace is independent on the inclusion of a feedback loop the even subspace fails to stabilize entanglement without feedback. As the feedback parameter  $f$  approaches the optimal value  $f = 1$  the amount of created entanglement increases. However, only the optimal feedback parameter stabilizes the entanglement indefinitely. The time is measured in units of the measurement time  $1/\Gamma_{eo}$ . Cf. [22]

is simulated again by a von Neumann type of measurement procedure with a coupling parameter  $\lambda_x$  and a detector noise  $D_x$ . The measurement rate of this second measurement therefore is given by  $\Gamma_x = \lambda_x^2/D_x$  [50].

The measurement procedure hence amounts to drawing a random variable from the distribution pertaining to the parity measurement, updating the state accordingly, then drawing another random variable pertaining to the  $P_x$  measurement and finally again updating the state.

After both measurements are performed, the phases (4.5.3, 4.5.4) are calculated and the bias energies are adjusted to incorporate both Markovian and Bayesian feedback via

$$\varepsilon_1^{i+1} \rightarrow \varepsilon_1^i + f\pi (I_3^i - I_1) \frac{\hbar}{e} + f_x \frac{\phi_e^i + \phi_o^i}{2} \quad (4.6.3)$$

$$\varepsilon_2^{i+1} \rightarrow \varepsilon_2^i + f\pi (I_3^i - I_1) \frac{\hbar}{e} + f_x \frac{\phi_e^i - \phi_o^i}{2}. \quad (4.6.4)$$

This loop is continued until the parity measurement clearly distinguishes both parity spaces. After postselection based on the parity measurement result the system is averaged over many realizations. This postselection allows one to track the average creation of entanglement in both subspaces.

As mentioned in section 4.5, the relevant dephasing is characterized by the dephasing rate  $\Gamma_\xi$ . While the qualitative features of Bayesian feedback saturate with a feedback parameter  $f_x \approx 1$  the strength of the measurement plays a significant role [46]. Figure 4.6.3 therefore shows the created entanglement (given by the conditional concurrence) for different measurement rates  $\Gamma_x$  and for several noise strengths  $\Gamma_\xi$ . While the absence of noise in the Hamiltonian renders the second feedback loop obsolete for any finite dephasing a finite amount of entanglement is still created and, importantly, stabilized. Surprisingly even for significant dephasing of the order of the parity measurement rate the implementation of a Bayesian feedback loop secures a decent amount of entanglement. This partial entanglement can then be used via the entanglement distillation protocol introduced in chapter 2.

Importantly, the implementation of both Markovian and Bayesian feedback loops allows for the on-demand creation of entangled states as for any parity measurement outcome a stable state is produced. Figure 4.6.4 shows that even and odd subspaces are indeed on equal footing as the amount of entanglement created is the same for any strength of dephasing. This amounts to a fidelity of theoretically 100% so that the effectivity of a parity meter to create entanglement is greatly improved.

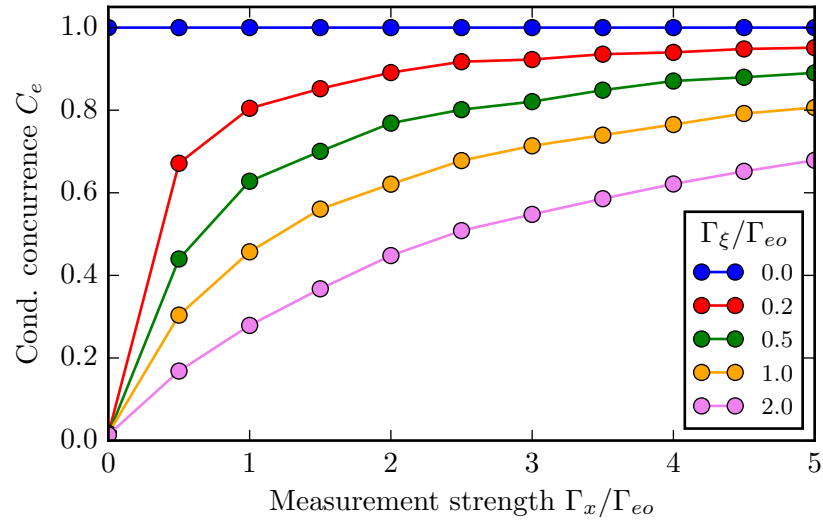


Figure 4.6.3: Deterministic creation of stable entangled states in the presence of external noise. The asymptotic conditional concurrence  $C_e$  is plotted for various measurement strengths given by the measurement rate  $\Gamma_x$  normalized by the dephasing/measurement rate  $\Gamma_{eo}$ . Different strength of external noise  $\Gamma_\xi$  are shown, again normalized by the parity measurement rate. For no external noise the Markovian feedback, that is included in all measurements, is sufficient to create fully entangled Bell states and no Bayesian feedback is necessary (blue line). For any finite environmental noise the Bayesian feedback loop allows for the creation and stabilization of partially entangled states. Cf. [22]

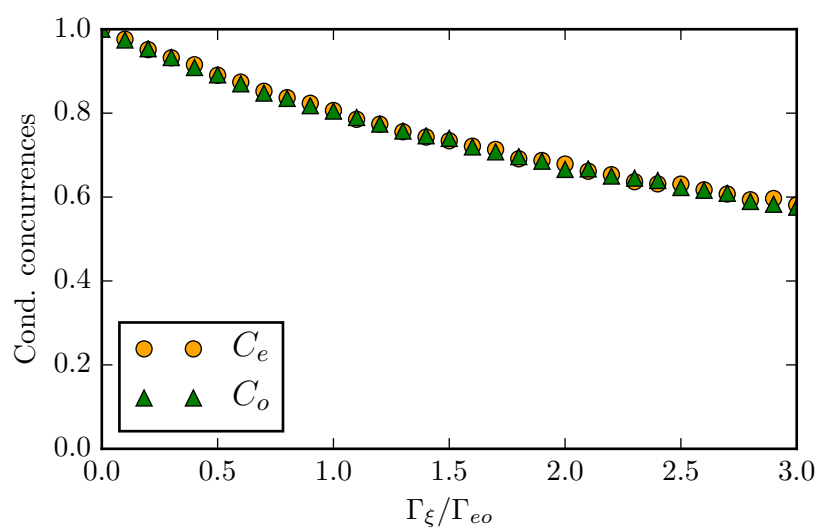


Figure 4.6.4: The asymptotic conditional concurrences are plotted against the strength of external noise. For noise strength smaller or of the order of the measurement strength  $\Gamma_{eo}$  a significant amount of entanglement can be stabilized with the inclusion of the presented Bayesian feedback. Both parity subspaces are on equal footing due to the prior inclusion of a Markovian feedback. Cf. [22]



## Chapter 5

# Summary and conclusions

We have presented the implementation of a parity measurement between two quantum bits to create entanglement. The specific architecture used was an electronic Mach-Zehnder interferometer that is capacitively coupled to two double quantum dots that form the qubits. It was previously shown that the interferometer can be tuned in such a way that the flux of electrons through its arms constitutes a parity measurement. With a properly chosen initial product state the resulting parity eigenstates are fully entangled Bell states. It was predicted theoretically and confirmed experimentally, however, that this specific architecture of a parity meter induces intrinsic dephasing within the even parity subspace. The creation of entanglement is therefore limited to the odd parity subspace so that the fidelity can maximally reach 50%.

Here we have shown that the underlying dephasing mechanism is closely connected to the parity measurement outcome so that a feedback loop can be implemented that counters said dephasing. We proved analytically and confirmed with subsequent numerical simulations that the incorporation of this feedback loop indeed leads to the creation of full entangled Bell states in both parity subspaces so that the theoretical fidelity is increased to 100%. It is important to notice that only with the inclusion of the presented feedback mechanism the Mach-Zehnder interferometer can be indeed tuned to represent a true parity meter.

While the intrinsic dephasing was shown to be a direct consequence of the specific measurement architecture, additional noise sources are present in any experimental setup. To stabilize the creation of entanglement also in such general noisy environments we implemented a second feedback loop. This feedback loop is based on the Bayesian update through information about the system acquired by a second measurement. Simulations done including both feedback mechanisms show that indeed entanglement can be created and stabilized for any realization of the measurement setup.

As an appropriate measure for the amount of created entanglement, we introduced the conditional entanglement concurrence that makes use of the

parity measurement outcome. In a noisy environment the stabilized entanglement is not maximal and decreases with increasing noise strength. However, even a partially entangled pair of qubits is of great use from a quantum informational point of view, as from an ensemble of partially entangled qubit pairs a subset of fully entangled pairs can be distilled with well known protocols.

We conclude therefore that we have presented a proof-of-concept for the fundamental building block of a quantum computational system. While experimental realization remains challenging, the introduced concepts can be applied and expanded to different solid-state architectures.



## Part II

# Ultrafast thermalization and equilibration dynamics



# Chapter 6

## Introduction

Much like psychologists distressing their subjects to study the genuine reactions of human nature, physicists learn about the behavior of matter by exciting it out of its equilibrium state. The subsequent return to a steady configuration, the *relaxation process*, then shines light on the equilibrium itself as well as the interactions governing its approach.

With the development of ultra-fast pulse lasers in the femto second regime a whole new world of relaxation processes emerged to be explored. In particular electron-electron and electron-phonon scattering processes could be studied in real time [62, 63, 64, 65] and the ultra-fast dynamics of magnetization became experimentally accessible [66, 67, 68, 69]. The newly achieved access to ultra-fast phenomena was of particular interest as the time-scale for establishment of quasi-equilibria tends to be of the order of femto to pico seconds. This allows for a deeper examination of non-equilibrium effects and the connected establishment of equilibrium. Furthermore the scattering time of a particle with impurities in a typical metal is of the order of several ten femto seconds as well. A transport analysis of a propagating excitation within the ultra-fast time scale therefore gives insights into the different involved transport mechanisms.

In the present work we apply the Boltzmann formalism to study the ultra-fast relaxation processes of a quasi-particle excitation due to impurity scattering, electron-electron interactions and collisions with the surrounding phonon bath. The Boltzmann approach is of particular use in this context as it allows for rather simple separation of the different contributing effects. For instance a dimensional approximation regarding the symmetry of the sample can readily be included. In the present text we focus on thin strip architectures that are translationally invariant in two directions, effectively reducing the transport into one dimension.

An excited quasi-particle pair is created by lifting a quasi-particle from an energy state below the Fermi energy to above and thus leaving a corresponding hole below the surface. In the first approximation of Fermi liquid theory

this excitation is treated as moving independently. However, the created excitation then starts to scatter with impurities, such as lattice imperfections, so that the initial directional momentum is smoothed out. The quasi-particle changes its type of transport from initially unperturbed ballistic motion to diffusive expansion.

We show that the impurity scattering is the main driving force of this transition and defines its timescale. While the analysis of anomalous diffusion does of course include super-diffusive (and sub-diffusive) behavior, the diffusion exponent is typically assumed to be constant [70]. Here we present a simple model to describe the dynamic change of the diffusion exponent from ballistic to linear diffusive behavior. Importantly the derived ballistic-diffusive equation allows for an analytical solution of the transition previously only described by ab-initio calculations [69].

As the elastic collisions mediate the transition between ballistic and diffusive transport, but do not affect the distributions energy space, we continue to include electron-electron scattering in the Boltzmann formalism. An excitation scatters with an electron below the Fermi sea and transfers energy due to the electron-electron collisions. The gain of energy by the collision partner lifts the particle above the Fermi level as well, creating a second excitation. The subsequent cascade of excited particles losing energy by exciting further particles from the Fermi sea leads to the asymptotic establishment of a new thermal distribution. Being interested in this equilibration within energy space we derive a coupled differential equation for the energy distribution that describes the thermalization of a non-equilibrium distribution. Discretizing energy space we reduce the equation to an eigenvalue problem that can be solved in a quasi-analytical manner.

For the analysis of equilibration of electron and phonon baths the two temperature model showed to be of great use [64, 65]. It has been applied, among others, to noble metals [71, 72, 73, 74], heavy fermion compounds [75] and magnetic thin films [66].

In its wake, Kaganov *et al.* calculated the energy exchange between electron and phonon systems, each at their respective temperatures, and Anisimov *et al.* used these findings to develop the two temperature model itself [76, 77]. The free electron model assumption of Kaganov *et al.* was relaxed by the treatment of Allen [78].

However, this take on the two temperature model presupposes both baths to be in quasi-equilibrium. This assumption is weary at best, as electron-electron relaxation rates are of similar order of magnitude as the equilibration time between electron and phonon baths [73, 79, 80].

Several extensions and refinements have thus been suggested. On one hand, the two temperature model can be extended by including a non-thermal electron distribution [81] within a relaxation time approximation [71, 82]. The implicit assumption is for the main part of the electron distribution to stay in quasi-equilibrium while the modulating non-thermal behavior is

limited to a fraction of the full distribution. On the other hand, a full solution of the coupled system using the Boltzmann formalism can be used to incorporate electron-electron scattering at the same time as electron-lattice relaxation processes [83]. While this requires less rigorous approximations, the phenomenological simplicity of the two temperature model is lost.

Here we extend the two temperature model by making use of the solution obtained from analyzing the equilibration of the electron system. We fit the distribution during thermalization and include the dynamics of the equilibration into the derivation of the two temperature model. Assuming that the interaction between electrons and phonons does not change the dynamics of the thermalization, but only acts as an effective energy drain from the higher electronic temperature to the lower phonon temperature, the extended two temperature model reflects the thermalization effects in a delayed interaction between electron and phonon bath. This delay recovers prior results obtained by a solution of the full Boltzmann problem [83] while still retaining the phenomenological simplicity of the two temperature model.

As the weapon of choice in the following chapters is the Boltzmann equation, we start by introducing the formalism in Chapter 7. Examples of single and two particle collisions and the corresponding collision integrals are presented with a focus on generality. Equipped with the necessary background we continue to include the scattering off impurities in Chapter 8 to derive a ballistic-diffusive equation. The formalism is then extended in the following Chapter 9 by adding electron-electron interactions. The resulting energy-space equation describes the dynamics of thermalization. Introducing the two temperature model in the last Chapter 10 we are provided with an approachable way to illustrate electron-phonon equilibration. Subsequently, we use the previously derived dynamics of thermalization to extend this model to include initial non-equilibrium evolution as well.



## Chapter 7

# Boltzmann equation

Before we start with the on hands calculation of any given problem the necessary tools have to be supplied. In the present part of this work we labor with the Boltzmann formalism. It is now therefore the time to introduce at least those parts that turn later out to be useful for our analysis. As there are countless introductions to the Boltzmann equation we also limit ourselves to these necessary technical details and refer the reader to the standard literature [84, 85, 86, 87, 88]. For the familiar reader the present chapter will probably have hidden nothing too exciting.

### 7.1 Classical part

Fundamentally the Boltzmann equation has two sides, the classical and the quantum, that can be discussed quite separately. The classical part of the Boltzmann equation can be considered to be sort of a continuity equation [89]. The space it adheres to is the single particle phase space and the solution it considers is the phase space density  $f(\mathbf{r}, \mathbf{p})$ . In the following we show the derivation of the Boltzmann equation from this generalized continuity equation. We denote the six dimensional phase space vector  $(\mathbf{r}, \mathbf{p})$  as  $x_\mu$ , so that the phase space density is  $f(x_\mu)$  and the flux in phase space  $\dot{x}_\mu f(x_\mu)$ . In integral form the continuity equation states that, for any volume of phase space  $V$ , the change of particles within this volume is due to a flux through its surface are. Or formally

$$\frac{\partial}{\partial t} \int_V dx_\mu f(x_\mu) = - \int_{\partial V} dx_\mu (\dot{x}_\mu f(x_\mu)) \cdot \hat{n}, \quad (7.1.1)$$

where  $\hat{n}$  denotes the unit vector normal to the surface  $\partial V$ , pointing outwards (hence the minus sign in front). Applying the Gaussian divergence theorem to the right hand side we have the continuity equation in integral form

$$\frac{\partial}{\partial t} \int_V dx_\mu f(x_\mu) = - \frac{\partial}{\partial x_\mu} \int_V dx_\mu (\dot{x}_\mu f(x_\mu)). \quad (7.1.2)$$

As this equation must hold for any volume  $V$ . This restriction, or rather universality leads to the differential form

$$\frac{\partial}{\partial t} f(x_\mu) + \frac{\partial}{\partial x_\mu} (\dot{x}_\mu f(x_\mu)) = 0. \quad (7.1.3)$$

Now the second term is a divergence in the six dimension of phase space and with the usual rules of differentiation  $\nabla \cdot (\mathbf{cb}) = (\nabla \cdot \mathbf{b})c + (\nabla c) \cdot \mathbf{b}$  we rewrite

$$\frac{\partial}{\partial t} f + \dot{x}_\mu \frac{\partial}{\partial x_\mu} f + \left( \frac{\partial}{\partial x_\mu} \dot{x}_\mu \right) f = 0. \quad (7.1.4)$$

Remembering the definition of  $x_\mu$  and applying now our knowledge of classical Hamilton mechanics<sup>1</sup> we see that the last term of equation (7.1.4) vanishes. In particular we have

$$\frac{\partial}{\partial x_\mu} \dot{x}_\mu = \left( \frac{\partial}{\partial \mathbf{r}}, \frac{\partial}{\partial \mathbf{p}} \right) \cdot (\dot{\mathbf{r}}, \dot{\mathbf{p}}) = \frac{\partial}{\partial \mathbf{r}} \frac{\partial H}{\partial \mathbf{p}} + \frac{\partial}{\partial \mathbf{p}} \left( -\frac{\partial H}{\partial \mathbf{r}} \right) = 0. \quad (7.1.5)$$

Keeping now the separation of space and momentum variables we arrive at what can be called the classical part of the Boltzmann equation

$$\frac{\partial}{\partial t} f(\mathbf{r}, \mathbf{p}) + \dot{\mathbf{r}} \cdot \frac{\partial}{\partial \mathbf{r}} f(\mathbf{r}, \mathbf{p}) + \dot{\mathbf{p}} \cdot \frac{\partial}{\partial \mathbf{p}} f(\mathbf{r}, \mathbf{p}) = 0. \quad (7.1.6)$$

The connection to Hamilton mechanics already points to the role of  $\mathbf{p}$  as being the canonical momentum conjugate to  $\mathbf{r}$ . In the common case of external forces independent of the velocity  $\dot{\mathbf{r}}$  the canonical momentum is the same as the kinetic one and we can identify  $\dot{\mathbf{p}} = \mathbf{F}$ . But in the case of velocity dependent forces, as in the presence of a magnetic field, canonical momentum differs from kinetic momentum. It turns out, however, that in this particular case the phase space volume  $d\mathbf{p}d\mathbf{r}$  is the same for canonical and kinetic momentum. As the particle number has to be equal as well, we may identify phase space density of canonical and kinetic momentum and thus arrive at the same equation as (7.1.6) for the kinetic momentum. Including thus the important special case of magnetic field we write as the commonly used classical part of the Boltzmann equation

$$\frac{\partial}{\partial t} f(\mathbf{r}, \mathbf{p}) + \dot{\mathbf{r}} \cdot \frac{\partial}{\partial \mathbf{r}} f(\mathbf{r}, \mathbf{p}) + \mathbf{F} \cdot \frac{\partial}{\partial \mathbf{p}} f(\mathbf{r}, \mathbf{p}) = 0. \quad (7.1.7)$$

This classical part, as is presented below, is also the left hand side of the full Boltzmann equation that includes instantaneous changes of the phase space density due to what is summarized in the physically appealing concept of collisions. Before we introduce the collision mechanisms in detail we quickly shed light on a fundamental approximation of the distribution itself, the so called two term approximation.

<sup>1</sup> $\dot{\mathbf{r}} = \frac{\partial H}{\partial \mathbf{p}}$  and  $\dot{\mathbf{p}} = -\frac{\partial H}{\partial \mathbf{r}}$  with the Hamilton function  $H(\mathbf{r}, \mathbf{p})$ .



## 7.2 Two term approximation

With classical and collision parts included, the Boltzmann equation is notoriously difficult to solve as it is an integro-differential equation of seven dimensions, three of each space and momentum and one of time. This has led to extensive advance in approximative treatments as it was discovered that many significant results can be obtained by these simpler approaches. Here we make two essential assumptions about the system at hand. First the spacial dependency is reduced to effectively one dimension, in particular the  $z$ -direction, by treating the other two as translationally invariant. This is the typical approximation of a thin film geometry. The translational symmetry of space then directly hints at the second approximation concerning the momentum space. With respect to this we expand the distribution function in spherical harmonics while only keeping the two lowest terms in the expansion, naming them the isotropic and the anisotropic part respectively. Treating the approach of an excited system towards equilibrium we separate the equilibrium distribution function such that

$$f(\mathbf{k}, \mathbf{r}, t) \approx f^{\text{eq}}(k, z, t) + \delta f^0(k, z, t) + \cos \theta \delta f^1(k, z, t), \quad (7.2.1)$$

where  $\theta$  denotes the angle between velocity and  $z$ -axis, and the translational invariance has been included. The above approximation is commonly known as the two term approximation, although often the isotropic part is equated with the equilibrium distribution. In the present text we are concerned with systems that are not subject to any external field so that  $\mathbf{F} = 0$ . Plugging in this and the two term approximation into the classical Boltzmann equation (7.1.7) we have

$$\begin{aligned} & \frac{\partial}{\partial t} \delta f^0(k, \mathbf{r}, t) + \cos \theta \frac{\partial}{\partial t} \delta f^1(k, \mathbf{r}, t) \\ & + v \cos \theta \frac{\partial}{\partial z} \delta f^0(k, \mathbf{r}, t) + v \cos^2 \theta \frac{\partial}{\partial z} \delta f^1(k, \mathbf{r}, t), = 0 \end{aligned} \quad (7.2.2)$$

for the left hand side as the Boltzmann equation vanishes for the equilibrium distribution. As hinted the right hand side contains the so called collision terms that lead to a instantaneous and non-continuous change of phase space density. In the following we introduce the main processes we are concerned with in the present text.

## 7.3 Collision part

Up to now we considered a classical single particle system with the help of its phase space density. The governing physics of this system was restricted by the continuity of phase space volume. While this description is

rather cumbersome for purely classical systems it has the advantage that we may now easily introduce enhancements, using a common language, that are connected to very different physical processes. Mathematically these enhancements amount to an instantaneous change of phase space density that is not due to external forces. We are therefore adding sources (and sinks) to the phase space.

This rather abstract concept has a very accessible physical interpretation, that is collisions. Thinking of these instantaneous changes of phase space density in the concept of collisions already points to the first restriction in these changes. To conform with common conception of a collision we demand that these changes happen at a defined point in physical space, i.e. at a fixed  $\mathbf{r}$ , the very nature of a collision is two distinct object finding each other occupying the same location in space. This restriction, that all instantaneous cause and effect shall be placed at the same location, is commonly referred to as the locality principle of nature and we shall make no exception to this fundamental law of nature in this work.

Other common concepts as number, momentum and energy conservation all can be readily applied to the language of collisions. And with a little flexibility in the interpretation on what processes can be considered collisions also the interaction between different types of (quasi)-particles can be included.

We write these changes due to sources and sinks in phase space on the right hand side of the Boltzmann equation that has previously conveniently been left empty. As the exact nature of these processes still has to be clarified a place holder will do for now. The Boltzmann equation in its most general form than reads

$$\frac{\partial}{\partial t} f(\mathbf{r}, \mathbf{p}) + \dot{\mathbf{r}} \cdot \frac{\partial}{\partial \mathbf{r}} f(\mathbf{r}, \mathbf{p}) + \mathbf{F} \cdot \frac{\partial}{\partial \mathbf{p}} f(\mathbf{r}, \mathbf{p}) = \left( \frac{\partial f}{\partial t} \right)_{\text{coll}}, \quad (7.3.1)$$

and the approximations of the previous section can be applied. As the notion of collisions is introduced to be applied to several different types of quasi-particle interactions it is of some use to see how these can be classified.

### 7.3.1 Single particle collisions

Let us first consider a process that involves moving phase space density from one point  $(\mathbf{r}, \mathbf{p})$  to another  $(\mathbf{r}, \mathbf{p}')$ . This surly changes the density at both points. If this change is the only change due to the considered process and only depends on the coordinates  $\mathbf{p}$  and  $\mathbf{p}'$ , we speak of a single particle collision. The physical concepts that lead to single particle collisions are for instance scattering off impurities or particles of a different phase space.

Before diving into the details of actual single particle processes that we intend to consider later on, let us make some general remarks. Most importantly, any processes involving collisions shall be regarded only in the

stochastical mean. This allows us to speak meaningfully of a *rate of change* of the density  $f(\mathbf{p})$ .<sup>2</sup> The rate of change is then proportional to the target volume element  $d\mathbf{p}'$  as well as the density at the original point  $f(\mathbf{p})d\mathbf{p}$ . Again we may drop the real space part  $d\mathbf{r}$  as it is kept constant. As we consider single particle collisions here the proportionality factor only depends on  $\mathbf{p}$  and  $\mathbf{p}'$  so that the rate of change for a particle being scattered from  $\mathbf{p}$  to  $\mathbf{p}'$  is

$$-w(\mathbf{p}', \mathbf{p}) f(\mathbf{p}) \frac{d\mathbf{p}}{(2\pi\hbar)^3} \frac{d\mathbf{p}'}{(2\pi\hbar)^3}, \quad (7.3.2)$$

where we introduced the common phase space volume factor  $(2\pi\hbar)^3$  to keep  $f$  dimensionless. The minus sign emphasizes that the density at point  $\mathbf{p}$  is reduced. Turning the reasoning above around, the equivalent rate of change for a particle being scattered from a point  $\mathbf{p}'$  to the element around  $\mathbf{p}$  is readily obtained as

$$w(\mathbf{p}, \mathbf{p}') f(\mathbf{p}') \frac{d\mathbf{p}}{(2\pi\hbar)^3} \frac{d\mathbf{p}'}{(2\pi\hbar)^3}. \quad (7.3.3)$$

So that the total change of particles in the phase space volume  $\frac{d\mathbf{p}}{(2\pi\hbar)^3}$  is given by

$$-\frac{d\mathbf{p}}{(2\pi\hbar)^3} \int \frac{d\mathbf{p}'}{(2\pi\hbar)^3} [w(\mathbf{p}', \mathbf{p}) f(\mathbf{p}) - w(\mathbf{p}, \mathbf{p}') f(\mathbf{p}')] \quad (7.3.4)$$

and the change of phase space density, what we earlier kept as a place holder, can finally be written as

$$\left(\frac{\partial f}{\partial t}\right)_{\text{coll}} = - \int \frac{d\mathbf{p}'}{(2\pi\hbar)^3} [w(\mathbf{p}', \mathbf{p}) f(\mathbf{p}) - w(\mathbf{p}, \mathbf{p}') f(\mathbf{p}')]. \quad (7.3.5)$$

The integral involved justifies the common denomination of the above: collision integral. In the present work single particle collisions manifest in two events. The scattering of electrons off impurities inside the crystal, e.g., lattice imperfections, and the emission or absorption of a phonon by an electron. We introduce both cases in the following.

### 7.3.1.1 Impurity scattering

The first and simplest scattering process we consider is the collision of electrons with impurities of the surrounding crystal. Now in the section above we considered a general phase space of quasi-particles. To specify the nature of these quasi-particles to be electrons (in a periodic crystal potential) demands some changes to the general single particle collision integral (7.3.5) that we derived above. On the one hand electrons have a spin that should

<sup>2</sup>As the principle of locality restricts all physics that is involved in a collision to occur at the same space point, we drop the real space dependence for now.

be reflected in the distribution function. As we, however, only treat interactions that do not involve change of spin state in this work, we disregard the spin altogether. This amounts to treating each spin direction to belong to a different pseudo band with no interaction between bands.

The other particularity of electrons that comes to mind and shall be included in our treatment right away is the fact that electrons are Fermions. The Pauli exclusion principle prohibits two electrons to occupy the same state and as we disregarded spin this amounts to occupying the same position in phase space. In the derivation of single particle collisions above we asserted that the rate of change from a phase space point  $\mathbf{p}$  should be proportional to the density at said point. While this is still valid, the exclusion principle introduces a further restriction with regard to the final state. In particular it shall not be occupied. To cut a long story short: An electron can only be scattered from a state that is occupied and only scattered into a state that is unoccupied.

The rate of change thus has to be augmented with a factor  $(1 - f(\mathbf{p}'))$  so that the collision integral takes the form

$$\left(\frac{\partial f}{\partial t}\right)_{\text{coll}} = - \int \frac{d\mathbf{p}'}{(2\pi\hbar)^3} \left[ w(\mathbf{p}', \mathbf{p}) f(\mathbf{p}) (1 - f(\mathbf{p}')) - w(\mathbf{p}, \mathbf{p}') f(\mathbf{p}') (1 - f(\mathbf{p})) \right]. \quad (7.3.6)$$

For elastic scattering this can be further simplified when taking advantage of the then symmetric collision probability  $w(\mathbf{p}', \mathbf{p}) = w(\mathbf{p}, \mathbf{p}')$  so that we have the compact form

$$\left(\frac{\partial f}{\partial t}\right)_{\text{coll}} = - \int \frac{d\mathbf{p}'}{(2\pi\hbar)^3} w(\mathbf{p}', \mathbf{p}) [f(\mathbf{p}) - f(\mathbf{p}')]. \quad (7.3.7)$$

We now assume that the scattering conserves energy and the energy dispersion is isotropic in momentum. It immediately follows that the magnitude of momentum is conserved in the process

$$p = p' \quad (7.3.8)$$

and expanding the distribution function in moments as in the two term approximation

$$f(\mathbf{p}) \approx f^0(p) + \cos \theta_p f^1(p), \quad (7.3.9)$$

gives the form

$$\begin{aligned} \left(\frac{\partial f}{\partial t}\right)_{\text{coll}} &= - \cos \theta_p f^1(p) \int \frac{d\mathbf{p}'}{(2\pi\hbar)^3} w(\mathbf{p}', \mathbf{p}) [1 - \cos \theta_{p'}] \\ &= - \frac{\cos \theta_p f^1(p)}{\tau}, \end{aligned} \quad (7.3.10)$$

that is frequently employed in literature under the name *relaxation time approximation*. The corresponding relaxation time being

$$\frac{1}{\tau} = \int \frac{d\mathbf{p}'}{(2\pi\hbar)^3} w(\mathbf{p}', \mathbf{p}) [1 - \cos \theta_{p'}]. \quad (7.3.11)$$

However, the approach is usually taken from the opposite side by assuming that scattering drives the system that is not far from equilibrium back to its equilibrium state. Hence the collision integral is written as

$$\left( \frac{\partial f}{\partial t} \right)_{\text{coll}} = - \frac{f - f^{\text{eq}}}{\tau} \quad (7.3.12)$$

that reduces to equation (7.3.10) if we identify the zero moment  $f^0$  with the equilibrium distribution  $f^{\text{eq}}$ . The above procedure of expanding the distribution function around the equilibrium is called *linearization* and is almost universally applied in treating collision integrals. The naming becomes more striking and the following examples when the assumption that the deviation from equilibrium, and hence also the magnitude of  $f^1$ , is small allows for disregarding any terms of higher order in  $f^1$ .

Above we treated a process that changes the electronic distribution function due to external influences such as defects in the lattice. Next we bring the lattice itself to life by letting it create its own excitations or quasi-particles, the phonons.

### 7.3.1.2 Phonon scattering

A locally dislocated lattice ion can be treated in the above formalism of an impurity that leads to a scattering of conduction electrons. This implicitly assumes that the ion is shifted from its “normal” position but fixed in time. The lattice ions of a crystal at finite temperature, however, also have degrees of freedom regarding their dynamic shifting around their equilibrium position: the lattice vibrates. Indeed this is the main reason we may speak of the crystal to be at a certain temperature. This deviation of lattice ions from their crystal structure again leads to scattering of electrons. Before we can treat these scattering processes, however, we first start to introduce the formalism of lattice vibrations themselves.

**Phononic vibrations** We introduce a set of suitable coordinates for the description of the lattice vibrations, where we restrict ourselves to crystals with one atomic basis. This part follows rather closely [90]. The results can then be easily generalized to crystals with multi-atomic base. But as the derivational difference is a mere notational one we stick to one atom here.

The position of each lattice site can be written as

$$R_l = \mathcal{X}_l + u_l, \quad (7.3.13)$$

where  $\mathcal{X}_l$  denotes the equilibrium position of the lattice site and  $u_l$  the displacement. For the ease of notation we refrain from emphasizing the vector nature of these terms by printing them in bold. The total potential energy of the distorted lattice can thus be expanded and the lattice Hamiltonian reads

$$\mathcal{H} = \sum_l \frac{p_l^2}{2m} + \frac{1}{2} \sum_{i,j} u_i \cdot \frac{\partial^2 \mathcal{V}}{\partial u_i \partial u_j} \cdot u_j = \sum_l \frac{p_l^2}{2m} + \frac{1}{2} \sum_{i,j} u_i \cdot G_{ij} \cdot u_j, \quad (7.3.14)$$

where we omitted the constant equilibrium energy and  $p_l = m\dot{u}_l$ . We continue to define the operators<sup>3</sup> as

$$u(q) = \frac{1}{\sqrt{NV}} \sum_l u_l e^{iq \cdot \mathcal{X}_l}; \quad p(q) = \frac{1}{\sqrt{NV}} \sum_l p_l e^{-iq \cdot \mathcal{X}_l}. \quad (7.3.15)$$

Plugging these new operators in the Hamiltonian 7.3.14 we get

$$\begin{aligned} \mathcal{H} &= \frac{1}{2m} \frac{1}{NV} \sum_l \sum_{q,q'} p_q \cdot p_{q'} e^{i(q+q') \cdot \mathcal{X}_l} \\ &\quad + \frac{1}{2} \frac{1}{NV} \sum_{l,l'} \sum_{q,q'} u_q \cdot G_{l,l'} \cdot u_{q'} e^{-i(q \cdot \mathcal{X}_l + q' \cdot \mathcal{X}_{l'})} \\ &= \frac{1}{2m} \sum_q p_q \cdot p_{-q} \\ &\quad + \frac{1}{2} \frac{1}{NV} \sum_{q,q'} u_q \cdot \sum_{l,l'} G_{l,l'} e^{-i(q+q') \cdot \mathcal{X}_l + iq' \cdot (\mathcal{X}_l - \mathcal{X}_{l'})} \cdot u_{q'}, \end{aligned} \quad (7.3.16)$$

where we have used the familiar relation

$$\frac{1}{NV} \sum_l e^{i(q-q') \cdot \mathcal{X}_l} = \delta_{qq'}. \quad (7.3.17)$$

We now observe that the operator  $G_{ll'} = G(\mathcal{X}_l - \mathcal{X}_{l'})$  is translationally invariant in the sense that it only depends on the distance between two lattice sites. This means that we may write the Hamiltonian in the form

$$\mathcal{H} = \sum_q \underbrace{\left( \frac{p_q \cdot p_q^*}{2m} + \frac{1}{2} u_q \cdot E(q) \cdot u_q^* \right)}_{\mathcal{H}_q}, \quad (7.3.18)$$

where

$$p_q^* = p_{-q}; \quad u_q^* = u_{-q}; \quad E(q) = \sum_l e^{-iq \cdot \mathcal{X}_l} G(\mathcal{X}_l). \quad (7.3.19)$$

<sup>3</sup>Notice that these operators are only defined up to a reciprocal lattice vector  $G$  as  $e^{iG \cdot \mathcal{X}_l} = 1$ .

Notice here that we sum over the lattice site numbers  $l$  and therefore interpret a shift in these numbers  $l' \rightarrow l + l'$  with a corresponding shift of site vectors  $\mathcal{X}_{l'} \rightarrow \mathcal{X}_l + \mathcal{X}_{l'}$ .

With the ansatz  $u_q^\alpha = m^{-\frac{1}{2}} \exp(i\omega_q t) e_q^\alpha$  and the Hamiltonian equations we have

$$\begin{aligned} \ddot{u}_q^\alpha &= \frac{d}{dt} \frac{\partial \mathcal{H}_q}{\partial p_q^\alpha} = -\frac{1}{2m^{\frac{3}{2}}} E_q^{\alpha\beta} \exp(i\omega_q t) e_q^\beta = -\frac{1}{\sqrt{m}} v_q^2 \exp(i\omega_q t) e_q^\alpha \\ \Rightarrow \left( \frac{1}{m} E_q^{\alpha\beta} - \omega_q^2 \delta_{\alpha\beta} \right) e_q^\beta &= 0 \end{aligned}$$

and see that this ansatz indeed is a valid solution, if we choose the  $\omega_q^2$  in a way to make vanish the determinant  $\det(\frac{1}{m} E_q^{\alpha\beta} - \omega_q^2 \delta_{\alpha\beta})$ . In other words we solve the eigenvalue problem  $\frac{1}{m} E_q^{\alpha\beta} e_q^\beta = \omega_q^2 e_q^\alpha$ . As  $E$  is real and symmetric,<sup>4</sup> it can be diagonalized, each separate eigenvalue  $\omega_{q,\lambda}^2$  being non-degenerate and thus having a different eigenvector given by its components  $e_{q,\lambda}^\alpha$ . These eigenvectors form an orthonormal system such that

$$e_{q,\lambda}^* \cdot e_{q,\lambda'} = \delta_{\lambda,\lambda'}. \quad (7.3.20)$$

These vectors form a basis and are called *normal coordinates*. Using this basis to express the displacement and momentum vectors via

$$A_q = \sum_{\lambda} (e_{q,\lambda}^* \cdot A) e_{q,\lambda} \equiv \sum_{\lambda} A_{q,\lambda} e_{q,\lambda} \quad (7.3.21)$$

$$A_q^* = \sum_{\lambda} (e_{q,\lambda} \cdot A^*) e_{q,\lambda}^* \equiv \sum_{\lambda} A_{q,\lambda}^* e_{q,\lambda}^* \quad (7.3.22)$$

diagonalizes also  $E$  and we can rewrite the Hamiltonian (7.3.18) in these new coordinates as

$$\mathcal{H} = \sum_{q,\lambda} \left( \frac{p_{q,\lambda}^2}{2m} + \frac{1}{2} m \omega_{q,\lambda}^2 u_{q,\lambda}^2 \right). \quad (7.3.23)$$

We continue in the line of second quantization by interpreting  $p$  and  $u$  as quantum mechanical operators from now on and consequently introducing

<sup>4</sup>As can be seen by the following transformation

$$\begin{aligned} E(q) &= \sum_l e^{-iq \cdot \mathcal{X}_l} G(\mathcal{X}_l) = \frac{1}{2} \sum_l (e^{-iq \cdot \mathcal{X}_l} G(\mathcal{X}_l) + e^{iq \cdot \mathcal{X}_l} G(-\mathcal{X}_l)) \\ &= \frac{1}{2} \sum_l G(\mathcal{X}_l) (e^{-iq \cdot \mathcal{X}_l} + e^{iq \cdot \mathcal{X}_l} - 2) \\ &= \frac{1}{2} \sum_l G(\mathcal{X}_l) \sin^2\left(\frac{1}{2} q \cdot \mathcal{X}_l\right), \end{aligned}$$

where we used that  $\sum_l G(\mathcal{X}_l) = 0$ .

the ladder operators know from the harmonic oscillator

$$\begin{aligned} a_{q,\lambda} &= \sqrt{\frac{\omega_{q,\lambda}m}{2\hbar}} u_{q,\lambda} + i \frac{1}{\sqrt{2\hbar\omega_{q,\lambda}m}} p_{q,\lambda} \\ a_{q,\lambda}^* &= \sqrt{\frac{\omega_{q,\lambda}m}{2\hbar}} u_{q,\lambda}^* - i \frac{1}{\sqrt{2\hbar\omega_{q,\lambda}m}} p_{q,\lambda}^*, \end{aligned} \quad (7.3.24)$$

so that the momentum and displacement in normal coordinates may be expressed as

$$p_{q,\lambda} = -i \frac{\sqrt{2\hbar\omega_{q,\lambda}m}}{2} (a_{q,\lambda} - a_{-q,\lambda}^\dagger) \quad (7.3.25)$$

$$u_{q,\lambda} = \sqrt{\frac{\hbar}{2\omega_{q,\lambda}m}} (a_{q,\lambda} + a_{-q,\lambda}^\dagger). \quad (7.3.26)$$

The Hamiltonian then finally receives the familiar form

$$\mathcal{H} = \frac{1}{2} \sum_{q,\lambda} \hbar\omega_{q,\lambda} \{a_{q,\lambda}, a_{q,\lambda}^\dagger\} = \sum_{q,\lambda} \hbar\omega_{q,\lambda} \left( a_{q,\lambda}^\dagger a_{q,\lambda} + \frac{1}{2} \right). \quad (7.3.27)$$

In real space this consequently translates to

$$\begin{aligned} p_l &= \frac{1}{\sqrt{NV}} \sum_{q,\lambda} e^{iq \cdot \mathcal{X}_l} p_{q,\lambda} e_{q,\lambda} = -i \sum_{q,\lambda} \sqrt{\frac{\hbar\omega_{q,\lambda}m}{2NV}} e^{iq \cdot \mathcal{X}_l} e_{q,\lambda} (a_{q,\lambda} - a_{-q,\lambda}^\dagger) \\ u_l &= \sum_{q,\lambda} \sqrt{\frac{\hbar}{2\omega_{q,\lambda}mNV}} e^{iq \cdot \mathcal{X}_l} e_{q,\lambda} (a_{q,\lambda} + a_{-q,\lambda}^\dagger). \end{aligned} \quad (7.3.28)$$

**Adiabatic principle** The translationally invariant potential that is due to a static lattice of ions does not lead to scattering of electrons. This is the central result of Bloch's Theorem. If locally the ions move away from their equilibrium position this translational symmetry is broken locally and electrons can scatter by the produced effective local electrostatic potential.

However, a single electron is not just influenced by this change due to the new ionic potential but also by the behavior of the other electrons that form a plasma that reacts to the ionic motion. This direct effect is particularly strong for quickly oscillating ions, when the phonon wavelength is of the order of screening length of the plasma.

The adiabatic Born-Oppenheimer approximation is employed to separate the time-scales of electronic and ionic movement. The whole problem has a Hamiltonian of

$$\mathcal{H} = \sum_l \frac{p_l^2}{2m_l} + \mathcal{V}(\mathcal{X}) + \sum_i \frac{p_i^2}{2m} + \sum_i \mathcal{U}(r_i; \mathcal{X}) + \sum_{i < j} \frac{e^2}{|r_i - r_j|}, \quad (7.3.29)$$



where  $\mathcal{X}$  represents the position of all ions  $\mathcal{X} = \mathcal{X}_1, \dots, \mathcal{X}_N$ . Here  $\mathcal{V}$  is the potential energy stored in the construction and deformation of the lattice, excluding the energy resulting from the subsequent distortion of the electronic system, as this is already included in the electronic part  $\mathcal{U}$ . The Born-Oppenheimer approximation now takes the electronic part to be solvable separately to give (i.e., we solve the eigenvalue equation and find a configuration of electronic states such that)

$$\sum_i \frac{p_i^2}{2m} + \sum_i \mathcal{U}(r_i; \mathcal{X}) + \sum_{i < j} \frac{e^2}{|r_i - r_j|} \equiv \mathcal{E}_{\mathcal{X}}. \quad (7.3.30)$$

Substituting this back in the full problem we may solve for the lattice system separately. This assumes that the lattice vibrations are largely independent on the exact electronic configuration. This can be justified by noting that

- The majority of the electrons are occupying the same states in every possible configuration, due to Fermi statistics, and only a small fraction of thermally excited electrons are “free” to change their states.
- It is not the absolute value of  $\mathcal{E}_{\mathcal{X}}$  that enters in the solution for the lattice vibrations but rather the second derivative with respect to lattice distortions, the effect thus should be small indeed.

The approximation above gives a satisfactory account for the energy of the system. For any dynamics, however, the terms that change lattice and electronic structure at the same time become significant. While still maintaining the adiabatic approximation picture these terms can be thought of as the two separate systems interaction with each other. We will follow this line of thought while remarking that:

- The interaction effect should be small in size compared to the static physics of the problem, so the separation into sub-systems is still valid. This on the same time permits for the inclusion of these interaction terms in a perturbative manner.
- The collective effect of the plasma is a renormalization of the interaction between individual electrons and lattice as well as a change of lattice frequency. This plasma effect can thus be disregarded at first analysis.

**Electron-phonon interaction** Above we introduced the adiabatic approximation to separate the time-scales of electron and lattice movements. By constructing the full Hamiltonian (7.3.29) we defined  $\mathcal{V}(\mathcal{X})$  to be the potential energy of the lattice and its vibrations while separating its effect on the electrons. This is included into  $\mathcal{U}(r_i; \mathcal{X})$  and is precisely the electron-phonon interaction that we turn to now. Separating time-scales allows us to solve

the electronic Hamiltonian (7.3.30) for a fixed lattice configuration.<sup>5</sup> Bloch's theorem greatly simplifies the treatment of electrons in a periodic potential. While the lattice exhibits this periodicity in equilibrium, the distortion due to phonons prohibits the employment of the theorem for  $T > 0$ . However, if we assume the contribution to the potential energy due to the lattice distortions to be small compared to the equilibrium term, we may reasonably expect to be able to treat these in the framework of perturbation theory. For this to apply we first have to separate the full potential energy into an equilibrium part and a perturbation part such as<sup>6</sup>

$$\mathcal{U}(r_i; R) = \mathcal{U}_0(r_i; \mathcal{X}) + \delta\mathcal{U}(r_i; u) = \sum_l [\mathcal{U}_0(r_i - \mathcal{X}_l) + \delta\mathcal{U}(r_i - \mathcal{X}_l - u_l)], \quad (7.3.31)$$

where  $u$  is the collection of lattice displacements  $u_l$ . Realizing that the perturbative nature of  $\delta\mathcal{U}$  is based on the assumption that every single displacement  $u_l$  is small we may expand

$$\delta\mathcal{U}(r_i; u) = \sum_l \delta\mathcal{U}(r_i - \mathcal{X}_l - u_l) \approx \sum_l u_l \cdot \left. \frac{\partial \mathcal{U}_0(r_i - \mathcal{X}_l - u_l)}{\partial u_l} \right|_{u_l=0}. \quad (7.3.32)$$

Notice that the total potential energy that the electronic system gains from the displacement of the lattice can be split into the contribution due to each lattice ion at position  $\mathcal{X}_l + u_l$  onto each electron at  $r_i$ , we may thus continue in a one electron picture and drop the electron index  $i$  from now on until needed again. This Hamiltonian is still written in real space while the perturbation theory is most conveniently written in second quantized form. As the interaction between an electron and a phonon is a one particle process in the electronic system we write

$$h_{\text{el-ph}} = \int d^3r \psi^\dagger(r) \delta\mathcal{U}(r; u) \psi(r) = \frac{1}{V} \sum_{k, k'} c_{k+k'}^\dagger \delta\mathcal{U}_{k'} c_k \quad (7.3.33)$$

with  $\psi(r)$  being the electronic field operators,  $c_k$  the creation operator in momentum space and  $\delta\mathcal{U}_k = \int d^3r e^{-ik \cdot r} \delta\mathcal{U}(r; u)$ . Inserting equation (7.3.32)

---

<sup>5</sup>Configuration here means the position and movement of the ions. However, as the lattice is seen as frozen from the point of view of the electrons, every phonon just contributes its distortion to the interaction, while its dynamic part is omitted here. Hence we continue to write  $\mathcal{U}(r_i; R)$  without any reference to  $\dot{R}$ .

<sup>6</sup>This is also called the rigid ion approximation.

and equation (7.3.33) yields

$$h_{\text{el-ph}} = \frac{1}{V} \sum_{k,k'} c_{k+k'}^\dagger c_k \int d^3 r e^{-ik' \cdot r} \sum_l u_l \cdot \frac{\partial \mathcal{U}_0(r - \mathcal{X}_l)}{\partial u_l} \quad (7.3.34)$$

$$= -\frac{1}{V} \sum_{k,k'} c_{k+k'}^\dagger c_k \sum_l u_l \cdot \int d^3 r e^{-ik' \cdot r} \frac{\partial \mathcal{U}_0(r - \mathcal{X}_l)}{\partial r} \quad (7.3.35)$$

$$= -\frac{1}{V} \sum_{k,k'} c_{k+k'}^\dagger c_k \sum_l \sum_{q,\lambda} \sqrt{\frac{\hbar}{2\omega_{q,\lambda} m N V}} e^{iq \cdot \mathcal{X}_l} (a_{q,\lambda} + a_{-q,\lambda}^\dagger) \times e_{q,\lambda} \cdot \int d^3 r e^{-ik' \cdot r} \frac{\partial \mathcal{U}_0(r - \mathcal{X}_l)}{\partial r} \quad (7.3.36)$$

$$= -\frac{1}{V} \sum_{k,k'} c_{k+k'}^\dagger c_k \frac{1}{\sqrt{V}} \sum_{q,\lambda} (a_{q,\lambda} + a_{-q,\lambda}^\dagger) \sqrt{\frac{\hbar}{2\omega_{q,\lambda} m N}} \sum_l e^{iq \cdot \mathcal{X}_l} \times e_{q,\lambda} \cdot \int d^3 r e^{-ik' \cdot r} \frac{\partial \mathcal{U}_0(r - \mathcal{X}_l)}{\partial r} \quad (7.3.37)$$

$$= \frac{1}{V} \sum_{k,k'} \frac{1}{\sqrt{V}} \sum_{q,\lambda} V^{\text{el-ph}}(k, k', q, \lambda) c_{k+k'}^\dagger c_k (a_{q,\lambda} + a_{-q,\lambda}^\dagger) \quad (7.3.38)$$

Where here the second quantized matrix element of the electron-phonon interaction is given by

$$\begin{aligned} V^{\text{el-ph}}(k, k', q, \lambda) &= -\sqrt{\frac{\hbar}{2\omega_{q,\lambda} m N}} e_{q,\lambda} \cdot \sum_l e^{iq \cdot \mathcal{X}_l} \int d^3 r e^{-ik' \cdot r} \frac{\partial \mathcal{U}_0(r - \mathcal{X}_l)}{\partial r} \\ &= -\sqrt{\frac{\hbar N}{2\omega_{q,\lambda} m}} \underbrace{\int d^3 r e^{-ik' \cdot r} e_{q,\lambda} \cdot \frac{\partial \mathcal{U}_0(r)}{\partial r}}_U \\ &= -\sqrt{\frac{\hbar N}{2\omega_{q,\lambda} m}} U. \end{aligned} \quad (7.3.39)$$

In the last transformation we approximated the integral over the lattice deviations to be constant.

The electronic collision integral again involves the transition rates between different electronic states. As now the creation or annihilation of a phonon is part of the process, the transition can happen in two ways, by absorbing or emitting said phonon:

$$\begin{aligned} w^{\text{abs}}(\mathbf{p} + \hbar\mathbf{q}, \mathbf{p}) &= \frac{2\pi}{\hbar} |V^{\text{el-ph}}|^2 \delta(E_{\mathbf{p}+\hbar\mathbf{q}} - E_{\mathbf{p}} - \hbar\omega_{\mathbf{q}\lambda}) \\ &= W_{\mathbf{p}+\hbar\mathbf{q}, \mathbf{p}} n_{\mathbf{q},\lambda} \delta(E_{\mathbf{p}+\hbar\mathbf{q}} - E_{\mathbf{p}} - \hbar\omega_{\mathbf{q}\lambda}) \\ w^{\text{em}}(\mathbf{p} + \hbar\mathbf{q}, \mathbf{p}) &= W_{\mathbf{p}+\hbar\mathbf{q}, \mathbf{p}} (n_{\mathbf{q},\lambda} + 1) \delta(E_{\mathbf{p}+\hbar\mathbf{q}} - E_{\mathbf{p}} + \hbar\omega_{\mathbf{q}\lambda}) \end{aligned} \quad (7.3.40)$$

with the transition amplitude  $W_{\mathbf{p}+\hbar\mathbf{q},\mathbf{p},\lambda} = \frac{\pi NU^2}{\omega_{\mathbf{q},\lambda} m}$ , and the phonon occupation function  $n_{\mathbf{q},\lambda}$ . The total transition rate is then the sum of both possible processes  $w = w^{\text{abs}} + w^{\text{em}}$  and plugging this into (7.3.6) gives the electron-phonon collision integral

$$\begin{aligned} \left(\frac{\partial f}{\partial t}\right)_{\text{coll}}^{\text{el-ph}} = & - \int \frac{d\mathbf{q}}{(2\pi\hbar)^3} \sum_{\lambda} \left\{ W_{\mathbf{p}+\hbar\mathbf{q},\mathbf{p},\lambda} \left[ n_{\mathbf{q},\lambda} f(\mathbf{p}) (1 - f(\mathbf{p}+\hbar\mathbf{q})) \right. \right. \\ & \left. \left. - (n_{\mathbf{q},\lambda} + 1) f(\mathbf{p}+\hbar\mathbf{q}) (1 - f(\mathbf{p})) \right] \right. \\ & \left. + W_{\mathbf{p},\mathbf{p}-\hbar\mathbf{q},\lambda} \left[ (n_{\mathbf{q},\lambda} + 1) f(\mathbf{p}) (1 - f(\mathbf{p}-\hbar\mathbf{q})) \right. \right. \\ & \left. \left. - n_{\mathbf{q},\lambda} f(\mathbf{p}-\hbar\mathbf{q}) (1 - f(\mathbf{p})) \right] \right\}. \end{aligned} \quad (7.3.41)$$

This now is the collision integral for the change of electronic states due to the emission or the absorption of a phonon. Consequently the same process can be view from the point of the phonon bath where we analogously have a similar collision integral of the form

$$\begin{aligned} \left(\frac{\partial n}{\partial t}\right)_{\text{coll}}^{\text{ph-el}} = & - \int \frac{d\mathbf{p}}{(2\pi\hbar)^3} W_{\mathbf{p}+\hbar\mathbf{q},\mathbf{p},\lambda} \left[ n_{\mathbf{q},\lambda} f(\mathbf{p}) (1 - f(\mathbf{p}+\hbar\mathbf{q})) \right. \\ & \left. - (n_{\mathbf{q},\lambda} + 1) f(\mathbf{p}+\hbar\mathbf{q}) (1 - f(\mathbf{p})) \right]. \end{aligned} \quad (7.3.42)$$

This concludes the two examples of single particle collisions and we turn to the next level of interactions where the state of not just one but the state of two particles<sup>7</sup> is changed.

### 7.3.2 Two particle collisions

Above we considered scattering events that only depend on two points in phase space. Accordingly we spoke of single particle collisions. The naming already hints to the existence of scattering processes that involve more than one particle. Incidentally the only process of higher order that commonly treated is the next order, meaning a collision of two particles. Again we stick to the principle of locality that restricts everything to a single point in real space so that we again restrict the nomenclature to momenta. In complete analogy to the preceding section we deduce the rate of change of the phase space density at some point  $\mathbf{p}$ . Now besides  $\mathbf{p}'$  two other phase space points  $\mathbf{p}_1$  and  $\mathbf{p}'_1$  are involved so that the rate of change becomes

$$w(\mathbf{p}', \mathbf{p}'_1; \mathbf{p}, \mathbf{p}_1) f(\mathbf{p}) f(\mathbf{p}_1) \frac{d\mathbf{p}_1}{(2\pi\hbar)^3} \frac{d\mathbf{p}'_1}{(2\pi\hbar)^3} \frac{d\mathbf{p}'}{(2\pi\hbar)^3}, \quad (7.3.43)$$

<sup>7</sup>As above the counting is meant to be within the bath of a single type of particles. In this sense the electron-phonon scattering is a single particle process as only one electron (and conversely one phonon) is involved.

where now also the density at the second initial point  $\mathbf{p}_1$  enters. The full collision integral includes the processes where one of the final states involves the phase space point  $\mathbf{p}$  so that we arrive at

$$\begin{aligned} \left(\frac{\partial f}{\partial t}\right)_{\text{coll}} = & - \int \frac{d\mathbf{p}_1}{(2\pi\hbar)^3} \frac{d\mathbf{p}'_1}{(2\pi\hbar)^3} \frac{d\mathbf{p}'}{(2\pi\hbar)^3} \left[ w(\mathbf{p}', \mathbf{p}'_1; \mathbf{p}, \mathbf{p}_1) f(\mathbf{p}) f(\mathbf{p}_1) \right. \\ & \left. - w(\mathbf{p}, \mathbf{p}_1; \mathbf{p}', \mathbf{p}'_1) f(\mathbf{p}') f(\mathbf{p}'_1) \right] \end{aligned} \quad (7.3.44)$$

The typical physical processes of these form are collisions of two (quasi)-particles of the same type. In the present work this involves electron-electron scattering and thus we turn a closer look on these collisions in the following.

### 7.3.2.1 Electron-electron scattering

As the quasi-particle of interest in the present text is the electron, we present now the fundamental two particle interactions of electrons, the electron-electron scattering. While the Coulomb interaction is the source of all elementary interactions in a solid state system, in the case of electron-electron collision it is also the direct mediator. In the formalism of second quantization the two particle Hamiltonian takes the form

$$H_2 = \frac{1}{2V} \sum_{\mathbf{k}_1, \mathbf{k}_2, \mathbf{q}} a_{\mathbf{k}_1 + \mathbf{q}}^\dagger a_{\mathbf{k}_2 - \mathbf{q}}^\dagger U_{\mathbf{q}} a_{\mathbf{k}_2} a_{\mathbf{k}_1},$$

where  $U_{\mathbf{q}} = \int d\mathbf{r} U(\mathbf{r}) e^{-i\mathbf{q}\mathbf{r}}$  denotes the Fourier transform of the Coulomb potential and  $a_{\mathbf{k}} \left( a_{\mathbf{k}}^\dagger \right)$  is the annihilation (creation) operator of an electron with wavevector  $\mathbf{k}$ . Again we, as previously done, dropped the spin dependence. To simplify the calculation we assume a constant matrix element  $U_{\mathbf{q}}$  that amounts to a strongly localized screened potential. Assuming, as above, that elastic scattering is dominated by anisotropic impurity scattering, qualitatively new phenomena are to be expected by the introduction of an isotropic scattering mechanism. And as inelastic scattering is to be expected to be the less dominant mechanism in general, we take only its isotropic part [84].

With the two term approximation the linearized collision integral then takes the form

$$\begin{aligned} I_{\text{inel}} &= -\frac{1}{\tau'(k)} \delta f^0(k) - \int dk' \frac{\delta f^0(k')}{\tau(k, k')} \\ &= -\frac{1}{\tau(E)} \delta f^0(E) - \int dE' \frac{\delta f^0(E')}{\tau(E, E')}, \end{aligned} \quad (7.3.45)$$

where we switched into energy space. Note here that we continue to use the notation of  $1/\tau$  to denote coupling constants. This honors the common

notational convention, however, the interpretation of the off-diagonal terms as scattering rates or live times is rather awkward as they may become negative. As collisions conserve quasi-particle number  $N = \int d^3r \int d^3k f(\mathbf{r}, \mathbf{k}, t)$  we can deduce a relation between the diagonal part of (7.3.45) and its off-diagonal rates.

Having

$$\int d^3r \int d^3k I_{\text{inel}} = 0, \quad (7.3.46)$$

or

$$\int dk k^2 \left( \frac{\delta(k' - k)}{\tau(k')} + \frac{1}{\tau(k, k')} \right) = 0 \quad (7.3.47)$$

$$\frac{\nu(E')}{\tau(E')} + \int dE \frac{\nu(E)}{\tau(E, E')} = 0, \quad (7.3.48)$$

where the density of states is given by

$$\nu(E) = \frac{3}{2} n \frac{\sqrt{E}}{E_F^{\frac{3}{2}}}.$$

Equivalently the total energy of the system  $E = \int d^3r \int d^3k E_{\mathbf{k}} f(\mathbf{r}, \mathbf{k}, t)$  is conserved as well, leading to

$$E' \frac{\nu(E')}{\tau(E')} + \int dE E \frac{\nu(E)}{\tau(E, E')} = 0. \quad (7.3.49)$$

The above conservation laws allow for the calculation of the diagonal terms  $1/\tau(E)$  from the off-diagonal ones that are given by

$$\begin{aligned} \frac{1}{\tau(E, E')} = & \frac{m\pi}{32\hbar^3} \frac{|U|^2}{(2\pi)^4} \left( \frac{2m}{\hbar^2} \right)^2 \tau_{\text{el}} \int \frac{d\epsilon}{\sqrt{E}} \\ & \left\{ H^+(E, E', \epsilon) [f(E) (1 - f(E + \epsilon) - f(E' - \epsilon)) \right. \\ & \quad \left. + f(E + \epsilon) f(E' - \epsilon)] \right. \\ & H^-(E, E', \epsilon) [f(E + \epsilon) (1 - f(E' + \epsilon) - f(E)) \\ & \quad \left. + f(E' + \epsilon) f(E)] \right\}, \end{aligned} \quad (7.3.50)$$

where  $f(E)$  is the Fermi distribution and we introduced the auxiliary func-

tions

$$H^+ = \begin{cases} 0 & \epsilon > E' \\ \min \left( \sqrt{E + \epsilon} + \sqrt{E}, \sqrt{E' - \epsilon} + \sqrt{E'} \right) & 0 < \epsilon < E' \\ -\max \left( \sqrt{E + \epsilon} - \sqrt{E}, -\sqrt{E' - \epsilon} + E' \right) & \\ \min \left( \sqrt{E + \epsilon} + \sqrt{E}, \sqrt{E' - \epsilon} + \sqrt{E'} \right) & -E < \epsilon < 0 \\ -\max \left( \sqrt{E + \epsilon} + \sqrt{E}, \sqrt{E' - \epsilon} - E' \right) & \\ 0 & \epsilon < -E \end{cases} \quad (7.3.51)$$

$$H^- = \begin{cases} 2\sqrt{\min(E, E')} & \epsilon > 0 \\ 2\sqrt{\min(E, E') + \epsilon} & -\min(E, E') < \epsilon < 0 \\ 0 & \text{else} \end{cases}$$

The electron-electron collision integral (7.3.45) leads to a thermalization of the excited out of equilibrium distribution as we present in the following chapters. This concludes the introduction to the formalism of the Boltzmann equation. We are now well equipped to take the theory to action and apply the different scattering mechanisms to analyze dynamics non-equilibrium distribution functions.





## Chapter 8

# Ballistic-diffusive crossover

### 8.1 Introduction

In the present chapter we begin to apply the Boltzmann approach introduced above. This semi-classical treatment of electrons in a crystal is well suited to describe a variety of situations and it tends to excel in particular at problems regarding transport of electrons or quasi-particles in general. As also presented in the previous chapter, the Boltzmann equation is too complex to allow for a direct treatment so that appropriate approximation are required.

The approximations that are applied to the various components constituting the Boltzmann equation depend on the specific situation that we want to describe. And therefore the most common approach is the definition of a certain physical situation first to then choose the various possible approximations and collisions that might describe said situation.

As the title suggests, and the introduction specified, the present work is concerned with the time evolution of a quasi-particle excitation and the successive approach of equilibrium. A quasi-particle excitation in the context of the Boltzmann equation is hence precisely an excess density that deviates from the equilibrium distribution. This excitation can be formed spontaneously but is usually studied by driving it with a pump laser.

Formally the specific excess density, however, is introduced into the problem as the boundary (or initial) condition of the Boltzmann equation. The first task therefore is to adapt the general and overwhelming Boltzmann equation to the problem at hand. On the one hand we limit our analysis to a bulk material with two translationally invariant axes opposed to a third axis (in our case that will be the  $z$ -axis) that is observed for transport effects. The physical architecture this setup resembles would be a thin metal film.

The geometry thus introduced allows for the application of the two term approximation as presented in section 7.2. While this reduces the dimensionality of the problem and simplifies the left hand side of the Boltzmann equation, the collision part is still unspecified. Assuming that the quasi-

particle excess density is excited with an initially directional momentum the quasi particles continue to travel in that direction until perturbed. In the Boltzmann formalism these perturbations take the form of collisions and the simplest is the impurity scattering. Before analyzing more complex scattering processes it is therefore worthwhile to see where the simple application of the relaxation time approximation takes us.

## 8.2 Ballistic-diffusive equation

As introduced above the collision integral for the present section is formed by impurity scattering (7.3.10) taking the form of the relaxation time approximation

$$I_{\text{el}} [f(\mathbf{p}, z, t)] = -\cos\theta \frac{\delta f^1(p, z, t)}{\tau_{\text{el}}}. \quad (8.2.1)$$

The life time  $\tau_{\text{el}}$ , or relaxation time, can be estimated via Fermi's Golden Rule as presented above (7.3.11). However, experimental data suggests values of the order of 10 femto seconds [91, 92]. The full Boltzmann equation in the present context therefore takes the form

$$\begin{aligned} \frac{\partial}{\partial t} \delta f^0(k, z, t) + \cos\theta \frac{\partial}{\partial t} \delta f^1(k, z, t) \\ + v \cos\theta \frac{\partial}{\partial z} \delta f^0(k, z, t) + v \cos^2\theta \frac{\partial}{\partial z} \delta f^1(k, z, t) = -\cos\theta \frac{\delta f^1(k, z, t)}{\tau_{\text{el}}}. \end{aligned} \quad (8.2.2)$$

Integrating the now established Boltzmann equation over moments, i.e., performing the operation  $\int d\theta \cos^n \theta$ , we obtain two coupled differential equations

$$n = 0 : \quad \frac{\partial}{\partial t} \delta f^0 + \frac{v}{3} \frac{\partial}{\partial z} \delta f^1 = 0 \quad (8.2.3)$$

$$n = 1 : \quad \frac{\partial}{\partial t} \delta f^1 + v \frac{\partial}{\partial z} \delta f^0 = -\frac{\delta f^1}{\tau_{\text{el}}}. \quad (8.2.4)$$

Notice that the two functions  $\delta f^0$  and  $\delta f^1$  still depend on the wave vector  $k$ . But as the applied impurity scattering is elastic in nature and therefore conserves magnitude of momentum we drop the dependency. Equations (8.2.3) and (8.2.4) can be decoupled to yield the ballistic-diffusive equation

$$\frac{\partial^2}{\partial t^2} \delta f^0 + \frac{1}{\tau_{\text{el}}} \frac{\partial}{\partial t} \delta f^0 - \frac{v^2}{3} \frac{\partial^2}{\partial z^2} \delta f^0 = 0, \quad (8.2.5)$$

that governs the dynamical evolution of the isotropic density distribution. As we are mainly interested in the general properties and dynamics of the equation, it is of use to switch to dimensionless parameters. This amounts

to measuring time in units of the scattering time  $\tau_{\text{el}}$  and space in units of the mean free path  $l = v_F \tau_{\text{el}}$ :

$$t/\tau_{\text{el}} = \tilde{t} \rightarrow t \quad (8.2.6)$$

$$z/v_F \tau_{\text{el}} = \tilde{z} \rightarrow z. \quad (8.2.7)$$

As we are treating isotropic cases in momentum space we use the energy representation  $E = \frac{1}{2}mv^2$  to obtain

$$\frac{\partial^2}{\partial t^2} \delta f^0 + \frac{\partial}{\partial t} \delta f^0 - \frac{1}{3} \frac{E}{E_F} \frac{\partial^2}{\partial z^2} \delta f^0 = 0. \quad (8.2.8)$$

Equation (8.2.8) can be solved via separation of variables, as presented below, and governs the full evolution of any quasi-particle density with energy  $E$  and hence describes the ballistic and diffusive transport as well as the transition between both.

Both diffusion equation and wave equation (governing ballistic motion) are limiting cases of (8.2.8) for  $\tau_{\text{el}} \ll dt$  and  $\tau_{\text{el}} \rightarrow \infty$ , respectively.

### 8.3 Diffusion and wave equations

When speaking about transport, the categories of ballistic and diffusive motion are frequently used. Ballistic motion is associated with a propagation that is unhampered by disruptions such as collisions. The governing equation is the wave equation, here in the one-dimensional version

$$\frac{\partial^2}{\partial t^2} \delta f^0 = v^2 \frac{\partial^2}{\partial z^2} \delta f^0. \quad (8.3.1)$$

The dynamics of the system before scattering sets in is effectively described by a diverging relaxation time

$$\tau_{\text{el}} \rightarrow \infty. \quad (8.3.2)$$

Inserting this in the ballistic-diffusive equation (8.2.5) recovers the wave equation immediately. With the initial condition  $\delta f^0(t=0) = \delta(z) = \frac{1}{2\pi} \int dz \exp(ikz)$  the solution of the wave equation reads

$$\begin{aligned} \delta f^0(z, t) &= \frac{1}{2\pi} \int dk \exp \left[ ik \left( z \pm \frac{v}{\sqrt{3}} t \right) \right] \\ &= \frac{1}{2} \left[ \delta \left( z + \frac{v}{\sqrt{3}} t \right) + \delta \left( z - \frac{v}{\sqrt{3}} t \right) \right] \end{aligned} \quad (8.3.3)$$

so that the mean square displacement<sup>1</sup> reads

$$\sigma^2(t) = \int dz z^2 \delta f^0(z, t) = \frac{v^2}{3} t^2 \quad (8.3.4)$$

<sup>1</sup>Technically the mean square displacement involves also an integration over momentum-space. As this dependence is delta-like in the elastic case, we omit it here.

and thus is quadratic as expected for ballistic motion.

To extract the diffusive limit [84] that is characterized by the case that the particles scatter many times in an observed dynamic interval  $dt$  and hence

$$\tau_{\text{el}} \ll dt, \quad (8.3.5)$$

we rewrite the Boltzmann equation (8.2.5)

$$\frac{1}{\tau_{\text{el}}} \frac{\partial}{\partial t} \left( \tau_{\text{el}} \frac{\partial}{\partial t} \delta f^0 + \delta f^0 \right) - \frac{v^2}{3} \frac{\partial^2}{\partial z^2} \delta f^0 = 0. \quad (8.3.6)$$

Omitting the first term in the brackets we obtain the diffusion equation

$$\frac{\partial}{\partial t} \delta f^0 - \underbrace{\frac{v^2}{3} \tau_{\text{el}}}_{D} \frac{\partial^2}{\partial z^2} \delta f^0 = 0. \quad (8.3.7)$$

Solving this via separation of variables and the initial condition  $\delta f^0(t=0) = \delta(z)$  gives

$$\delta f^0(z, t) = \frac{1}{2\pi} \int dk \exp[ikz - Dk^2t] \quad (8.3.8)$$

and a linear mean square displacement

$$\sigma^2(t) = 2Dt. \quad (8.3.9)$$

These two limiting cases for ballistic and diffusive transport are entrenched in the ballistic-diffusive equation, so that we now turn to derive a dynamic equation for the mean square displacement.

## 8.4 Mean square displacement

Above we already looked at the mean square displacement as a convenient way to classify the type of transport state. A linear mean square displacement corresponds to a diffusive behavior while an exponent larger than one in general refers to super-diffusive expansion. This culminates in collision-less ballistic transport for a quadratic mean square displacement.

Both limits have been shown to naturally arise from the ballistic-diffusive equation (8.2.8). We may, however, integrate this equation to form from it a differential equation that governs the complete dynamic evolution of the mean square displacement and thus the change of transport type. In general the mean square displacement is given by

$$\sigma^2(t) = \int dE' \nu(E') \int dz z^2 \delta f^0, \quad (8.4.1)$$

with a density of state  $\nu(E)$  so that the ballistic diffusive equation (8.2.8) becomes

$$\frac{\partial^2}{\partial t^2} \sigma^2(t) + \frac{1}{\tau_{\text{el}}} \frac{\partial}{\partial t} \sigma^2(t) - \frac{2}{3} \frac{E}{E_F} = 0, \quad (8.4.2)$$

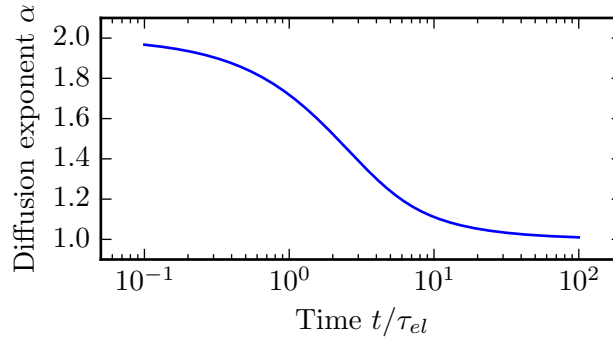


Figure 8.4.1: The evolution of the diffusion exponent  $\alpha$  is plotted against time. Here the time is measured in terms of the elastic scattering rate  $\tau_{el}$ . An exponent of two defines a ballistic motion and dominates the transport for times below the impurity scattering time. With increasing scattering processes the transport changes from ballistic to diffusive, denominated by an exponent of one, recovering previous ab-initio results [93].

where we took  $\int dE' \nu(E') E' \int dz \delta f^0 = E$ . This takes the energy dependence to be delta like. In the general case of a non-trivial energy dependence of the quasi-particle distribution this gives the average energy as used below. The solution is straightforwardly obtained to be

$$\sigma^2(t) = \frac{2 \langle E \rangle}{3 E_F} (t + (e^{-t} - 1)). \quad (8.4.3)$$

The evolution of the type of transport from ballistic to diffusive is best described by a (time dependent) transport exponent [93, 70]  $\alpha$  via  $\sigma^2(t) \propto t^\alpha$ , with

$$\alpha = \frac{\frac{\partial}{\partial t} \sigma^2(t)}{\sigma^2(t)} t = \frac{t(e^t - 1)}{1 + e^t(t - 1)}, \quad (8.4.4)$$

where  $\alpha = 2$  denotes ballistic and  $\alpha = 1$  diffusive transport as presented in figure 8.4.1.

With common approximative approaches to treat the Boltzmann problem we have thus given an analytical expression for the crossover between ballistic to diffusive transport of an excited quasi-particle density. This crossover is characterized by the mean square displacement. However the ballistic-diffusive equation can also be solved directly to give the dynamical evolution of the distribution function at any point in space.

## 8.5 Solution to the ballistic-diffusive equation

In the previous sections we took different looks on the ballistic-diffusive equation (8.2.8). We discussed how the wave equation and diffusion equation are

natural limits for collision-less transport and the opposite case where collisions completely randomized the directional properties of initial momentum. We derived an equation for the evolution of the mean square equation that conveniently allows for the dynamical classification of the type of transport.

In the present section we now turn back to the ballistic-diffusive equation itself to solve it analytically. The partial differential equation (8.2.8) can be solved by a separation of variables ansatz

$$\delta f^0(z, t) = a(t)b(z). \quad (8.5.1)$$

The solutions of the individual equations then are given by

$$a(t) \propto \exp \left[ -\frac{t}{2} \left( 1 \pm \sqrt{1 - \frac{4E}{3E_F} k^2} \right) \right] \quad (8.5.2)$$

$$b(z) \propto \exp [\pm ikz], \quad (8.5.3)$$

and the general solution is obtained by plugging these into (8.5.1). With the general solution given we can now turn to the specific physical situation at hand. Here we model the quasi-particle excitation as a initial excitation on the  $z$ -plane, that is normally distributed with a standard deviation  $\sigma$  in space and isotropic in  $k$ -space. This gives as first initial condition

$$\delta f^0(z, t = 0) = \frac{1}{\sqrt{2\pi\sigma^2}} e^{-\frac{z^2}{2\sigma^2}} = \frac{1}{2\pi} \int dk e^{ikz} e^{-\frac{\sigma^2 z^2}{2}}. \quad (8.5.4)$$

And as there are no anisotropic contributions at time  $t = 0$  equation (8.2.3) gives the second initial condition

$$\frac{\partial \delta f^0(z, t = 0)}{\partial t} = 0, \quad (8.5.5)$$

that translates to the demand  $A(k) + B(k) = 1$ . Plugging both in we obtain a full solution of

$$\begin{aligned} \delta f^0(z, t) = & \frac{1}{4\pi} \int dk e^{ikz} e^{-\frac{\sigma^2 z^2}{2}} \\ & \left\{ \left( 1 + \frac{1}{\sqrt{1 - \frac{4E}{3E_F} k^2}} \right) \exp \left[ -\frac{t}{2} \left( 1 - \sqrt{1 - \frac{4E}{3E_F} k^2} \right) \right] \right. \\ & \left. + \left( 1 - \frac{1}{\sqrt{1 - \frac{4E}{3E_F} k^2}} \right) \exp \left[ -\frac{t}{2} \left( 1 + \sqrt{1 - \frac{4E}{3E_F} k^2} \right) \right] \right\}. \end{aligned} \quad (8.5.6)$$

This gives the full dynamical evolution of a initially ballistic transport that turns into a diffusive expansion after the first couple of collisions. Figure 8.5.1 shows the density of such an excitation propagating through the

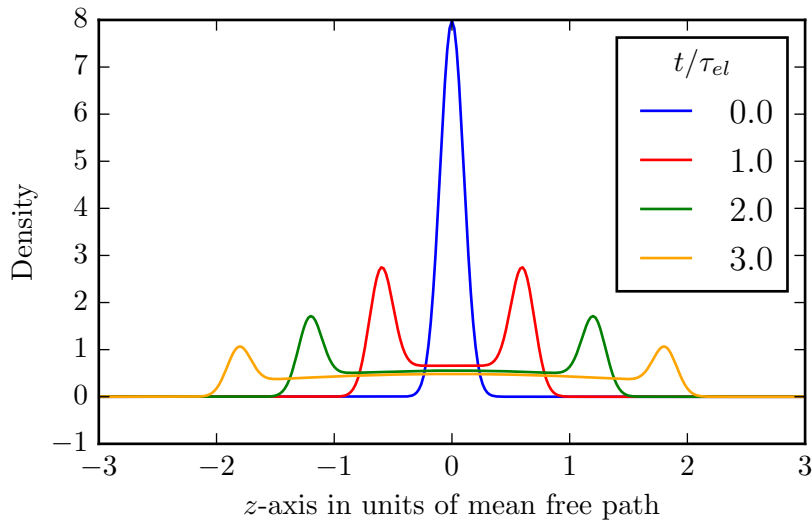


Figure 8.5.1: The density of a localized excitation that propagates through the bulk. The fast moving ballistic contributions is diminished by impurity scattering and makes way for a diffusive expansion.

material and depicts how collisions lead to a decrease in ballistic density while more weight is shifted into a normal distribution that expands diffusively.

In the present chapter we were concerned with the spacial propagation of a localized quasi-particle excitation. The geometry of the problem leads to a directed transport of excess density that interacts with the material via impurity scattering. As this impurity scattering is elastic in nature there is no mechanism present that relaxes the kinetic energy of the excitation. In the next chapter we therefore introduce electron-electron collisions as a means of inelastic scattering that leads to a relaxation of the excitation not only in real space but also in momentum or energy space.





## Chapter 9

# Thermalization

### 9.1 Introduction

As introduced before, the Boltzmann equation is an equation for the quasi-particle distribution. This distribution is in general a function of seven degrees of freedom, three spacial ones, three in momentum space and the time axis. The whole previous chapter was concerned with the evolution of this quasi-particle distribution in its spacial degrees of freedom. The means of this evolution were the combination of classical deterministic phase space evolution and a collisions with the environment mediated by impurity scattering. This impurity scattering then lead to any directional momentum to be evened out so that an initially ballistic motion slowly turns into an isotropic diffusive transport.

As the impurity scattering is elastic in nature, the collision integral only connected phase space volume elements of equal magnitude of momentum and an excitation could be treated as living freely without regard to the rest of the conduction electrons. In reality, however, a quasi-particle excitation is created by providing an electron that is situated below the Fermi surface in momentum space with enough energy to “lift” it above the Fermi surface. On the one hand this leaves a hole below the Fermi surface, a fact that we ignored in the treatment of the previous chapter. And on the other hand it becomes clear by this view of an excitation that the approach of a new equilibrium necessary includes the interaction with this excitation and the rest of the electron sea. By colliding with an electron near the Fermi surface inelastically energy is transferred from the initially excited electron to its collision partner which is in turn lifted above the Fermi surface. This effectively leaves two excitations, each at its respective energy level.

In a first order approximation these two excitations can be treated independently so that their subsequent interaction with the Fermi sea is again described by the same formalism as the initial collision. In practice the collision integral that is employed here is the one of electron-electron scattering.

As we are interested in the relaxation of energy we integrate the distribution function over space and reduce the problem thus to two dimensions, energy and time.

The first collision leaves the system with two particle-hole excitations and subsequent collisions keep exchanging energy with the Fermi sea until a new equilibrium is reached. This approach of equilibrium is usually coined *thermalization* as the reaching of a new equilibrium allows again to describe the system with a temperature that is now adjusted to incorporate the additional energy of the initial excitation.

## 9.2 Thermalization of the electron system

As we have started the analysis of the previous chapter with the collision integral for impurity scattering we start the present one with the corresponding one pertaining to electron-electron scattering. The linearized collision integral for inelastic electron-electron scattering (7.3.45) reads

$$I_{\text{inel}} = -\frac{1}{\tau(E)}\delta f^0(E) - \int dE' \frac{\delta f^0(E')}{\tau(E, E')}, \quad (9.2.1)$$

where we again take the energy state representation and the energy dependent collision rates  $1/\tau(E)$  and  $1/\tau(E, E')$  are given by equations (7.3.50) and (7.3.49).

The Boltzmann equation now becomes an partial-integro-differential equation whose naming already points at the cumbersomeness of its solution process. As we are concerned only with the evolution in energy space we restrict the analysis to the energy space density  $\mathcal{G}(E) = \int dz \delta f^0$ . Integrating therefore the Boltzmann equation leaves us with treating the simpler coupled system

$$\frac{\partial}{\partial t}\mathcal{G}(E) + \int dE' \left( \frac{\delta(E' - E)}{\tau(E')} + \frac{1}{\tau(E, E')} \right) \mathcal{G}(E') = 0, \quad (9.2.2)$$

which diagonalization, after discretizing energy space, amounts to an eigenvalue problem that given algorithms are willing to solve.

It is of particular importance that the solution of (9.2.2) is obtained not by iterative methods but by eigenvalue decomposition. This allows for a semi-analytic solution, where only the eigenvalues and coefficients are calculated with the help of a machine, the solution itself, however, has an analytic expression. Because of this semi-analytic nature of the solution it yields applicable results for all time scales, spanning from the first few femto seconds up to reaching a new equilibrium. This crucially admits for an analysis of the transient behavior and, as we show below, its characterization in terms of a quasi-equilibrium.

To analyze the relaxation of energy in an excited system out of equilibrium<sup>1</sup> we take a single particle-like excitation that leaves a hole below the Fermi level by moving the taken particle to an energy level above at time  $t = 0$ . This quasi-particle scatters with quasi particles in the Fermi sea exciting an additional density above the Fermi level. This process, also called electron cascade [94], then is repeated until an equilibrium is reached between the excess density of particles above the Fermi level and of holes below. This amounts to a Fermi distributed system at a new (higher) temperature. The new temperature and thus the final state can also be calculated from the amount of additional energy induced into the system  $\delta u$ .

In particular the temperature dependent total internal energy  $u$  of a system is given by means of the Sommerfeld expansion

$$u = \frac{3}{5}nE_F + \frac{\pi^2}{4} \frac{(k_B T)^2}{E_F} = u_0 + \frac{\pi^2}{4} \frac{(k_B T)^2}{E_F}, \quad (9.2.3)$$

with  $n$  being the particle density,  $k_B$  the Boltzmann constant and  $E_F$  the Fermi energy. So the final temperature can be expressed via

$$T = \sqrt{T_0^2 + \frac{12E_F^2}{5\pi^2 k_B^2} \frac{\delta u}{u_0}}, \quad (9.2.4)$$

where the added energy  $\delta u$  is given in units of the zero temperature internal energy  $u_0$  and  $T_0$  is the initial temperature taken to be at room temperature. The final state has then the simple form  $\mathcal{G}^{\text{eq}}(E) = f^{\text{eq}}(E, T) - f^{\text{eq}}(E, T_0)$ . With the new temperature  $T$  given by (9.2.4).

The approach of said equilibrium is governed by the Boltzmann equation (9.2.2) and the solution is depicted in figure 9.2.1. In principle this approach is an asymptotic process but as depicted in the figure after the initial excitation scattered around 1000 times a new equilibrium is established. On the other hand the prominent signature of the initial excitation looses its non-continuous shape, as shown in figure 9.2.2, within the first few scattering events and a continuous excitation density is established. In the next section we therefore analyze how this distribution develops to finally form the new equilibrium.

### 9.3 Approaching the equilibrium

We can distinguish two phases of this approach of equilibrium. In phase one the excited quasi-particle collides with the Fermi sea and looses its energy.

---

<sup>1</sup>The system is assumed to be “not-far” from equilibrium, this hand-wavy demand can be concretized in terms of our analysis. Excluding non-linear behavior in the collision integral we implicitly assume the quasi-particle density involved in the excitation to be small compared to the rest of the Fermi sea.

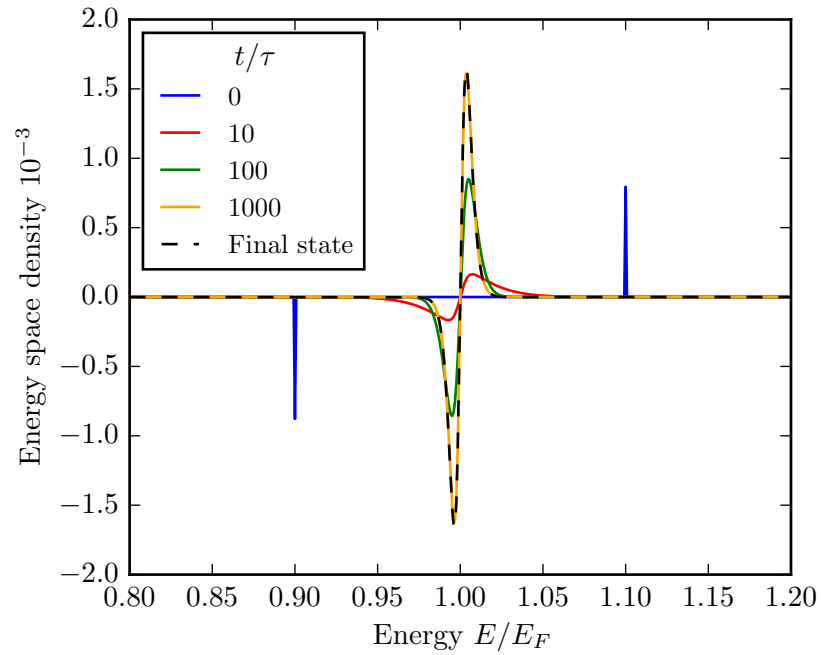


Figure 9.2.1: The approach of a new equilibrium final state is mediated via electron-electron collisions. Between the initial state that is clearly out of equilibrium and the establishment of a final state, the system undergoes a cascade of quasi-equilibrium like states that can be described by a fraction of a system in equilibrium at a higher temperature (cf. section 9.3). The non-equilibrium state defined here as a non-continuous distribution decays on a short timescale of a few femto seconds and a new continuous transient distribution is established.

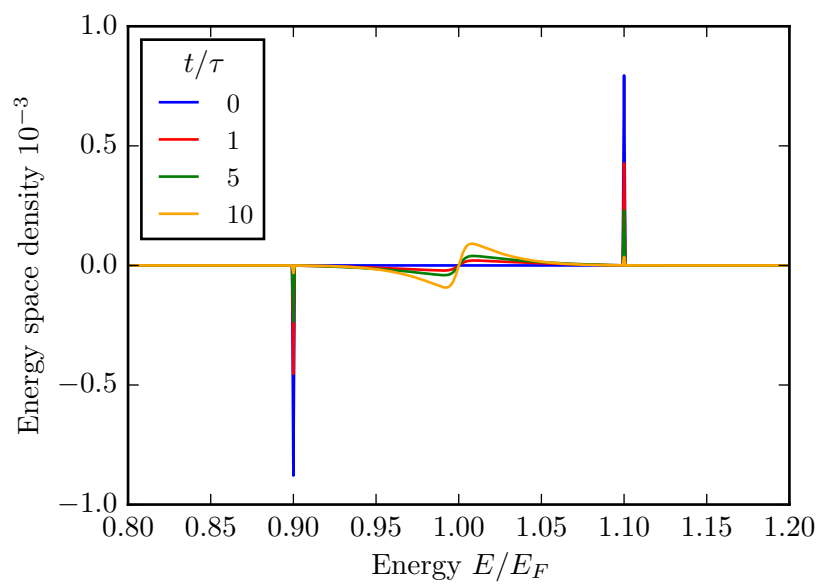


Figure 9.2.2: The non-equilibrium distribution interacts with the Fermi sea. After the first few collisions the strong non-continuous peaks of the initial quasi-particle excitation makes way to a transient continuous distribution. As predicted by Fermi liquid theory the electron-electron scattering dynamics subsequently slow down for particles around the Fermi surface.

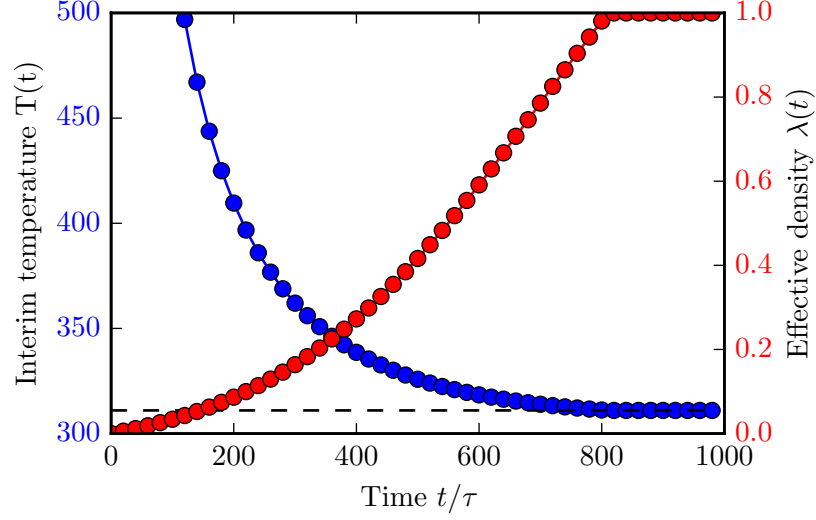


Figure 9.3.1: An interim temperature  $T(t)$  can be defined by approximating the system as a fraction of a larger system with said temperature  $T$ . The solution to the Boltzmann equation (9.2.2) is fitted with the model (9.3.1) at different times approaching the new equilibrium.

This amounts to a diminishing of the singular non-equilibrium peak and a building up of an continuous excitation density. This phase ends once the particle density reaches a continuous state. As depicted, this is the case already before  $10\tau$ . This phase is the phase of strong non-equilibrium and has to be treated as such by the full theory presented so far.

The second stage, however, beginning with the establishment of a continuous particle density up to the new equilibrium distribution, can be described by a dynamic quasi equilibrium. A fit of the form

$$\mathcal{G}(E, t) = \lambda(t) [f^{\text{eq}}(T(t)) - f^{\text{eq}}(T_0)], \quad (9.3.1)$$

with the fitting parameter  $\lambda(t)$  and  $T(t)$  suggests that the transient system at any time  $t$  behaves as it were a fraction  $\lambda(t)$  of a larger system at temperature  $T(t)$ , where  $\lambda$  approaches unity while  $T$  approaches  $T_0$ . Demanding as a sentient control for the fit that the internal energy stays constant we arrive at a relation between both parameters of

$$\lambda(t) = \frac{12E_F^2 \frac{\delta u}{u_0}}{5\pi^2 k_B^2 (T(t)^2 - T_0^2)} = \frac{T_{\text{final}}^2 - T_0^2}{T(t)^2 - T_0^2}, \quad (9.3.2)$$

shown in figure 9.3.1.

This interpretation contrasts earlier work [71, 82] that treats the transient regime as a system separated into main bath in (quasi)-equilibrium and an

non-equilibrium part that exponentially decays in time. This decay amounts to an energy transfer from non-equilibrium part to quasi-equilibrium part. The prefix “quasi” then is justified as the influx of energy leads to a change of equilibrium temperature. It is this rising temperature that the literature adhering to said model usually coins *transient* temperature [95].

However, our analysis proves the concept of any transient temperature or even the establishment of a quasi-equilibrium on electron-electron scattering time scales to be weary. The solution to the Boltzmann equation (9.3.1) does indeed contain a dynamic parameter  $T(t)$  that mathematically resembles a temperature. However, the interpretation of the physicality of the transient regime is remarkably different. Instead of viewing the system as a main part that is always in quasi-equilibrium and a non-equilibrium part our analysis suggest the interpretation of two separate systems, one at the original temperature  $T_0$  and one hot system, also in quasi-equilibrium, that cools down quickly following the temperature dynamics given by  $T(t)$ . The weight between both systems is mediated by the function  $\lambda(t)$  so that it is suggestive to write the dynamics of the whole system as

$$f(t) = (1 - \lambda(t)) f^{\text{eq}}(T_0) + \lambda(t) f^{\text{eq}}(T(t)), \quad (9.3.3)$$

to show the shifting of weight between both fictitious subsystems. It is important to take care with interpreting these result physically, however.

None-the-less the solution (9.3.3) can be used, together with the fitted dynamics for the variable  $T(t)$  shown in figure 9.3.1, to analyze the interaction of the electron system with its environment. Making use of the solution (9.3.3) allows for a simpler treatment of the electron-phonon interaction without the need of solving the fully coupled system. Next we therefore investigate how the above insights can be incorporated into the two temperature model that proved useful to describe the interaction of a thermalized electron system with its environment.





## Chapter 10

# Two temperature model

The two temperature model [76, 77, 78] (TTM) has been well established to describe the exchange of energy between an electron system and a phonon bath, both in equilibrium internally but at different temperatures [63, 64, 65].

As the temperatures are the only defining parameter in these equilibrium systems, the model analyzes their dynamics. The change in lattice temperature is due to the flux of energy from the (hotter) electron system.

In the present chapter we use the two temperature model to describe the interaction of an thermalized electron system with its environment, namely the surrounding phonon bath. Once the model is established we turn to incorporate the dynamics of electron thermalization derived in the previous chapter.

The internal energy of the electron system is given by

$$u_{\text{el}} = \int d\varepsilon \varepsilon \nu(\varepsilon) f(\varepsilon, t), \quad (10.0.1)$$

where  $\nu(\varepsilon)$  is the density of states and  $f(\varepsilon, t)$  is the electronic distribution function. In equilibrium this is just the Fermi distribution.

To describe then the equilibration between electron and phonon system we formally introduce the concept of a quasi-equilibrium. This assumes the electron system<sup>1</sup> to be describable by a Fermi function with a time dependent temperature  $T_{\text{el}}(t)$  with the further restriction that this temperature change should be adiabatic. We thus have

$$f^{\text{eq}}(\varepsilon, T_{\text{el}}(t)) = \frac{1}{1 + \exp\left[\frac{\varepsilon - \varepsilon_F}{k_B T_{\text{el}}(t)}\right]} \quad (10.0.2)$$

and a corresponding internal energy of

$$u[T_{\text{el}}(t)] = \int d\varepsilon \varepsilon \nu(\varepsilon) f^{\text{eq}}(\varepsilon, T_{\text{el}}(t)). \quad (10.0.3)$$

---

<sup>1</sup>We continue to speak of the electron system in the present derivation, but the same insights naturally apply to the phonon bath as well.

The general dynamics of this quasi-equilibrium distribution is governed by electron-phonon scattering and described by the Boltzmann equation. We continue to use the partial derivative to denote the temporal change even though this change is not explicit, but via the change of temperature. The implicit time dependence of temperature results in conservation of particle number but not of energy. The driver of this change of distribution function, and thus of the change of temperature, are the electron-phonon collisions. We therefore write

$$\begin{aligned}\frac{\partial f(\varepsilon, t)}{\partial t} &= \frac{\partial f^{\text{eq}}(\varepsilon, T_{\text{el}}(t))}{\partial t} \\ &= \left( \frac{\partial f^{\text{eq}}}{\partial t} \right)_{\text{el-ph}}.\end{aligned}\quad (10.0.4)$$

Now the change of distribution also amounts to a change of energy so that by differentiation of equation (10.0.1) in time we obtain

$$\frac{\partial u_{\text{el}}}{\partial t} = \int d\varepsilon \varepsilon \nu(\varepsilon) \frac{\partial f(\varepsilon, t)}{\partial t}.\quad (10.0.5)$$

Or again taking the electron system in quasi-equilibrium we may insert the electron-phonon collision integral, as in equation (10.0.4), to describe the change due to electron-phonon scattering. The evaluation of the integrals [76, 78] then gives

$$\begin{aligned}\frac{\partial u_{\text{el}}}{\partial t} &= \int d\varepsilon \varepsilon \nu(\varepsilon) \frac{\partial}{\partial t} f^{\text{eq}}(\varepsilon, T_{\text{el}}(t)) \\ &= \int d\varepsilon \varepsilon \nu(\varepsilon) \left( \frac{\partial f}{\partial t} \right)_{\text{el-ph}}\end{aligned}\quad (10.0.6)$$

$$= \kappa(T_{\text{ph}}(t) - T_{\text{el}}(t)).\quad (10.0.7)$$

Here we used that electrons and phonons constitute a closed system so that energy conservation requires

$$\frac{\partial u_{\text{el}}}{\partial t} = -\frac{\partial u_{\text{ph}}}{\partial t}.\quad (10.0.8)$$

Notice that the assumption of quasi-equilibrium means that the change of electron distribution function is only driven by the change of temperature on first sight. The underlying mechanism is, however, the drain of energy from the electron system. The change of a system's energy is connected to the change of its temperature via the heat capacity  $C$  that is typically split into a linear electronic and a cubic lattice contribution part [96],

$$\frac{\partial u}{\partial t} = C(T) \frac{\partial T}{\partial t}.\quad (10.0.9)$$

	Au	Ru	Units
$\kappa$	2.3	185	$10^{10} \text{ W cm}^{-3} \text{ K}^{-1}$
$C_{\text{el}}$	0.021	0.12	$\text{J cm}^{-3} \text{ K}^{-1}$
$C_{\text{ph}}$	2.5	2.9	$\text{J cm}^{-3} \text{ K}^{-1}$
$\tau_{\text{el-ph}}$	918	62	fs

Table 10.1: Electron-phonon coupling constant  $\kappa$  and the electronic  $C_{\text{el}}$  and lattice  $C_{\text{ph}}$  contribution to the heat capacity at room temperature for gold and ruthenium. From these quantities a electron-phonon relaxation time as defined in equation (10.0.12) can be derived [82, 87, 97, 98]. We choose here gold and ruthenium as example materials as they differ in their strength of electron-phonon coupling by two orders of magnitude. This then allows for the analysis of electron-phonon coupling strength on the equilibration dynamics.

After collecting equations (10.0.7), (10.0.8) and (10.0.9) we finally arrive at the two temperature model

$$\begin{aligned} C_{\text{el}}(T_{\text{el}}) \frac{\partial T_{\text{el}}}{\partial t} &= \kappa (T_{\text{ph}}(t) - T_{\text{el}}(t)) \\ C_{\text{ph}}(T_{\text{ph}}) \frac{\partial T_{\text{ph}}}{\partial t} &= -\kappa (T_{\text{ph}}(t) - T_{\text{el}}(t)). \end{aligned} \quad (10.0.10)$$

These coupled differential equations describe the equilibration between electron and phonon bath and are well established in theoretical and experimental literature. In theory the coupling parameter  $\kappa$  can be calculated microscopically but in practice determining it experimentally is more practicable.

In equation (10.0.10) the heat capacity of electron and phonon bath is taken to be temperature dependent. While this is true in general and one of the fundamental results of developing the theory of the free electron Fermi gas in the early days of condensed matter theory [87], here we assume to be in the perturbative regime where  $T_{\text{el}} \approx T_{\text{ph}}$  so that the change of heat capacity is negligible. With constant heat capacities the two temperature model (10.0.10) can be solved directly, giving for the electron temperature

$$T_{\text{el}}(t) = \frac{C_{\text{el}}T_{\text{el},0} + C_{\text{ph}}T_{\text{ph},0}}{C_{\text{el}} + C_{\text{ph}}} + \frac{C_{\text{ph}}(T_{\text{el},0} - T_{\text{ph},0})}{C_{\text{el}} + C_{\text{ph}}} e^{-\frac{t}{\tau_{\text{el-ph}}}} \quad (10.0.11)$$

with the relaxation time

$$\tau_{\text{el-ph}} = \frac{C_{\text{el}}C_{\text{ph}}}{(C_{\text{el}} + C_{\text{ph}})\kappa}. \quad (10.0.12)$$

Table 10.1 gives values for selected materials.

The two temperature model assumes both the electron and the phonon system to be in quasi-equilibrium. As we have presented in the previous section the thermalization time of an isolated electron system is of the order of pico seconds. For a quasi instantaneous excitation of the electron system the thermalization and the exchange of energy with the phonon bath therefore are of the same order of magnitude. It is therefore necessary to include the non-equilibrium effects of the dynamics of thermalization into account. In the next section we therefore use the fitted thermalization model (10.1.1) to extend the usual two temperature model.

## 10.1 Extension of the two temperature model

As the thermalization of the electron system and the coupling of electrons with the phonon bath are of a similar time-scale, both effects have to be taken into account for more detailed description of the relaxation process [73, 79, 82, 83]. In the previous section we derived a model for the equilibration of the electron system by the means of electron-electron interaction.

$$f(\varepsilon, t) = (1 - \lambda(t)) f^{\text{eq}}(\varepsilon, T_{\text{el,initial}}) + \lambda(t) f^{\text{eq}}(\varepsilon, T(t)). \quad (10.1.1)$$

We therefore now turn to incorporate the thermalization dynamics of the electron system into the two temperature model (10.0.10) above. The solution (10.1.1) suggests an interpretation of the transient regime to consist of two baths, one at initial temperature  $T_{\text{el,initial}}$  and the other at the transient temperature  $T(t)$  that asymptotically approaches the final temperature  $T_{\text{el,final}}$ . So that we have

$$T(t) = T_{\text{el,final}} + \tilde{T}(t), \quad \text{with } \tilde{T}(t) \rightarrow 0. \quad (10.1.2)$$

Both temperature baths are modulated by the shifting weight factor  $\lambda(t)$  that describes the electron-electron interaction dynamics.

We assume now that this interaction dynamics is not directly effected by the electron-phonon coupling. Instead the two respective temperature baths couple directly to the phonon system via their base temperature. The change of energy of the electron system is therefore given by

$$\begin{aligned} \frac{\partial u_{\text{el,tot}}}{\partial t} &= (1 - \lambda(t)) \int d\varepsilon \varepsilon \nu(\varepsilon) \frac{\partial f^{\text{eq}}(\varepsilon, T_{\text{el,initial}}(t))}{\partial t} \\ &\quad + \lambda(t) \int d\varepsilon \varepsilon \nu(\varepsilon) \frac{\partial f^{\text{eq}}(\varepsilon, T(t))}{\partial t} \\ &\equiv \frac{\partial u_{\text{el,initial}}}{\partial t} + \frac{\partial u_{\text{el,final}}}{\partial t}, \end{aligned} \quad (10.1.3)$$

where the omission of time derivatives of  $\lambda(t)$  amounts to ignoring the effect of electron-phonon scattering on the dynamics of electron-electron collisions.

Plugging in the two temperature model calculation (10.0.7) then yields

$$\frac{\partial u_{\text{el,final}}}{\partial t} = \kappa \lambda(t) \left( T_{\text{ph}} - T_{\text{el,final}} - \tilde{T}(t) \right) \quad (10.1.4)$$

$$\frac{\partial u_{\text{el,initial}}}{\partial t} = \kappa (1 - \lambda(t)) (T_{\text{ph}} - T_{\text{el,initial}}). \quad (10.1.5)$$

Now, as the only physical temperatures are the base temperatures  $T_{\text{el,initial}}$  and  $T_{\text{el,final}}$ , we assume that the drain of energy affects the electron bath only via a change of these base temperatures, omitting any effect of the dynamical temperature  $\tilde{T}(t)$  that represents the approach of a new quasi-equilibrium via electron-electron collisions. We therefore have

$$C_{\text{el}} [T_{\text{el,final}}] \frac{\partial}{\partial t} T_{\text{el,final}} = \kappa \lambda(t) \left( T_{\text{ph}} - T_{\text{el,final}} - \tilde{T}(t) \right) \quad (10.1.6)$$

$$C_{\text{el}} [T_{\text{el,initial}}] \frac{\partial}{\partial t} T_{\text{el,initial}} = \kappa (1 - \lambda(t)) (T_{\text{ph}} - T_{\text{el,initial}}) \quad (10.1.7)$$

for the dynamics of the electron bath under electron-phonon scattering and with the conservation of energy the corresponding phonon temperature is governed by the analogous relation

$$C_{\text{ph}} (T_{\text{ph}}) \frac{\partial T_{\text{ph}}(t)}{\partial t} = -\kappa \lambda(t) \left( T_{\text{el,initial}} - T_{\text{el,final}} - \tilde{T}(t) \right) - \kappa (T_{\text{ph}} - T_{\text{el,initial}}). \quad (10.1.8)$$

The weigh factor  $\lambda$  is then given by

$$\lambda(t) = \frac{T_{\text{el,final}}^2 - T_{\text{el,initial}}^2}{\left( T_{\text{el,final}} + \tilde{T}(t) \right)^2 - T_{\text{el,initial}}^2}. \quad (10.1.9)$$

Equations (10.1.6) to (10.1.8) now incorporate the dynamics of electron thermalization into the evolution of energy exchange between electron and phonon bath. Notice that as the time approaches the thermalization time  $t \rightarrow \tau_{\text{therm}}$  where the electronic quasi-equilibrium is established we have

$$\lambda(t) \rightarrow 1 \quad (10.1.10)$$

$$\tilde{T}(t) \rightarrow 0, \quad (10.1.11)$$

and the extended two (three) temperature model approaches the conventional one for times greater than the thermalization time. As  $\lambda(t)$  is a smooth function increasing from zero at  $t = 0$  to one over the time of thermalization (cf. figure 9.3.1) the change of temperatures at  $t = 0$  should also be vanishing. This slows down the initial dynamics of the two temperature equilibration compared to the original model (10.0.10) as shown in

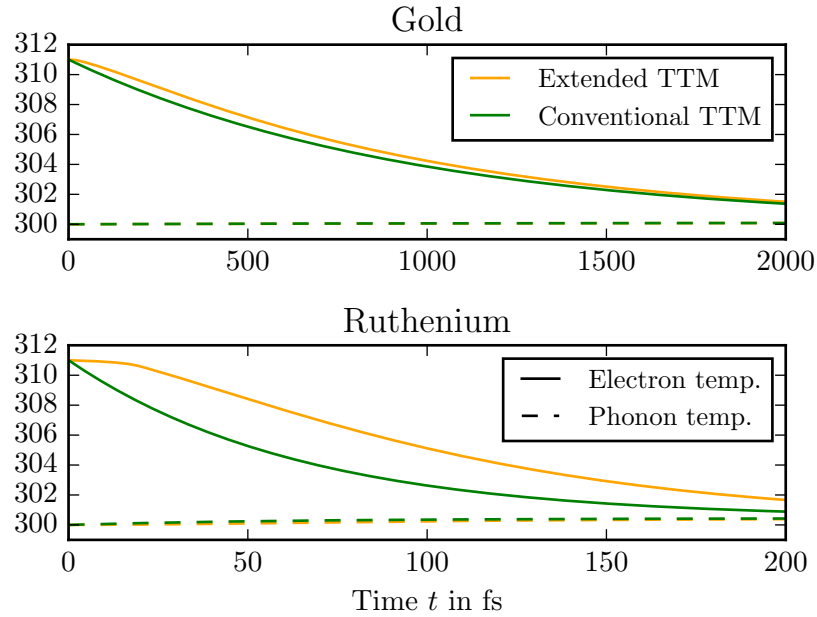


Figure 10.1.1: The inclusion of thermalization dynamics in the two temperature model leads to a delayed interaction between electron and phonon bath. Here we compare the interaction of an excited electron bath with its surroundings. Before the excitation is induced at  $t = 0$  both systems are in equilibrium at room temperature ( $T = 300\text{K}$ ). The conventional model assumes an established quasi-equilibrium of the electron system and the energy drain from electron bath to phonon bath sets in immediately. This interaction is delayed in the extended model as the hot electrons in the non-equilibrium electron distribution do not interact with the phonon bath.

figure 10.1.1. Here we used the heat capacities and electron-phonon coupling parameters for gold and ruthenium (cf. table 10.1) .

Figure 10.1.1 also shows that this delay of electron-phonon interaction prior to thermalization is much more apparent in a material such as ruthenium where the time-scales electron-phonon interaction  $\tau_{\text{el-ph}}$  is two orders of magnitude smaller than for instance in gold. However, in both cases the change of phonon temperature is less effected due to the small contribution of the lattice to the overall heat capacity. None-the-less a delay in electron-phonon energy exchange is present, recovering the result of a full numerical solution of the coupled Boltzmann problem [83].

# Chapter 11

## Summary and conclusions

In this part, we have presented the application of the Boltzmann formalism to electron relaxation processes on the ultra-fast time scale in a solid-state architecture. We show the treatment of three dominant scattering mechanisms: collisions of electrons with lattice imperfections and impurities, the interaction between electrons and the energy exchange of electrons with the surrounding lattice, represented by a phonon bath.

The experimental setup in mind is a thin film geometry of a generic metal. The film is excited with a laser uniformly in two dimensions, leaving a spacial variation to the third dimension. This effectively reduces the problem to one spacial dimension and the distribution function can be expanded into moments.

Including impurity scattering in the relaxation time approximation, we derived a ballistic-diffusion equation for the excited particle distribution. This equation not only describes the transport of a locally created excitation but allows for the classification of transport as well. To this end, we analyzed the mean square displacement and derived an expression for the dynamic change of the diffusion exponent from ballistic transport initially to a diffusive expansion after many scattering events.

The elastic impurity scattering was then supplemented with the inelastic electron-electron collision integral to describe the relaxation of a non-equilibrium distribution in energy space. A particle-hole pair was shown to excite particles from the Fermi sea in an energy cascade until a new equilibrium is established. The process can be described heuristically by introducing a fictional superposition of two thermalized electron systems with a weight factor shifting from the old to the new system during equilibration.

Having at hand a description of the electron thermalization process we then turn to the equilibration of the electron system with its surrounding phonon bath. The common description of energy exchange between an electron and phonon bath, each in quasi-equilibrium, is the two temperature model. We incorporated the thermalization dynamics of the electron system

to extend the two temperature model. With the equilibration dynamics of the electrons included we observe a delayed energy exchange between electron and phonon baths, reproducing earlier results.

In conclusion, the Boltzmann formalism can be readily applied to the ultra-fast dynamics of non-equilibrium systems. While the high dimensionality of the problem makes strong approximations unavoidable, the resulting equations still exhibit all expected features of the approach of equilibrium and can be treated in an analytical or quasi-analytical manner.



# Bibliography

- [1] J. Palmer, “Quantum leaps - Technology quarterly,” mar 2017.
- [2] A. Trabesinger, “Quantum computing: towards reality,” *Nature*, vol. 543, pp. S1–S1, mar 2017.
- [3] A. Trabesinger, “Quantum leaps, bit by bit,” *Nature*, vol. 543, pp. S2–S3, mar 2017.
- [4] R. Ruskov and A. N. Korotkov, “Entanglement of solid-state qubits by measurement,” *Phys. Rev. B*, vol. 67, p. 241305, jun 2003.
- [5] H.-A. Engel and D. Loss, “Fermionic Bell-State Analyzer for Spin Qubits,” *Science*, vol. 309, no. 5734, pp. 586–588, 2005.
- [6] W. A. Coish, V. N. Golovach, J. C. Egues, and D. Loss, “Measurement, control, and decay of quantum-dot spins,” *physica status solidi (b)*, vol. 243, no. 14, pp. 3658–3672, 2006.
- [7] R. Ionicioiu, “Entangling spins by measuring charge: A parity-gate toolbox,” *Phys. Rev. A*, vol. 75, p. 32339, mar 2007.
- [8] N. S. Williams and A. N. Jordan, “Entanglement genesis under continuous parity measurement,” *Phys. Rev. A*, vol. 78, p. 62322, dec 2008.
- [9] O. Zilberberg, B. Braunecker, and D. Loss, “Controlled-NOT gate for multiparticle qubits and topological quantum computation based on parity measurements,” *Phys. Rev. A*, vol. 77, p. 12327, jan 2008.
- [10] J. Kerckhoff, L. Bouten, A. Silberfarb, and H. Mabuchi, “Physical model of continuous two-qubit parity measurement in a cavity-QED network,” *Phys. Rev. A*, vol. 79, p. 24305, feb 2009.
- [11] S. G. Hofer, D. V. Vasilyev, M. Aspelmeyer, and K. Hammerer, “Time-Continuous Bell Measurements,” *Phys. Rev. Lett.*, vol. 111, p. 170404, oct 2013.
- [12] B. Trauzettel, A. N. Jordan, C. W. J. Beenakker, and M. Büttiker, “Parity meter for charge qubits: An efficient quantum entangler,” *Physical Review B - Condensed Matter and Materials Physics*, 2006.

- [13] A. Blais, R.-S. Huang, A. Wallraff, S. M. Girvin, and R. J. Schoelkopf, “Cavity quantum electrodynamics for superconducting electrical circuits: An architecture for quantum computation,” *Physical Review A*, vol. 69, p. 062320, jun 2004.
- [14] D. Ristè, M. Dukalski, C. A. Watson, G. de Lange, M. J. Tiggelman, Y. M. Blanter, K. W. Lehnert, R. N. Schouten, and L. Dicarlo, “Deterministic entanglement of superconducting qubits by parity measurement and feedback,” *Nature*, vol. 502, pp. 350–354, oct 2013.
- [15] K. Lalumière, J. M. Gambetta, and A. Blais, “Tunable joint measurements in the dispersive regime of cavity QED,” *Physical Review A*, vol. 81, p. 040301, apr 2010.
- [16] L. Tornberg and G. Johansson, “High-fidelity feedback-assisted parity measurement in circuit QED,” *Physical Review A*, vol. 82, p. 012329, jul 2010.
- [17] O. P. Saira, J. P. Groen, J. Cramer, M. Meretska, G. de Lange, and L. DiCarlo, “Entanglement Genesis by Ancilla-Based Parity Measurement in 2D Circuit QED,” *Physical Review Letters*, vol. 112, p. 070502, feb 2014.
- [18] L. V. Litvin, A. Helzel, H.-P. Tranitz, W. Wegscheider, and C. Strunk, “Edge-channel interference controlled by Landau level filling,” *Physical Review B*, vol. 78, p. 075303, aug 2008.
- [19] E. Bieri, M. Weiss, O. Göktas, M. Hauser, C. Schönenberger, and S. Oberholzer, “Finite-bias visibility dependence in an electronic Mach-Zehnder interferometer,” *Physical Review B*, vol. 79, p. 245324, jun 2009.
- [20] P. Roulleau, F. Portier, P. Roche, A. Cavanna, G. Faini, U. Gennser, and D. Mailly, “Tuning Decoherence with a Voltage Probe,” *Physical Review Letters*, vol. 102, p. 236802, jun 2009.
- [21] G. Haack, H. Förster, and M. Büttiker, “Parity detection and entanglement with a Mach-Zehnder interferometer,” *Phys. Rev. B*, vol. 82, p. 155303, oct 2010.
- [22] C. Meyer Zu Rheda, G. Haack, and A. Romito, “On-demand maximally entangled states with a parity meter and continuous feedback,” *Physical Review B - Condensed Matter and Materials Physics*, vol. 90, no. 15, 2014.
- [23] H. M. Wiseman, “Quantum theory of continuous feedback,” *Physical Review A*, vol. 49, pp. 2133–2150, mar 1994.

- [24] A. C. Doherty, S. Habib, K. Jacobs, H. Mabuchi, and S. M. Tan, “Quantum feedback control and classical control theory,” *Physical Review A*, vol. 62, p. 012105, jun 2000.
- [25] J. Wang and H. M. Wiseman, “Feedback-stabilization of an arbitrary pure state of a two-level atom,” *Physical Review A*, vol. 64, p. 063810, nov 2001.
- [26] H. M. Wiseman, S. Mancini, and J. Wang, “Bayesian feedback versus Markovian feedback in a two-level atom,” *Physical Review A*, vol. 66, p. 013807, jul 2002.
- [27] R. Vijay, C. Macklin, D. H. Slichter, S. J. Weber, K. W. Murch, R. Naik, A. N. Korotkov, and I. Siddiqi, “Stabilizing Rabi oscillations in a superconducting qubit using quantum feedback,” *Nature*, vol. 490, pp. 77–80, oct 2012.
- [28] C. H. Bennett, H. J. Bernstein, S. Popescu, and B. Schumacher, “Concentrating partial entanglement by local operations,” *Physical Review A*, vol. 53, pp. 2046–2052, apr 1996.
- [29] C. Bennett, D. DiVincenzo, J. Smolin, and W. Wootters, “Mixed-state entanglement and quantum error correction,” *Physical Review A*, vol. 54, pp. 3824–3851, nov 1996.
- [30] C. H. Bennett, G. Brassard, S. Popescu, B. Schumacher, J. A. Smolin, and W. K. Wootters, “Purification of Noisy Entanglement and Faithful Teleportation via Noisy Channels,” *Physical Review Letters*, vol. 76, pp. 722–725, jan 1996.
- [31] A. Ekert, “Entangled quantum systems and the Schmidt decomposition,” *American Journal of Physics*, vol. 63, no. 5, p. 415, 1995.
- [32] V. Coffman, J. Kundu, and W. K. Wootters, “Distributed entanglement,” *Physical Review A*, vol. 61, p. 52306, apr 2000.
- [33] A. Wong and N. Christensen, “Potential multiparticle entanglement measure,” *Physical Review A - Atomic, Molecular, and Optical Physics*, vol. 63, pp. 1–4, mar 2001.
- [34] R. Horodecki, P. Horodecki, M. Horodecki, and K. Horodecki, “Quantum entanglement,” *Reviews of Modern Physics*, vol. 81, pp. 865–942, jun 2009.
- [35] W. Wootters, “Entanglement of formation and concurrence,” *Quantum Information and Computation*, vol. 1, no. 1, pp. 27–44, 2001.
- [36] W. K. Wootters, “Entanglement of Formation of an Arbitrary State of Two Qubits,” *Phys. Rev. Lett.*, vol. 80, pp. 2245–2248, mar 1997.

- [37] S. Hill and W. K. Wootters, “Entanglement of a Pair of Quantum Bits,” *Physical Review Letters*, vol. 78, no. 26, pp. 5022–5025, 1997.
- [38] M. A. Nielsen and I. L. Chuang, *Quantum Computation and Quantum Information: 10th Anniversary Edition*. Cambridge University Press, 2011.
- [39] J. von Neumann, *Mathematische Grundlagen der Quantenmechanik*, vol. 42. Verlag von Julius Springer Berlin, 1935.
- [40] J. J. Sakurai, *Modern Quantum Mechanics*. Pearson new international edition, Pearson, 1994.
- [41] A. N. Korotkov, “Continuous quantum measurement of a double dot,” *Physical Review B*, vol. 60, no. 8, p. 6, 1999.
- [42] A. N. Korotkov, “Selective quantum evolution of a qubit state due to continuous measurement,” *Phys. Rev. B*, vol. 63, p. 15, feb 2000.
- [43] A. Stuart and K. Ord, *Kendall’s Advanced Theory of Statistics: Volume 1: Distribution Theory*. Wiley, 2009.
- [44] S. a. Gurvitz, “Measurements with a noninvasive detector and dephasing mechanism,” *Physical Review B*, vol. 56, pp. 15215–15223, dec 1997.
- [45] J. W. Lewis, *Feedback Control Systems Demystified: Volume 1 Designing PID Controllers*. Surber Press, 2014.
- [46] R. Ruskov and A. Korotkov, “Quantum feedback control of a solid-state qubit,” *Physical Review B*, vol. 66, no. 4, p. 041401, 2002.
- [47] Q. Zhang, R. Ruskov, and A. N. Korotkov, “Continuous quantum feedback of coherent oscillations in a solid-state qubit,” *Physical Review B*, vol. 72, p. 245322, dec 2005.
- [48] M. Sarovar, H.-S. Goan, T. P. Spiller, and G. J. Milburn, “High-fidelity measurement and quantum feedback control in circuit QED,” *Physical Review A*, vol. 72, p. 062327, dec 2005.
- [49] M. A. Castellanos-Beltran, K. D. Irwin, G. C. Hilton, L. R. Vale, and K. W. Lehnert, “Amplification and squeezing of quantum noise with a tunable Josephson metamaterial,” *Nature Physics*, vol. 4, pp. 929–931, dec 2008.
- [50] A. A. Clerk, M. H. Devoret, S. M. Girvin, F. Marquardt, and R. J. Schoelkopf, “Introduction to quantum noise, measurement, and amplification,” *Reviews of Modern Physics*, vol. 82, pp. 1155–1208, apr 2010.

- [51] N. Roch, M. E. Schwartz, F. Motzoi, C. Macklin, R. Vijay, A. W. Ed-  
dins, A. N. Korotkov, K. B. Whaley, M. Sarovar, and I. Siddiqi, “Ob-  
servation of Measurement-Induced Entanglement and Quantum Tra-  
jectories of Remote Superconducting Qubits,” *Physical Review Letters*,  
vol. 112, p. 170501, apr 2014.
- [52] Y. Ji, Y. Chung, D. Sprinzak, M. Heiblum, D. Mahalu, and H. Shtrik-  
man, “An electronic Mach-Zehnder interferometer,” *Nature*, vol. 422,  
pp. 415–418, mar 2003.
- [53] I. Neder, M. Heiblum, Y. Levinson, D. Mahalu, and V. Umansky, “Un-  
expected Behavior in a Two-Path Electron Interferometer,” *Physical  
Review Letters*, vol. 96, p. 016804, jan 2006.
- [54] G. Haack, M. Moskalets, J. Splettstoesser, and M. Büttiker, “Coherence  
of single-electron sources from Mach-Zehnder interferometry,” *Physical  
Review B*, vol. 84, p. 081303, aug 2011.
- [55] P. Roulleau, F. Portier, P. Roche, A. Cavanna, G. Faini, U. Gennser,  
and D. Mailly, “Direct Measurement of the Coherence Length of Edge  
States in the Integer Quantum Hall Regime,” *Physical Review Letters*,  
vol. 100, p. 126802, mar 2008.
- [56] L. V. Litvin, A. Helzel, H.-P. Tranitz, W. Wegscheider, and C. Strunk,  
“Edge-channel interference controlled by Landau level filling,” *Physical  
Review B*, vol. 78, p. 075303, aug 2008.
- [57] P. Roulleau, F. Portier, P. Roche, A. Cavanna, G. Faini, U. Gennser,  
and D. Mailly, “Tuning Decoherence with a Voltage Probe,” *Physical  
Review Letters*, vol. 102, p. 236802, jun 2009.
- [58] P.-A. Huynh, F. Portier, H. le Sueur, G. Faini, U. Gennser, D. Mailly,  
F. Pierre, W. Wegscheider, and P. Roche, “Quantum Coherence Engi-  
neering in the Integer Quantum Hall Regime,” *Physical Review Letters*,  
vol. 108, p. 256802, jun 2012.
- [59] V. S.-W. Chung, P. Samuelsson, and M. Büttiker, “Visibility of current  
and shot noise in electrical Mach-Zehnder and Hanbury Brown Twiss  
interferometers,” *Physical Review B*, vol. 72, p. 125320, sep 2005.
- [60] B. Misra and E. C. G. Sudarshan, “The Zeno’s paradox in quantum  
theory,” *Journal of Mathematical Physics*, vol. 18, pp. 756–763, apr  
1977.
- [61] H. Risken and T. Frank, *The Fokker-Planck Equation: Methods of So-  
lution and Applications*. Springer Series in Synergetics, Springer Berlin  
Heidelberg, 2012.

- [62] G. L. Eesley, "Observation of Nonequilibrium Electron Heating in Copper," *Phys. Rev. Lett.*, vol. 51, no. 23, 1983.
- [63] J. G. Fujimoto, J. M. Liu, and E. P. Ippen, "Femtosecond laser interaction with metallic tungsten and non equilibrium electron and lattice temperature," *Physical Review Letters*, vol. 53, no. 19, pp. 1837–1841, 1984.
- [64] H. E. Elsayed-Ali, T. B. Norris, M. A. Pessot, and G. A. Mourou, "Time-resolved observation of electron-phonon relaxation in copper," *Physical Review Letters*, vol. 58, no. 12, pp. 1212–1215, 1987.
- [65] R. W. Schoenlein, W. Z. Lin, J. G. Fujimoto, and G. L. Eesley, "Femtosecond studies of nonequilibrium electronic processes in metals," *Physical Review Letters*, vol. 58, no. 16, pp. 1680–1683, 1987.
- [66] E. Beaurepaire, J.-C. Merle, A. Daunois, and J.-Y. Bigot, "Ultrafast Spin Dynamics in Ferromagnetic Nickel," *Physical Review Letters*, vol. 76, p. 4250, may 1996.
- [67] C. Stamm, T. Kachel, N. Pontius, R. Mitzner, T. Quast, K. Holl-dack, S. Khan, C. Lupulescu, E. F. Aziz, M. Wietstruk, H. a. Dürr, and W. Eberhardt, "Femtosecond modification of electron localization and transfer of angular momentum in nickel," *Nature materials*, vol. 6, pp. 740–3, oct 2007.
- [68] K. Vahaplar, A. M. Kalashnikova, A. V. Kimel, D. Hinzke, U. Nowak, R. Chantrell, A. Tsukamoto, A. Itoh, A. Kirilyuk, and T. Rasing, "Ultrafast Path for Optical Magnetization Reversal via a Strongly Nonequilibrium State," *Physical Review Letters*, vol. 103, p. 117201, sep 2009.
- [69] M. Battiato, K. Carva, and P. M. Oppeneer, "Superdiffusive spin transport as a mechanism of ultrafast demagnetization," *Physical Review Letters*, vol. 105, no. 2, 2010.
- [70] R. Metzler and J. Klafter, "The random walk's guide to anomalous diffusion: a fractional dynamics approach," *Physics Reports*, vol. 339, no. 1, pp. 1–77, 2000.
- [71] W. S. Fann, R. Storz, H. W. K. Tom, and J. Bokor, "Electron thermalization in gold," *Physical Review B*, vol. 46, no. 20, pp. 13592–13595, 1992.
- [72] C. K. Sun, F. Vallée, L. H. Acioli, E. P. Ippen, and J. G. Fujimoto, "Femtosecond-tunable measurement of electron thermalization in gold," *Physical Review B*, vol. 50, no. 20, pp. 15337–15348, 1994.

- [73] R. H. M. Groeneveld, R. Sprik, and A. Lagendijk, “Femtosecond spectroscopy of electron-electron and electron-phonon energy relaxation in Ag and Au,” *Physical Review B*, vol. 51, no. 17, pp. 11433–11445, 1995.
- [74] N. Del Fatti, C. Voisin, M. Achermann, S. Tzortzakis, D. Christofilos, and F. Vallée, “Nonequilibrium electron dynamics in noble metals,” *Physical Review B*, vol. 61, no. 24, pp. 16956–16966, 2000.
- [75] J. Demsar, R. D. Averitt, K. H. Ahn, M. J. Graf, S. A. Trugman, V. V. Kabanov, J. L. Sarrao, and A. J. Taylor, “Quasiparticle relaxation dynamics in heavy fermion compounds,” *Physical review letters*, vol. 91, p. 27401, jul 2003.
- [76] M. L. Kaganov, I. M. Lifshitz, and L. V. Tanatarov, “Relaxation between Electrons and the Crystalline Lattice,” *JETP*, vol. 4, no. 2, p. 173, 1957.
- [77] S. I. Anisimov, B. L. Kapeliovich, T. L. Perel ’man, and L. D. Landau, “Electron emission from metal surfaces exposed to ultrashort laser pulses,” *Zh. Eksp. Teor. Fiz.*, vol. 66, pp. 776–781, 1974.
- [78] P. B. Allen, “Theory of thermal relaxation of electrons in metals,” *Physical Review Letters*, vol. 59, no. 13, pp. 1460–1463, 1987.
- [79] R. H. M. Groeneveld, R. Sprik, and A. Lagendijk, “Effect of a non-thermal electron distribution on the electron-phonon energy relaxation process in noble metals,” *Physical Review B*, vol. 45, no. 9, pp. 5079–5082, 1992.
- [80] W. S. Fann, R. Storz, H. W. K. Tom, and J. Bokor, “Direct measurement of nonequilibrium electron-energy distributions in sub-picosecond laser-heated gold films,” *Phys. Rev. Lett.*, vol. 68, no. 18, 1992.
- [81] D. Bejan and G. Raseev, “Nonequilibrium electron distribution in metals,” *Physical Review B*, vol. 55, no. 7, pp. 4250–4256, 1997.
- [82] E. Carpene, “Ultrafast laser irradiation of metals: Beyond the two-temperature model,” *Physical Review B - Condensed Matter and Materials Physics*, vol. 74, p. 24301, jul 2006.
- [83] B. Rethfeld, A. Kaiser, M. Vicanek, and G. Simon, “Ultrafast dynamics of nonequilibrium electrons in metals under femtosecond laser irradiation,” *Physical Review B - Condensed Matter and Materials Physics*, vol. 65, no. 21, pp. 2143031–21430311, 2002.
- [84] T. T. Heikkilä, *The Physics of Nanoelectronics: Transport and Fluctuation Phenomena at Low Temperatures*. Oxford Master Series in Physics, OUP Oxford, 2013.

- [85] J. M. Ziman, *Electrons and Phonons: The Theory of Transport Phenomena in Solids*. International series of monographs on physics, OUP Oxford, 1960.
- [86] B. C. Taylor and O. Madelung, *Introduction to Solid-State Theory*. Springer Series in Solid-State Sciences, Springer Berlin Heidelberg, 2012.
- [87] C. Kittel, *Introduction to Solid State Physics*. Wiley, 2004.
- [88] N. W. Ashcroft and N. D. Mermin, *Solid State Physics*. HRW international editions, Holt, Rinehart and Winston, 1976.
- [89] W. J. Beek and K. M. Muttzall, *Transport phenomena*, vol. - of *Oxford science publications*. Clarendon Press, 1975.
- [90] H. Bruus and K. Flensberg, *Many-Body Quantum Theory in Condensed Matter Physics: An Introduction*. Oxford Graduate Texts, OUP Oxford, 2004.
- [91] R. Knorren, G. Bouzerar, and K. H. Bennemann, “Theory for the dynamics of excited electrons in noble and transition metals,” *Journal of Physics: Condensed Matter*, vol. 14, p. 201, jul 2002.
- [92] V. P. Zhukov, E. V. Chulkov, and P. M. Echenique, “Lifetimes and inelastic mean free path of low-energy excited electrons in Fe, Ni, Pt, and Au: Ab initio GW + T calculations,” *Physical Review B*, vol. 73, p. 125105, mar 2006.
- [93] M. Battiato, K. Carva, and P. M. Oppeneer, “Theory of laser-induced ultrafast superdiffusive spin transport in layered heterostructures,” *Physical Review B*, vol. 86, p. 024404, jul 2012.
- [94] P. A. Wolff, “Theory of Secondary Electron Cascade in Metals,” *Physical Review*, vol. 95, no. 1, 1954.
- [95] M. Lisowski, P. A. Loukakos, U. Bovensiepen, J. Stähler, C. Gahl, and M. Wolf, “Ultra-fast dynamics of electron thermalization, cooling and transport effects in Ru(001),” *Applied Physics A: Materials Science and Processing*, vol. 78, no. 2, pp. 165–176, 2004.
- [96] Z. Lin, L. V. Zhigilei, and V. Celli, “Electron-phonon coupling and electron heat capacity of metals under conditions of strong electron-phonon nonequilibrium,” *Physical Review B - Condensed Matter and Materials Physics*, vol. 77, no. 7, 2008.
- [97] M. Bonn, D. N. Denzler, S. Funk, M. Wolf, S.-S. Wellershoff, and J. Hohlfeld, “Ultrafast electron dynamics at metal surfaces: Competition between electron-phonon coupling and hot-electron transport,” 1999.



- [98] W. M. Haynes, *CRC Handbook of Chemistry and Physics, 97th Edition*.  
CRC Press, 2016.



# List of publications

C. Meyer Zu Rheda, G. Haack, and A. Romito, “On-demand maximally entangled states with a parity meter and continuous feedback,” *Physical Review B - Condensed Matter and Materials Physics*, vol. 90, no. 15, 2014.



# Curriculum Vitae

2005	Abitur	Gymnasium Othmarschen, Hamburg
2005–2006	Zivildienst	AFS Japan, Tokio, Japan
2006–2010	Bachelor Studium	Freie Universität Berlin
2007–2008	Erasmus Aufenthalt	Universita degli Studi di Genova, Genua, Italien
2010	Bachelor Arbeit	CNRS Strasbourg, Straßburg, Frankreich
2010–2012	Master Studium	Freie Universität Berlin und Technische Universität Berlin
2012	Gaststudent	Weizmann institute, Rehovot, Israel
2013–2017	Wissenschaftlicher Mitarbeiter	Freie Universität Berlin



# Acknowledgements

This thesis would not have been possible without the help of a number of people. Foremost I am indebted to my supervisor Tamara Nunner, who supported me throughout my work both scientifically and mentally.

Furthermore I would like to thank Alessandro Romito and Geraldine Haack for the fruitful collaboration leading to the first part of this work.

The groups of the Dahlem Center for Complex Quantum Systems have been a lovely work environment and our secretary Brigitte Odeh was of great support. Last but not least I give my thanks to Felix von Oppen for his support during my final year.